UNIVERSITÀ DEGLI STUDI DI PADOVA
DIPARTIMENTO DI INGEGNERIA CIVILE, EDILE E AMBIENTALE
Department of Civil, Environmental and Architectural Engineering

Corso di Laurea Magistrale in Ingegneria Civile

TESI DI LAUREA

STUDY OF THE EFFECTS INDUCED BY THE INTRODUCTION OF AUTOMATED VEHICLES ON VEHICULAR TRAFFIC FLOW IN URBAN AREAS

Relatori:
PROF. ING. RICCARDO ROSSI
PROF. ING. BERNHARD FRIEDRICH

Correlatori:
ING. FEDERICO ORSINI
M. SC. SEFA YILMAZ-NIEWERTH

Laureando: ALBERTO PELIZZA
Matricola 2242257

ANNO ACCADEMICO 2021-2022

Contents

Abstract vii

Sommario ix

1 Literature Review 1
- 1.1 Overview of Lane Changing Models . . . 1
- 1.2 Overview of LC2013 Model . . . 5
  - 1.2.1 Strategic Lane Change . . . 5
  - 1.2.2 Cooperative Lane Change . . . 8
  - 1.2.3 Tactical Lane Change . . . 9
  - 1.2.4 Regulatory Lane Change . . . 9
  - 1.2.5 Gap Acceptance Theory . . . 11
- 1.3 Overview of the Macroscopic Fundamental Diagram . . . 13
- 1.4 Overview of Surrogate Safety Measures . . . 17
  - 1.4.1 Time to Collision . . . 18
  - 1.4.2 Post Encroachment Time . . . 20
  - 1.4.3 Deceleration Rate to Avoid Collision . . . 20
- 1.5 Related Works . . . 21
- 1.6 Aim of the Study . . . 26

2 Methodology 27
- 2.1 SUMO Software . . . 27
- 2.2 Network Setup . . . 30
- 2.3 Vehicles Modeling . . . 32
  - 2.3.1 Automated Vehicles . . . 32
  - 2.3.2 Conventional Vehicles . . . 39
- 2.4 Demand Modeling . . . 39
- 2.5 Simulation Runs . . . 42

3 Results 47
- 3.1 About Lane Changes . . . 48
- 3.2 About Travel Time and Speed . . . 51
- 3.3 About Macroscopic Fundamental Diagram . . . 56
- 3.4 About Surrogate Safety Measures . . . 63

4 Discussion and Future Outlook **69**
4.1 About Efficiency 69
4.2 About Safety 70
4.3 Future Outlook 71

A Macroscopic Fundamental Diagram **73**

Bibliography **79**

List of Figures

1.1 Lane change scenario . . . 2
1.2 Generic structure of lane changing models . . . 3
1.3 `bestLaneOffset` parameter . . . 5
1.4 Urgent lane change, adapted from [29] . . . 6
1.5 Speed adjustment to support lane change . . . 7
1.6 Cooperative lane change . . . 8
1.7 Tactical lane change, adapted from [29] . . . 10
1.8 Regulatory lane change, adapted from [29] . . . 12
1.9 `requiredGap` parameter . . . 13
1.10 Traffic states in the Macroscopic Fundamental Diagram . . . 15
1.11 TTC in the event of rear end and crossing/lane change conflict . . . 19
1.12 PET . . . 20

2.1 Screenshot of SUMO traffic simulator . . . 28
2.2 Screenshot of continuous lane changing . . . 30
2.3 Real world Hannover Vahrenwald-List traffic network . . . 31
2.4 Number of lanes in the real world Hannover Vahrenwald-List traffic network . . . 32
2.5 Schematic view of driving task showing DDT portion [5] . . . 35
2.6 Level 5 Automated Vehicle sensors . . . 37
2.7 Scene for the Level 5 and Argoverse dataset . . . 38
2.8 Demand profile: real traffic flow and intensified flow . . . 40
2.9 Number of run of the simulation model, adapted from [10] . . . 43
2.10 Desired range vs number of runs . . . 45

3.1 Change in number of lane change maneuver from Scenario 0 . . . 49
3.2 Automated vehicle's lane change maneuver . . . 50
3.3 Change in mean travel time from Scenario 0 . . . 53
3.4 Change in mean speed from Scenario 0 . . . 54
3.5 50% penetration rate Macroscopic Fundamental Diagram . . . 58
3.6 Hysteresis cycle in the seed 1 simulation, 50% penetration rate Macroscopic Fundamental Diagram . . . 59
3.7 Change in maximum flow from Scenario 0 . . . 61
3.8 Change in optimum density from Scenario 0 . . . 62
3.9 Change in optimum speed from Scenario 0 . . . 62
3.10 Screenshot of a lane change conflict between vehicles . . . 65
3.11 Change in the ratio conflicts/lane changes from Scenario 0 . . . 66
3.12 Change in the ratio conflicts/conventional vehicles from Scenario 0 . . . 66

4.1 Change from the Scenario 0 of mean travel time and speed 71

A.1 MFD of the 0% automated vehicles penetration rate, *Scenario 0* 73
A.2 MFD of the 10% automated vehicles penetration rate 74
A.3 MFD of the 20% automated vehicles penetration rate 74
A.4 MFD of the 30% automated vehicles penetration rate 75
A.5 MFD of the 40% automated vehicles penetration rate 75
A.6 MFD of the 50% automated vehicles penetration rate 76
A.7 MFD of the 60% automated vehicles penetration rate 76
A.8 MFD of the 70% automated vehicles penetration rate 77
A.9 MFD of the 80% automated vehicles penetration rate 77
A.10 MFD of the 90% automated vehicles penetration rate 78
A.11 MFD of the 100% automated vehicles penetration rate 78

List of Tables

1.1 SUMO parameters related to urgency for strategic lane-changing [8], [29] 6
1.2 Surrogate Safety Measures . . . 17
1.3 Lane change model parameters by Lackey (2019) [23] and Kavas et al. (2021) [19] . . . 21
1.4 Lane change model parameters by Mintsis et al. (2019) [29] . . . 23
1.5 Lane change model parameters by Berrazouane (2019) [6] . . . 25

2.1 SUMO parameters [8] . . . 29
2.2 SUMO network charateristics . . . 31
2.3 Automation levels [5] . . . 34
2.4 Automated Vehicles sensors . . . 36
2.5 Parameter set for modeling Automated Vehicles . . . 38
2.6 Parameter set for modeling Conventional Vehicles . . . 39
2.7 Minimum number of runs [10] . . . 42
2.8 Number of runs per each scenario . . . 44

3.1 Number of inserted vehicles for the real traffic flow demand profile . . . 47
3.2 SUMO lane change measures . . . 48
3.3 Number of lane change maneuver . . . 49
3.4 SUMO edge-based measures . . . 51
3.5 Change in mean travel time from Scenario 0 for all vehicles . . . 53
3.6 Change in mean speed from Scenario 0 for all vehicles . . . 54
3.7 Change in mean travel time from Scenario 0 for conventional and automated vehicles . . . 55
3.8 Change in mean speed from Scenario 0 for conventional and automated vehicles . . . 55
3.9 MFD: maximum flow, optimum density and optimum speed . . . 57
3.10 MFD: linear regression analysis . . . 60
3.11 SUMO SSM measures . . . 63
3.12 Number of conflicts . . . 64
3.13 Change in number of conflicts from Scenario 0 . . . 67
3.14 Conflicts/conventional vehicles: linear regression analysis . . . 68

Abstract

In recent years, the interest of car manufacturers in the development of self-driving vehicles has grown, and automated vehicles are expected to circulate in increasing numbers in the next years. These predictions lead to the need to analyse how automated vehicles will interface with conventional vehicles and existing infrastructure. Given the small number of automated vehicles in circulation, the available literature proposes various tools for modelling them within microsimulation software and shows results in terms of system efficiency referring to highway scenarios. Few publications focus on urban scenarios and no publication concentrates on the exclusive analysis of a lane change maneuver. This thesis aims to close this gap in the literature by analyzing how the lane change behaviour of automated vehicles impacts efficiency and safety within the vehicular flow in an urban network. To achieve this goal, initially the urban network of the city of Hannover, Germany, was modeled and two different demand profiles were loaded. The first one refers to the profile of a typical working day, while the second profile represents a fictitious demand, obtained by increasing and subsequently decreasing the number of vehicles in circulation. An analysis of the available literature was then carried out to find parameters with which to model both automated and conventional vehicles. Eleven different scenarios are created, with the reference Scenario 0 consisting of the circulation of conventional vehicles only, in which the number of autonomous vehicles in circulation is increased by 10% for each subsequent scenario. The final scenario consists of only autonomous vehicles in circulation within the network. The results and final considerations are presented in terms of efficiency, i.e. through the analysis of travel times, average travel speeds and through the analysis of fundamental network diagrams, and in terms of safety with reference to Scenario 0. The results show a moderate but statistically significant worsening in both efficiency and safety. Results presented in this thesis can form the basis for further research aimed at studying the actual lane change behaviour of automated vehicles by developing ad-hoc models, or aimed at improving the efficiency and safety of lane change manoeuvers of automated vehicles.

Sommario

Negli anni recenti è cresciuto l'interesse delle case automobilistiche nello sviluppo di veicoli a guida autonoma e si prevede che veicoli autonomi circoleranno in numero sempre crescente negli anni a venire. Da queste previsioni nasce l'esigenza di analizzare come i veicoli autonomi si interfacceranno con i veicoli convenzionali e con le infrastrutture esistenti. Data l'esiguità del numero di veicoli autonomi in circolazione, la letteratura disponibile propone diversi strumenti per la modellazione dei veicoli autonomi all'interno di software di microsimulazione e mostra risultati in termini di efficienza del sistema riferiti a scenari autostradali. Poche pubblicazioni si concentrano sugli scenari urbani e nessuna pubblicazione concentra l'attenzione sull'analisi esclusiva di una manovra di lane change. Il presente lavoro di tesi si prefigge di chiudere questo gap della letteratura, analizzando come il comportamento di lane change dei veicoli autonomi impatti in termini di efficienza e di sicurezza all'interno del deflusso veicolare in una rete di trasporto urbana. Per raggiungere l'obiettivo, inizialmente è stata modellata la rete urbana della città di Hannover, in Germania, caricando su di essa due diversi profili di domanda. Il primo si riferisce al profilo di una giornata lavorativa tipo, mentre il secondo profilo rappresenta una domanda fittizia, ottenuta incrementando e successivamente decrementando il numero di veicoli in circolazione. In seguito si è effettuata un'analisi della letteratura disponibile per trovare i parametri con cui modellare sia i veicoli autonomi sia i veicoli convenzionali. Si creano 11 diversi scenari, con lo Scenario 0 di riferimento composto dalla circolazione di soli veicoli convenzionali, in cui si incrementa del 10% il numero di veicoli autonomi in circolazione per ogni scenario successivo. Lo scenario finale è composto da soli veicoli autonomi in circolazione all'interno della rete. I risultati e le considerazioni finali sono presentati in termini di efficienza, ovvero mediante l'analisi di tempi di percorrenza, di velocità medie di viaggio e tramite l'analisi dei diagrammi fondamentali di rete, e in termini di sicurezza con riferimento allo Scenario 0. I risultati mostrano un peggioramento moderato ma statisticamente significativo sia in termini di efficienza sia in termini di sicurezza. I risultati qui presentati possono formare la base per ulteriori ricerche mirate a studiare il reale comportamento di lane change dei veicoli autonomi, sviluppando dei modelli ad-hoc, oppure mirate a migliorare l'efficienza e la sicurezza delle manovre di lane change dei veicoli autonomi.

Chapter 1

Literature Review

1.1 Overview of Lane Changing Models

The lane change model describes the lateral movement of vehicles and includes the motivation for lane change and the choice of the destination lane. Most models classify lane change behavior into two categories: mandatory and discretionary. To follow a certain path, a vehicle has to perform mandatory lane change in order to avoid dead-end lane, for example if the vehicle has to turn left in an intersection, the driver will have to move in the turning lane in order to complete the maneuver. A desire to improve driving conditions cause a discretionary lane change, for example by overtaking a slow vehicle to gain speed. The execution of the maneuver is associated with the gap acceptance theory. Depending on the vehicles involved, different types of gaps are distinguished based on the decision to carry out the maneuver, as shown in Figure 1.1. The general structure of the lane change model is shown in Figure 1.2.
In dense traffic conditions it is possible to observe two different lane change behaviors: forced merging and cooperative merging. Forced merging occurs when there is no acceptable size gap in the target lane and the next vehicle is forced to decelerate in order to create a sufficiently large gap. Cooperative merging occurs when the next vehicle changes lanes in order to facilitate the ego vehicle to perform a lane change.
Moridpour et al. (2010) [30] published a critical review regarding lane change models and some of them are described below. According to their work there are two different categories of lane changing models: stimulus response and discrete choice model. The first category requires vehicles to decide to change lanes after evaluating the surrounding traffic conditions; the first category includes the Gipps model (1986), the Wiedemann and Reiter model (1992), the Hidas model (2002; 2005) and the Krajzewicz model (2009). On the other hand the second category involves the use of probabilistic models both for the choice of lane and for the choice of gaps in the selected lane. In accordance with this thesis, it is considered appropriate to present the models belonging to the stimulus response model category.
Gipps (1986) proposed a decision structure for the lane change model valid both in the urban context and in the motorway context. Lane change is performed when three factors occur: safety, necessity and desirability. Gipps also defines three zones that characterize the intention to change lanes, based on the distance from the ego vehicle to the exit point. In the farthest zone there is no need to change lanes and the driver

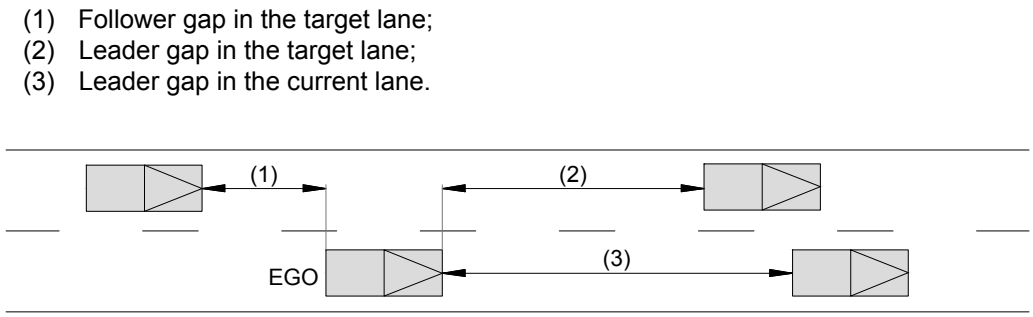

Figure 1.1: Lane change scenario

focuses on the desired speed. In the intermediate zone the driver concentrates on driving the vehicle to its final destination, ignoring the opportunities for speed gain. In the closest zone, the driver feels the need to drive the vehicle to its final destination, without any consideration of speed. The Gipps model, however, is based on some simplifications, including the presence of a sufficiently large gap to carry out the maneuver. This means that the model is not applicable in conditions of dense traffic, in which the mechanisms of forced merging and cooperative merging come into play.
Wiedemann and Reiter (1992) developed a lane changing decision model that considers the driver's perception of surrounding vehicles. The perception of the surrounding traffic is subjective, therefore in this model it is assumed that the drivers all have different characteristics. Wiedemann and Reiter assume that lane changes should occur following a speed gain. Therefore, they distinguish two different scenarios: lane change from the slowest to the fastest lane and vice versa. The lane change to the faster lane is due to the obstruction due to the presence of a slow vehicle. The obstruction is a function of the difference in speed between the front vehicle speed and the ego vehicle driver's desired speed the lane change occurs after a certain threshold is exceeded. The lane change to the slower lane takes place instead for the continuation of the path, to let the overtaking lane be free and allow a faster vehicle to pass.
Hidas (2002; 2005) developed a lane change model based on the courtesy of the follower vehicle in the target lane during the lane change maneuver. He also defined three different types of lane change: free, cooperative and forced lane change. In the first case, there are no variations in the gap between the leading vehicle and the follower in the destination lane during the maneuver, while in the second and third cases, yes. Forced lane change is based on the concept of the follower driver's courtesy: driver's ego vehicle sends courtesy request signals to the follower vehicle through the use of direction indicators. The follower vehicle's driver can decide whether to accept or reject the request: in case of acceptance, the follower vehicle's driver moderates the speed in order to create a large enough gap for the insertion of the ego vehicle. Cooperative lane change is the result of two decisions: the willingness of the follower vehicle's driver in the target lane to slow down and the feasibility to slow down. The maneuver is feasible if two conditions exist: the gap in the target lane is large enough for the ego vehicle to

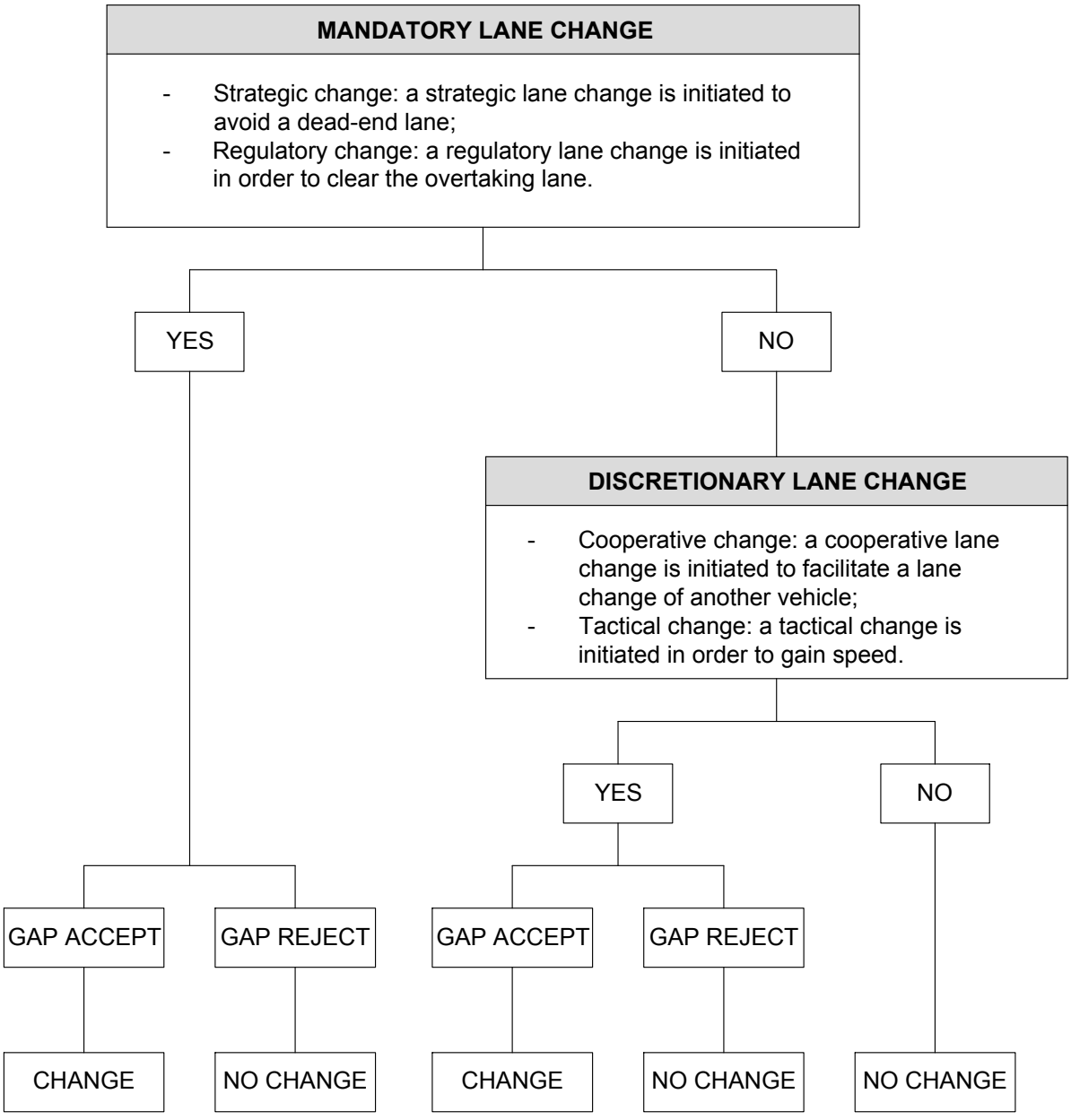

Figure 1.2: Generic structure of lane changing models

carry out the maneuver safely and the acceleration and deceleration components must be acceptable.
Krajzewicz's lane change model (2009) [20] is the model originally implemented within the SUMO software. The model considers three different lane change motivations called mandatory, tactical, cooperative lane change. Firstly, a valid route in the network is calculated, consisting of a set of links that allow the vehicle to reach its final destination. The lane change is carried out to continue within the valid route. Lane change occurs if the remaining distance is less than the distance required to make a lane change.

$$d_{lc}(t) = \begin{cases} v(t) \cdot t_1 + 2 \cdot l & \text{if } v(t) \leq v_{thres} \\ v(t) \cdot t_2 + 2 \cdot l & \text{if } v(t) > v_{thres} \end{cases}$$

Where:

- $v(t)$ is the current speed, in m/s;
- v_{thres} is the threshold speed, which discriminates between urban and highway environment, in m/s;
- t_1 and t_2 represent the time required to make a lane change maneuver, in s;
- l is the length of the vehicle, in m.

The method also considers the occupation of the target lane, so the situation of remaining in a dead-end lane due to a queque in the adjacent lane is avoided. Similar considerations are made in case of leaving the valid lane in order to overtake a slow vehicle: return to the valid lane must be possible within the remaining distance.
The lane change associated with the speed gain is associated with the benefit obtained.

$$b_{lc}(t) = \frac{v(t, \text{LC}) - v(t, \text{CL})}{v_{max}(\text{CL})} \tag{1.1}$$

Where $v(t, \text{LC})$ and $v(t, \text{CL})$ are the speeds in the adjacent lane and at the current lane. $v_{max}(t, \text{CL})$ is the maximum speed in the adjacent lane.
Using the benefit function, a memory variable is then created, whose numerical value represents the benefit associated with the lane change and whose sign represents the direction of the lane change. The maneuver is completed if the benefit exceeds a predetermined threshold.
When the lane change is not possible, the ego vehicle begins to interact with the other vehicle-drivers, accelerating or decelerating as appropriate.

$$v_{next}(t) = \begin{cases} v_{decel}(t) & \text{if blocking/blocked at own back and front} \\ v_{decel}(t) & \text{if blocking/blocked at own front} \\ v_{accel}(t) & \text{if blocking/blocked at own back} \end{cases}$$

Where $v_{accel}(t)$ and $v_{decel}(t)$ are the vehicle speed after accelerating or decelerating. Paragraph 1.2 describes the lane changing model currently implemented in SUMO, based on the described Krajzewicz model.

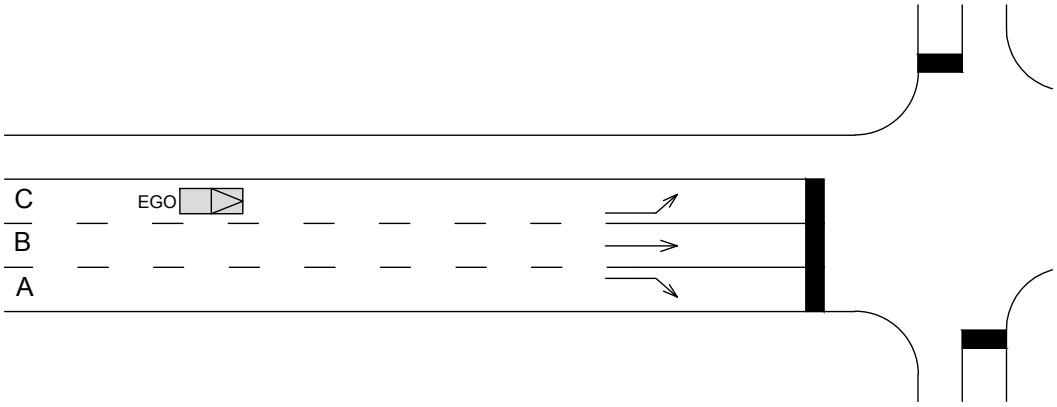

Figure 1.3: `bestLaneOffset` $= -2$ if the vehicle has to turn right

1.2 Overview of LC2013 Model

The LC2013 model is the default lane changing model implemented in SUMO. Based on the model by Krajzewicz described above, LC2013 was developed by Erdmann [12]. The lane changing model is a special case of the gap acceptance theory: the vehicle-driver, after making the decision to change lane, will have to accept, by carrying out the maneuver, a sufficient size gap to complete the maneuver in safety conditions. The paragraph describes the various reasons that lead the vehicle-driver to carry out the maneuver. Referring to Figure 1.2 the mandatory lane change is divided in strategic and regulatory, while the discretionary one is divided in cooperative and tactical.

1.2.1 Strategic Lane Change

A strategic lane change is initiated to avoid a dead-end lane. It is considered a mandatory lane change because it is necessary for the conclusion of the trip. Whenever a vehicle-driver is on a dead-end lane, it must change its lane to reach the next edge of its route. For example, the lane reserved for the right turn is considered a dead-end lane for those who wish to continue straight or turn left.
Vehicles have to choose the sequence of lanes to follow, taking into consideration that some of them are dead-end and that, if more lanes are possible, the choice must fall on the best one. Each vehicle, for each simulation step, has a numerical parameter, `bestLaneOffset`, which selects the possible lanes and takes into account the lane with the lowest traffic density.

$$\texttt{bestLaneOffset} \begin{cases} > 1 & \text{if the best lane is on the left} \\ = 0 & \text{if the current lane is the best lane} \\ < 1 & \text{if the best lane is on the right} \end{cases}$$

Referring to Figure 1.3, if the vehicle has to turn right, the lane A has a value of `bestLaneOffset` $= 0$, the lane B has a `bestLaneOffset` $= -1$ and the current lane has a `bestLaneOffset` $= -2$. This means that the sign is the direction in which to change lanes and the numerical value the number of lanes to change. It is important

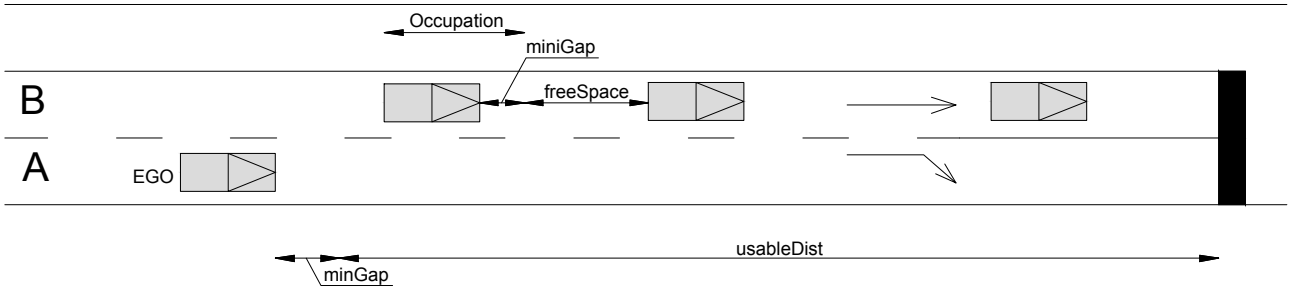

Figure 1.4: Urgent lane change, adapted from [29]

Table 1.1: SUMO parameters related to urgency for strategic lane-changing [8], [29]

Model parameters	Description
`myLookAheadSpeed`	Virtual speed used to calculate the ideal space needed to perform a lane change maneuver, in m/s. It increases proportionally as the speed of the ego vehicle increases.
`bestLaneOffset`	Indicates the number of lane changes required by the ego vehicle to reach an advisable lane, described above.
`miniGap`	Safe bumper-to-bumper vehicle distance in a jam, in m.
`laneOccupation`	The sum of the individual occupations of the vehicles in a line including their `minigap` downstream of the ego vehicle, in m.
`freeSpace`	The available free space on a lane downstream of the ego vehicle.
`usableDist`	The available distance between the vehicle and the dead-end line, in m.
`laDist`	The ideal longitudinal distance for the ego vehicle to execute a lane change manoeuvre.

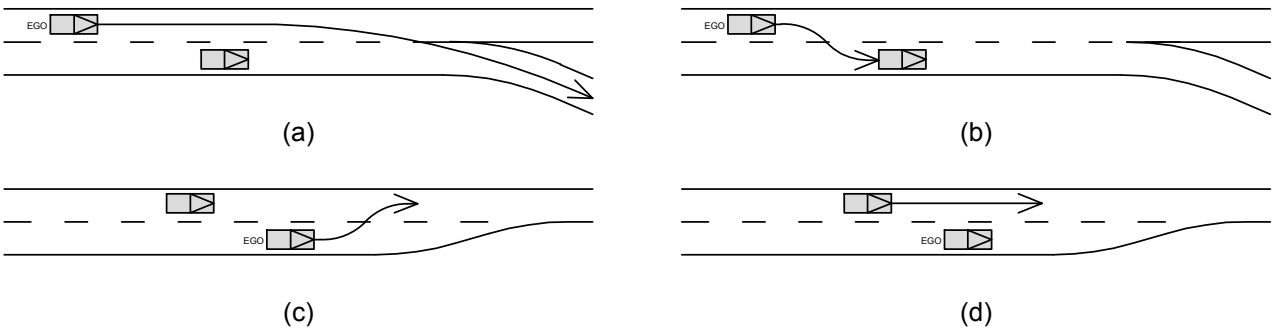

Figure 1.5: Speed adjustment to support lane change

to evaluate the urgency of the lane change. A vehicle may not be able to carry out the maneuver at the most appropriate moment, but doing it gradually closer to the dead-end line. Table 1.1 shows the parameters related to an urgent strategic lane change. Referring to Figure 1.4 a strategic lane change is defined urgent when the remaining distance is less than the distance needed to make a lane change, i.e. if the following inequality is true.

$$\texttt{usableDist} < \texttt{laDist}$$

$$d - \texttt{laneOccupation} < \texttt{lookAheadSpeed} \times |\texttt{bestLaneOffset}| \times f \qquad (1.2)$$

Whose parameters are already defined, except for d and f which represent the distance to the end of the lane and the time tipically needed to perform a successfull change maneuver respectively.
Two cases can be distinguished applied to a road consisting of two lanes in each direction.

1. In the first case, the left lane is empty. The ego vehicle will make the lane change when the relationship 1.2 is satisfied.

2. In the second case there are some vehicles in the left lane. The ego vehicle will make the lane change when the distance required to make a lane change is less than the sum of the spaces available downstream of the ego vehicle.

The two cases described take place thanks to the `laneOccupation` variable, by which the vehicle-drivers check the surrounding traffic to be sure that there are no deadlocks. If a lane change is not possible due to some vehicles that prevent the maneuver, the ego vehicle can adjust its speed to be able to carry out the lane change maneuver in the following phases. The speed adjustment is not exclusive to the ego vehicle, but also to the surrounding vehicles which can adjust their speed after observing the direction indicators of the ego vehicle. Since lane change is mandatory for the ego vehicle, it is assumed that it adopts all the necessary precautions to complete the maneuver. Figure 1.5 shows how different situations can be distinguished, which are solved by comparing the `plannedSpeed` variable with the speed of the leading vehicle.

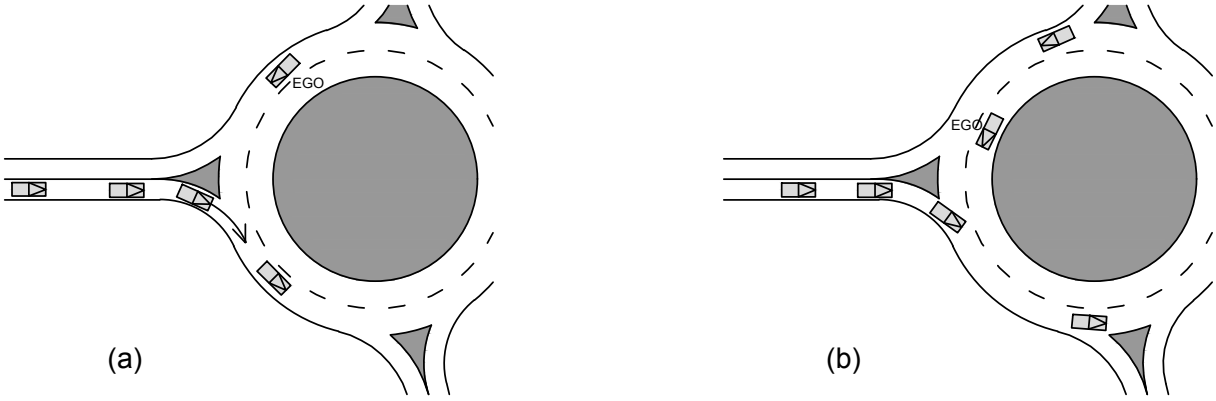

Figure 1.6: Cooperative lane change

(a) The ego vehicle is able of overtaking the leader. The leader must refrain from accelerating to allow the ego vehicle to complete the maneuver.

(b) The ego vehicle is unable of overtaking the leader. The ego vehicle will have to moderate its speed and position itself behind the leader.

(c) The ego vehicle is able of inserting itself before the follower. The follower will have to refrain from accelerating if the gap between the two vehicles is wide enough, or will have to moderate the speed to allow lane change if the gap is not wide enough.

(d) The ego vehicle is unable to insert itself before the follower. The follower will have to try to get past the ego vehicle quickly.

1.2.2 Cooperative Lane Change

In real situations, some vehicles decide to change lanes at the entry points to allow a vehicle to make a mandatory lane change. The ego vehicle is informed to be a blocking follower by observing the direction indicators of the vehicle being blocked. If there are no strategic reasons to stay in the current lane, the ego vehicle may change lanes to create a gap for the blocked vehicle. Figure 1.6 shows a multi-lane roundabout, an example of cooperative lane change in an urban scenario. Given the short distances involved, vehicles should be encouraged to use the outermost lane while traveling the ring. Some of them, however, move to the innermost lane to allow vehicles on subsequent approaches an easier entry. This behavior leads to an improvement in the performance of the roundabout. As shown in the Figure 1.6 (a) the ego vehicle proceeds in the outermost lane of the roundabout, but moves into the innermost lane (b) to allow a vehicle to enter the roundabout more easily.
The follower vehicle which cannot change lane to facilitate the lane change maneuver of the ego vehicle will have to moderate the speed to increase the probability that the ego vehicle will be able to carry out the maneuver in the subsequent simulation steps.

1.2.3 Tactical Lane Change

A tactical lane change is performed by the ego vehicle to overtake a blocking vehicle. This lane change occurs only to allow the ego vehicle to gain speed. Lane change must also be balanced with the need to keep the overtaking lane free as much as possible. Otherwise, slow moving vehicles with minor speed differences might significantly block traffic flow.
Each vehicle has a `speedGainProbability` variable which is updated at each simulation step and which represents the utility associated with the lane change. If the magnitude of this parameter exceeds a threshold value, a tactical lane change is desired: threshold value is represented by the parameter `speedGainProbabilityLeft` for the left lane, and `speedGainProbabilityRight` for the right one. Parameter `speedGainProbability` is calculated by normalizing the difference in speed between the expected ego vehicle speed in the case of lane change and the expected ego vehicle speed for remaining in current lane.

$$\texttt{speedGainProbability}_1 = \pm \left(\texttt{speedGainProbability}_0 + \frac{v-u}{v} \right) \tag{1.3}$$

Where:

- v is the speed in the adjacent lane;
- u is the speed in the current lane.

The sign of the variable indicates the direction of the lane change, > 1 if the maneuver must be to the right and < 1 otherwise. If a lane change succeed, the value is reset to 0. The numerical value is associated with the utility that derives from the lane change. The relationship between the SUMO parameters described in the paragraph 2.1 and the variables described above is explained below. `speedGainProbability` is divided by the parameter `lcSpeedGain`, as shown in the following Equation.

$$\text{threshold} = \frac{\texttt{speedGainProbability}}{\texttt{lcSpeedGain}} \tag{1.4}$$

The higher the value of `lcSpeedGain`, the lower the threshold above which a tactical lane change occurs.
Figures 1.7 shows tactical lane change behavior. (a) A slow vehicle precedes the ego vehicle in lane A, while lane B is free. (b) The `speedGainProbability` parameter increases until it exceeds the threshold value, at which time a tactical lane change is made by vehicle ego (c).

1.2.4 Regulatory Lane Change

Legislation provides using of the left lanes for overtaking. These lanes must be cleared once overtaking has been made and because of this the behavior described in this paragraph is mandatory. As regarding Figure 1.8, each vehicle, for each simulation step, has a numerical parameter called `keepRightProbability` which is decreased over time and leads to a lane change maneuver when a tolerance threshold is reached. The analyst can check the threshold value by acting on the `lcKeepRight` parameter, with the foresight to use negative values in parallel with the variable described. The Formula for

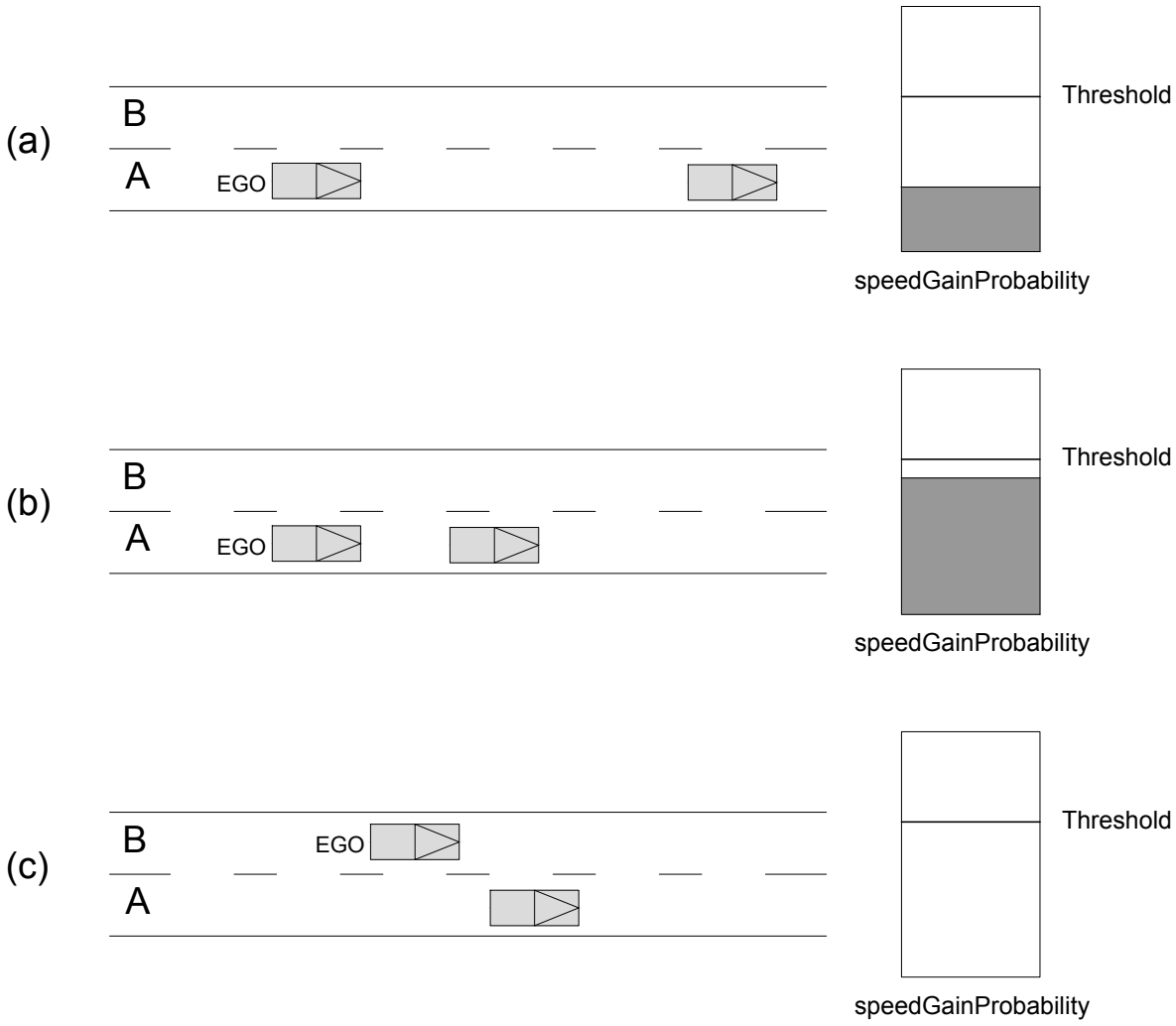

Figure 1.7: Tactical lane change, adapted from [29]

calculating the `keepRightProbability` parameter prevents fluctuations due to frequent lane changes due to continuous vehicle overruns. If a lane change succeed, the value is reset to 0.

$$\texttt{keepRightProbability}_1 = \texttt{keepRightProbability}_0 - \frac{t \cdot L}{V \cdot v \cdot T} \tag{1.5}$$

Where:

- t is the time to spend in the fast lane before making the next overtaking;
- L is the speed limit;
- V is the ego vehicle's maximum speed;
- v is the ego vehicle's current speed;
- T is a parameter, currently set at $T = 5$.

Figure 1.8 shows a situation which calls for regulatory lane changing, also called keep right lane changing. (a) The ego vehicle is overtaking a slow vehicle and the `keepRightProbability` value is low. (b) The ego vehicle is finishing overtaking the slow vehicle but the conditions are not yet in place to return to lane A; the value of `keepRightProbability` is close to the threshold. (c) The ego vehicle can move into lane A in a safe condition; the value of `keepRightProbability` is beyond the threshold. (d) The ego vehicle has returned to lane A and the value of `keepRightProbability` is set to 0.

1.2.5 Gap Acceptance Theory

The gap acceptance theory is based on the evaluation of the gaps available on the target lane. The vehicle-driver will choose to accept, by carrying out the maneuver, a gap of sufficient size to complete the maneuver in safety conditions. To better understand the application of the gap acceptance theory to the lane changing model, some fundamental quantities are defined.
Lag is defined as the residual part of a gap, or the time interval between the decision to make the lane change maneuver and the crossing of the first vehicle on the target lane. *Gap* is defined as the net time interval between the arrival of two subsequent vehicles. Very often the term *gap* is also used to indicate *lag*. *Critical gap* t_c is defined as the minimum gap considered acceptable by the driver to carry out the lane change maneuver in safe conditions. *Follow-up time* t_f is defined as the time interval between the instant in which a vehicle performs the lane change maneuver and the instant in which the maneuver itself is carried out by the following vehicle, in the hypothesis that the same gap is used by both vehicles. The quantities introduced are measured in s. There are several methods for estimating gap acceptance parameters [4]:

- Regression analysis between the number of users who accept a given range and the size of the range itself;
- Estimation of the distributions of t_f and t_c which occurs independently using a probabilistic approach.

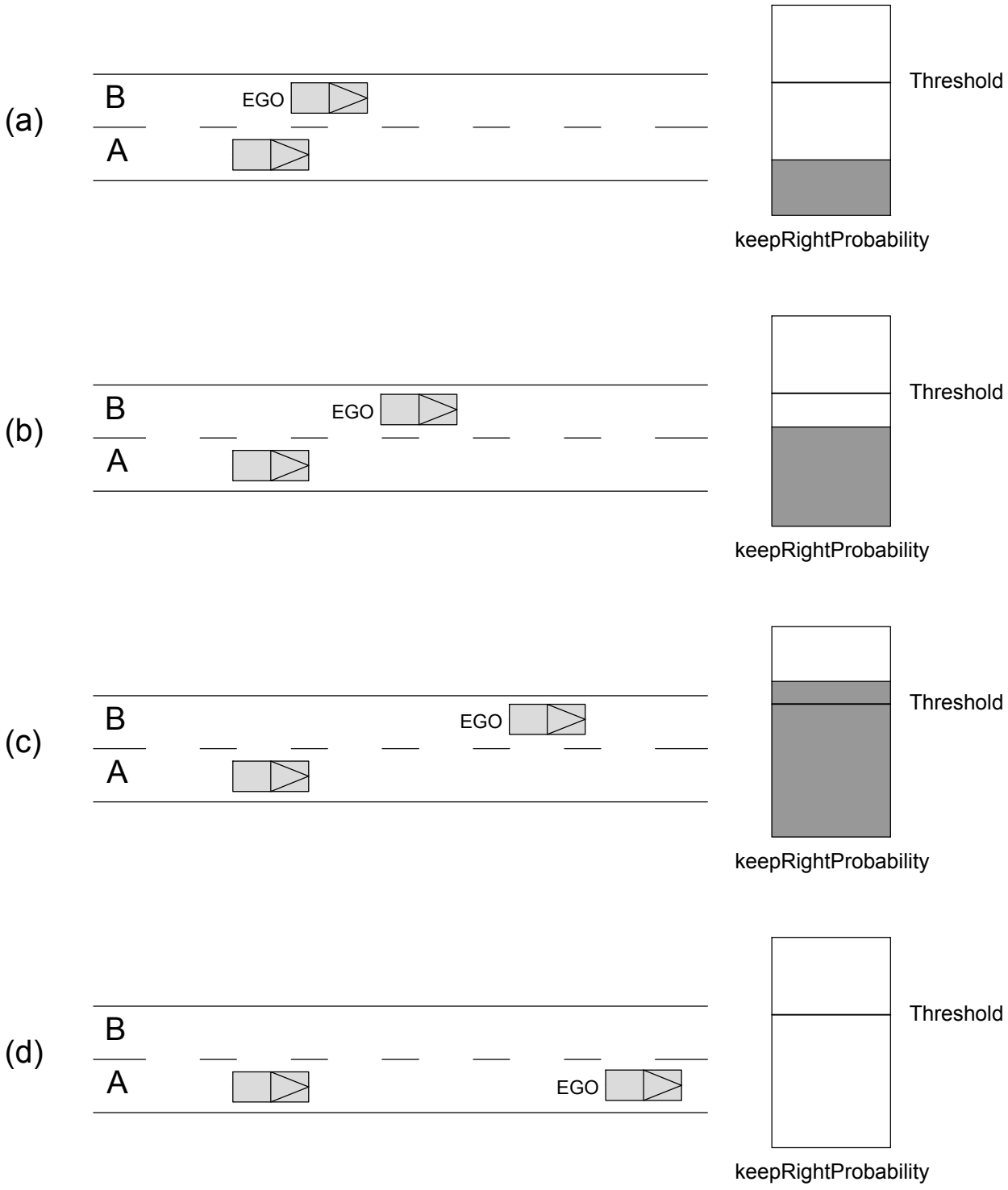

Figure 1.8: Regulatory lane change, adapted from [29]

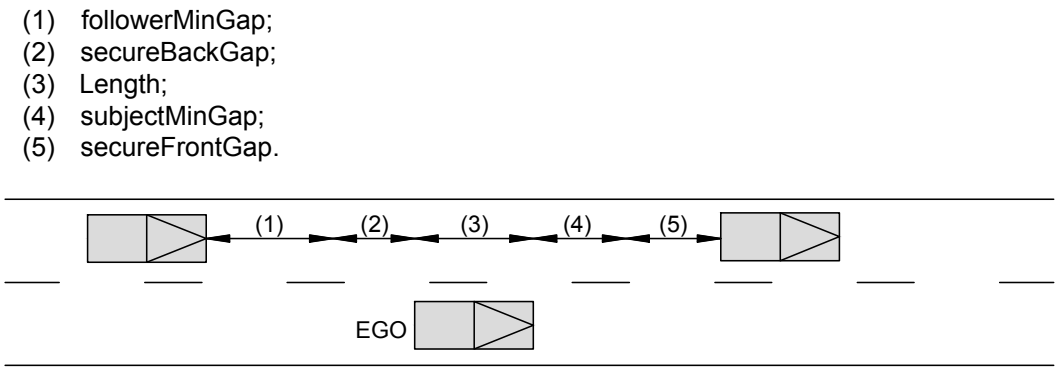

Figure 1.9: `requiredGap` parameter

It is possible to apply the gap acceptance theory in case of homogeneous drivers, with similar characteristics, and in the case of coherent drivers, i.e. those who accept gaps greater than all the gaps rejected.
The parameter through which the previously presented gap acceptance theory is inserted into SUMO is `lcAssertive`: the `requiredGap` is divided by its value. The `requiredGap` is an attribute calculated for each pair of vehicles for each simulation step and is given by the sum of different components, as described in the following Equation.

$$\begin{aligned}\texttt{requiredGap} = \texttt{secureBackGap} + \texttt{followerMinGap} + \texttt{length} + \\ + \texttt{subjectMinGap} + \texttt{secureFrontGap}\end{aligned} \tag{1.6}$$

Where `secureBackGap` and `secureFrontGap` are calculated according to the car following model, while the other parameters are defined within Figure 1.9.

$$g_c = \frac{\texttt{requiredGap}}{\texttt{lcAssertive}} \tag{1.7}$$

SUMO measures these parameters in m, so the name g_c is used here instead of t_c to name the critical gap. Critical gap g_c is then compared with the available gap in the target lane. The lane change maneuver is carried out if the available gap is greater than or at the same limit as the calculated critical gap. It is possible to notice how, by increasing the value of the `lcAssertive` parameter, the vehicle-driver will accept lower gap values, resulting in more aggressive driving behavior.

1.3 Overview of the Macroscopic Fundamental Diagram

The Macroscopic Fundamental Diagram (MFD) describes the relationship between accumulation and production in a large urban area. *Accumulation* and *production* are links' length weighted average respectively of the densities and of the flows. The evidence of the existence of MFD in a small network is thanks to Geroliminis and Daganzo

(2007) [14], [9]. The authors demonstrated that there is a relationship between the accumulation and the trip completion rate. The accumulation is defined as the number of vehicles within the network, while the trip completion rate is the rate at which vehicles leave the network. The authors demonstrated that accumulation is predictable independently of their O/D tables. The use of the MFD is an interesting result in terms of assessing the network's level of service and, consequently, planning traffic management interventions in real time. The MFD as introduced by Geroliminis and Daganzo exists under the hypothesis of homogeneity, i.e. with a level of demand that varies slowly over time and space and with the network formed by links of a similar type. The authors then showed the existence of MFD, under the hypotheses previously introduced, using real data from the city of Yokohama, the second largest city in Japan.
Ji et al. (2010) [18] removed the hypotheses previously introduced by Geroliminis and Daganzo to observe how the shape of the MFD changes as the demand for mobility and the type of link changes. The observations were made within the Amsterdam network, which consists of different types of roads: freeways, major urban roads and urban links. The authors observed a decrease in the level of flow due to inefficient use of the network following a rapid decrease in the demand for mobility.
Other factors affecting the shape of the MFD were summarized by Zhang et al. (2020) [48], and classified into four types: traffic factors, network settings, control settings, and route choice behaviors. It was also observed that the car is the mode of transport that most influences the shape of the MFD, with a greater dispersion of the values observed as the number of circulating vehicles increases. The capacity value is reached with lower levels of density in case of high turning traffic flow and of shorter length links. Finally, the authors observed a benefit due to signal coordination. The better the traffic light coordination is and the better the quality of circulation.
As regards the functional form, the authors agreed in defining three different states within the MFD, similar to what happens for the single link's fundamental diagram. Free flow condition occurs when there are few vehicles in the network and the flow is low. As the number of vehicles in circulation increases, the flow increases accordingly until a maximum value is reached. When the flow reaches its maximum value, the corresponding critical density value is the weak point of the network. Exceeded this value, as the number of vehicles in circulation increases, the drivers are delayed until reaching the jam state, in which the vehicles block each other and the flow decreases.
To construct the MFD it is necessary to calculate the average network flow Q, density K and speed V using the following equations proposed by Geroliminis and Daganzo [9].

$$K = \frac{\sum_{i=1}^{N} k_i \cdot l_i}{\sum_{i=1}^{N} l_i} \tag{1.8}$$

$$V = \frac{\sum_{i=1}^{N} q_i \cdot l_i}{\sum_{i=1}^{N} k_i \cdot l_i} \tag{1.9}$$

$$Q = K \cdot V = \frac{\sum_{i=1}^{N} k_i \cdot l_i}{\sum_{i=1}^{N} l_i} \tag{1.10}$$

Where:

- K, V, Q are the average network density (in veh/km), speed (in km/h) and flow (in veh/h);

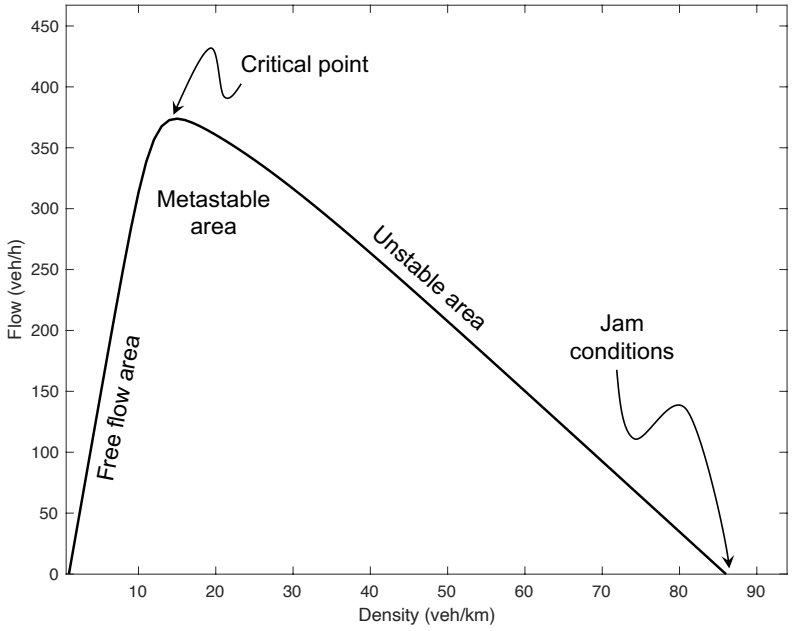

Figure 1.10: Traffic states in the Macroscopic Fundamental Diagram

- N is the total number of link i;
- l_i is the length of the single link i, in km;
- k_i, q_i are the density and flow on the single link i, in veh/km.

These formulas can be easily used in case of modeling with microsimulation software. They are difficult to use in the case of field measurements, since detectors uniformly distributed along all the links are required for their use. To overcome this problem, Geroliminis and Daganzo [9] used data from both fixed sensors and data from mobile sensors. The mobile sensors are represented by taxis that perform passenger service within the network.
Geroliminis and Daganzo [9] proposed a method to approximate the MFD called "method of cuts". Three families of equations were presented to allow the approximation of the MFD. Firstly the authors demonstrated how the MFD always stays below the limit functions; they then reported the formulas of the families of equations. These formulas derive from observations that are carried out near the most constraining intersections and involve the following parameters: free-flow speed, backward wave speed, optimal density, saturation flow, green time ratio and traffic light cycle time, distance between intersections and number of intersections. In empirical settings those values might not be identifiable as they are very hard to measure or to obtain.
Ambuhl et al. (2020) [2] proposed a mathematical formula of the MFD that contains easily obtainable parameters of physical significance plus a λ parameter that must be calibrated.

$$q(k) = -\lambda \cdot \ln\left[\exp\left(-\frac{u_f \cdot k}{\lambda}\right) + \exp\left(-\frac{Q}{\lambda}\right) + \exp\left(-\frac{(\kappa - k) \cdot w}{\lambda}\right)\right] \tag{1.11}$$

Where:

- u_f is the free flow speed, in km/h;
- k is the density, in veh/km;
- Q is the intersection capacity, in veh/h;
- κ is the jam density, in veh/km;
- w is the backward wave speed, in km/h;
- λ is a parameter.

The λ parameter has a double physical meaning. The first meaning represents the efficiency with which the network is used. Low values of λ increase the network capacity, i.e. lead to more efficient use of the network. The greater efficiency is attributed to less interference between vehicles. The second meaning of λ is obtained by observing its variation over time. Variation of λ can be used as a measure of intra and inter day heterogeneity. The proposed formula combines two different sources of information: the availability of field measurements and the possibility of estimating the required parameters. Based on this information, three different cases can occur.

1. In the first case both information are available. λ needs to be estimate, which has also a robust physical meaning. In this case, a value of λ between 0.03 and 0.07 is observed.

2. In the second case it is possible to estimate the required parameters, without having any field measurements. This may be the case in cities without traffic monitoring systems, where the necessary measurements can be obtained from historical data or with manual measurements. The authors indicate that this estimate gives less information than case 1 and is less accurate than case 3.

3. In the third case, only field measurements are available, without the possibility of estimating the required parameters. In this case the Equation 1.11 can be used for a conventional curve fitting. This approach shows the best fit to the data due to more degrees of freedom. However, the λ parameter loses its physical meaning.

The described MFD finds application in various fields of transport engineering, such as in road pricing measurements. Road pricing provides the payment of a fee to access an urban area, delimited by a fixed border. The rate can be fixed or dynamic, i.e. increasing as the level of congestion increases. In the second case, the historical MFD is compared with the real time data to decide which rate to apply for entry into the area. This kind of measurements are introduced to reduce the effect of congestion, environmental impacts and accidents within the area subject to the tariff.
The MFD can be used as a measure to compare the macroscopic performance of the network with varying microscopic characteristics. Ji et al. (2010) [18] suggested the use of the MFD to evaluate how the macroscopic characteristics of the network vary with the introduction of automated vehicles and connected vehicles, having different behaviors at a microscopic level compared to conventional vehicles.

Table 1.2: Surrogate Safety Measures

SSM	Unit of measure	Description
Time to collision (TTC)	s	Expected time for two vehicles to collide if they keep their current speed and path
Post encroachment time (PET)	s	Time lapse between end of encroachment of the ego vehicle and the time that the foe vehicle arrives at the potential point of collision
Deceleration rate to avoid collision (DRAC)	m/s^2	Deceleration rate for the follower vehicle to avoid collision

1.4 Overview of Surrogate Safety Measures

Surrogate Safety Measures (SSM) allow to indirectly assess the probability of an accident by studying the conflicts between vehicles. These measures are proximity indicators that can be used to identify conflicts between vehicles. Such conflicts occur more frequently than accidents and allow the analyst to approximate the probability of an accident: the higher the number of conflicts, the higher the probability of an accident. As shown in Table 1.2, the following measures are presented as SSM:

- Time to collision (TTC);
- Post encroachment time (PET);
- Deceleration rate to avoid collision (DRAC).

The SSM presented can be used to measure the severity of the conflict [15]. The values of TTC, PET and DRAC indicate the severity of the conflict event, which is related to the probability that a collision could result from a conflict.

- A lower TTC indicates a higher probability of a collision;
- A lower PET indicates a higher probability of a collision;
- A higher DRAC indicates a higher probability of a collision.

Research on traffic conflicts techniques has started in 1960s at General Motors in the USA. In 1967 General Motors published a study evaluating the basic causes of accidents near the intersections [36]. Within the study, conflict is defined as “discrete, observable events involving two or more road users, in which the action of one road user causes the other road user to make an evasive maneuver to avoid a collision”. A development of studies similar to those proposed by General Motors is observed between the 1980s and 1990s. The SSM proposed by the Federal Highway Administration (FHWA) [37] are currently being used. FHWA defines safety as “the expected number of crashes, by type, expected to occur at an entity in a certain period, per unit of time”. Authors define crash as “unintended collisions between two or more motor vehicles”, which excludes

single-vehicle crashes. FHWA also has a very similar definition of conflict as the one presented by General Motors. The conflict is an interaction between two vehicles that can lead to an accident (crash). It is necessary that the involved vehicles occupy the same space at the same instant time to have a conflict. The FHWA defines three different types of conflicts related to the angle at which vehicles approach the potential point of collision.

1. Rear end conflict. The situation occurs for vehicles that occupy the same lane and travel in the same direction. The conflict occurs when the first vehicle slows or changes direction and it places the following vehicle in danger of a rear end collision. The second vehicle brakes or swerves to avoid the collision, then continues to proceed through the intersection area.

2. Crossing conflict. The situation occurs within the intersections for vehicles traveling in different directions. The conflict occurs when a vehicle in the cross street turns or crosses into the path of a second vehicle on the main street who has the right of way and places the second vehicle in danger of collision. The second vehicle brakes or swerves to avoid the collision, then proceeds through the intersection area.

3. Lane change conflict. The situation occurs in roads composed by two or more lanes, when a vehicle decides to change lane. Conflict occurs when a vehicle performs a lane change maneuver, placing the vehicle in the adjacent lane in danger of collision. The vehicle in the adjacent lane brakes or swerves to avoid the collision, then proceeds through the intersection area.

The presented SSM can be collected by microsimulation software, together with information on vehicle acceleration, deceleration, position as a substitute for field studies. SUMO, the software used within this thesis, is able to generate the output concerning the SSM, in which the three different types of conflict can be recognized.
The SSM introduced at the beginning of the paragraph are presented below.

1.4.1 Time to Collision

Time to Collision (TTC) is the expected time for two vehicles to collide if they keep their current speed and path. The TTC value is defined for each time step during the encounter and it can assume values ranging from 0 to $+\infty$, where TTC$= 0$ indicates the occurrence of an accident. The minimum value of TTC recorded during the encounter is taken as an indicative value of the observed collision proximity.
There is a threshold value of TTC, called critical TTC, which is used to identify which of the encounters are conflicts. Users' danger perception is subjective and it can vary depending on numerous factors. Therefore, in the literature it is possible to observe different thresholds of critical TTC. In recent years, many researchers have looked for critical TTC values to be implemented as a warning parameter within the lane change warning system. Minderhoud et al. (2001) [28] and Wang et al. (2018) [43] published a review on the critical TTC and some of which are reported below. Olsen et al. (2002) [33] and Suzanne et al. (2004) [24] agree in split the collision urgency of lane change into four point scale.

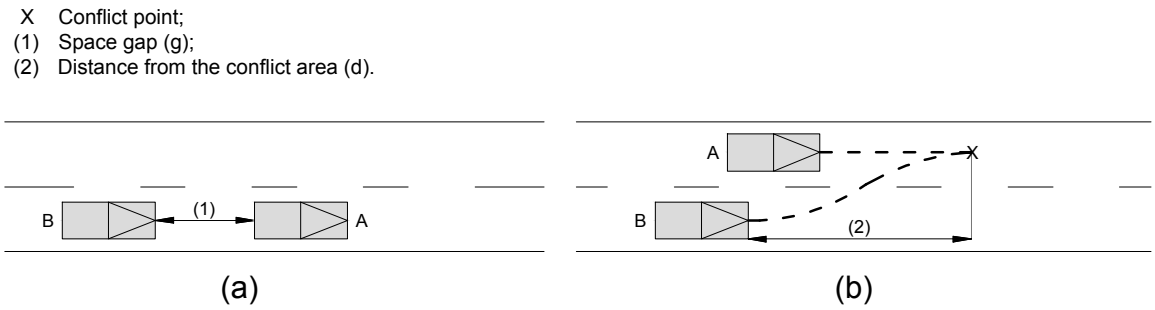

Figure 1.11: TTC in the event of (a) rear end and (b) crossing/lane change conflict

- Non urgent, when TTC > 5.0 s;
- Urgent, when $3.0 <$ TTC < 5.0 s;
- Forced, when TTC < 3.0 s;
- Collision.

Hirst and Graham (1997), using data from a field test, found that a TTC of 4.0 s can be used to distinguish between safe and unsafe lane change behavior. Authors also discovered that the found threshold can lead to false alarms. A subsequent study by Minderhoud (2001) shows how a TTC threshold value of 3.0 s leads to a decrease in the number of false alarms. Some studies provide variable TTC thresholds on the basis of the relative speed between the vehicle ego and a target vehicle in the adjacent lane. Other studies provide variable TTC thresholds on the basis of relative distance between the vehicle ego and a target vehicle in the adjacent lane. These critical values range between 2.5 s and 3.5 s. SUMO considers a critical TTC value equal to 3.0 s. From the values presented, it can be seen that there is no unique TTC threshold for identifying conflicts. More sophisticated probabilistic approaches are currently used for this purpose [34], [39].
TTC can be calculated in the case of a rear end conflict and in the case of a crossing/lane change conflict. Figure 1.11 (a) shows the case of rear end conflict. TTC is calculated when the follower vehicle is moving faster than the leader vehicle, i.e. when the likelihood of a conflict occurs. TTC is calculated by dividing the spatial gap between vehicles by the speed difference between vehicles.

$$TTC = \frac{g}{v_B - v_A} \tag{1.12}$$

Figure 1.11 (b) shows the case of crossing/lane change conflict. TTC is calculated only if the expected exit time from the conflict area of vehicle A is greater than the expected entry time from the conflict area of vehicle B.

$$TTC = \frac{d}{v_B} \tag{1.13}$$

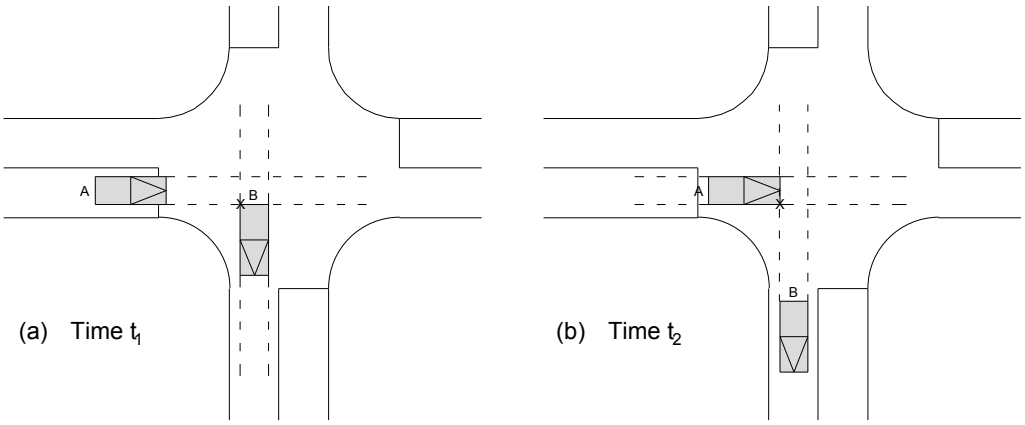

Figure 1.12: PET

1.4.2 Post Encroachment Time

Post Encroachment Time (PET) is the minimum post invasion time observed during the conflict, i.e. the time interval between the instant the first vehicle occupies a position and the instant the second vehicle arrives at the same position. During the encounter, a PET value is assigned to each time interval, which can assume values between 0 and $+\infty$, where PET= 0 indicates the occurrence of an accident. There is a threshold value of PET, called critical PET, which is used to identify which of the encounters are conflicts. SUMO considers a critical PET value equal to 2.0 s.
Referring to Figure 1.12, it is possible to calculate the PET value using the following equation.

$$PET = t_2 - t_1 \tag{1.14}$$

PET value is calculated for crossing conflicts only. If the vehicles occupy the same lane, no PET value is calculated.

1.4.3 Deceleration Rate to Avoid Collision

Deceleration Rate to Avoid Collision (DRAC) is the initial deceleration rate of the follower vehicle to avoid collision. DRAC is recorded as the instantaneous deceleration rate. If the follower vehicle reacts to the stimulus from the leader vehicle, DRAC is the deceleration value recorded during the encounter. If the follower vehicle does not react, DRAC is the smallest deceleration value recorded during the encounter. SUMO considers a critical DRAC value of $3m/s^2$.
DRAC can be calculated in the case of a rear end conflict and in the case of a crossing/lane change conflict. As for the TTC, Figure 1.11 shows (a) the case of rear end conflict, and (b) the case of crossing/lane change conflict. For the rear end conflict, DRAC is the deceleration rate for the vehicle B to avoid collision.

$$DRAC = \frac{1}{2} \cdot \frac{(v_B - v_A)^2}{g} \tag{1.15}$$

In the situation of crossing/lane change conflict, the DRAC is calculated only if the expected conflict area exit time for the vehicle A is larger than the conflict area entry

Table 1.3: Lane change model parameters by Lackey (2019) [23] and Kavas et al. (2021) [19]

Parameters	Conventional vehicles	Automated Vehicles		
		Level 2	Level 3	Level 4
`speedFactor`	1.0	normc(1, 0.1, 0.99, 1.01)	normc(1, 0.1, 0.98, 1.02)	normc(1, 0.1, 0.99, 1.1)
`lcStrategic`	1.0	1.2	1.6	3.0
`lcCooperative`	1.0	1.0	1.0	1.0
`lcSpeedGain`	1.0	1.2	1.6	5.0
`lcKeepRight`	1.0	2.0	1.8	1.2
`lcAssertive`	1.0	1.0	1.0	1.0
`lcOpposite`	1.0	0.23	1.0	1.0
`lcLookAheadLeft`	2.0	2.0	2.5	3.0
`lcSpeedGainRight`	0.1	0.1	0.1	0.1

time for the vehicle B.

$$DRAC = 2 \cdot \left(v_B - \frac{d_B}{t_A} \right) \cdot \frac{1}{t_A} \tag{1.16}$$

Where t_A is the expected conflict area exit time for the vehicle A, and d_B is the distance between the conflict point and the vehicle B.

1.5 Related Works

In the literature, the modeling of automated vehicles has become increasingly important in order to study their impact on mobility. This paragraph will present some works with this objective, with particular attention to the parameters used for modeling within SUMO, the microsimulation software presented in paragraph 2.1.
The UK Department of Transport has developed an automated vehicles modelling within the Vissim software [38]. The objective of Lackey (2019) [23] and Kavas et al. (2021) [19] was to adapt this automated vehicles modeling to the SUMO software. Authors then evaluated the interaction between automated vehicles and conventional vehicles and how average speeds, travel duration and time loss vary as the level of autonomy increases. Table 1.3 shows the parameters of the SUMO lane change model used. The parameters are different according to the different level of autonomy of the vehicles. As reported in the Table, it is possible to see how automated vehicles have been modeled to have more frequent lane change maneuver as the level of automation increase. A strategic lane change occurs in advance for level 4 automated vehicles. They are able to plan lane changes more and more in advance of the dead end point than lower level vehicles. At the same time, the desire to gain speed also increases as the level of autonomy increases. A level 4 automated vehicle will be more likely to overtake a slow vehicle than a lower level automated vehicle. A low variability of vehicle speeds can also be noted as automated vehicles are more likely to travel at the set speed limit, with little variation. Authors also reported non-modified parameters with respect to

the default values as they are considered to be relevant for the lane change behavior.
The parameterized model was applied in different situations, each of which foresees 40 simulative runs. The work was divided into two parts. In the first part, each simulation run contains a share of vehicles of the same level of autonomy and the remaining part of conventional vehicles. In the second part, automated vehicles of different levels of autonomy and conventional vehicles are made to travel simultaneously. The used maps make it possible to evaluate lane changes in different contexts: urban context, where most of the interactions take place near intersections; motorway; freeway with frequent lane changes inside it due to merge in and merge out ramps.
The first part of the work uses all three maps. The simulation was divided into four parts according to the type of vehicle, each of which is characterized by 10 simulation runs:

- "Solution 0": 100% of conventional vehicles;
- 97.9% of conventional vehicles and 2.1% level 2 automated vehicles;
- 98.5% of conventional vehicles and 1.5% level 3 automated vehicles;
- 96.6% of conventional vehicles and 3.4% level 4 automated vehicles.

For each map the values of average speed, average trip duration and time loss were compared with the "solution 0". Authors note how automated vehicles bring benefits to overall mobility. Including automated vehicles, the more the level of autonomy increases, the more the average speed increases. Similarly, the more the level of autonomy increases, the more trip duration and time loss decrease.
In the second part of the work, only the freeway was used in the simultaneous presence of vehicles with different levels of autonomy and conventional vehicles. The penetration rate of automated vehicles circulating in this case is 26.5%, divided by the different levels of automation. In this case, lower speeds were observed than in the case of the same level of autonomy, but higher than in the case of conventional vehicles only. Authors made the same consideration as regards the values of average trip duration and time loss, with a worsening compared to the case of homogeneous level of autonomy, and with an improvement compared to the case of conventional vehicles only.
In any case, the authors noted benefits on global mobility following the inclusion of automated vehicles in traffic. However, it should be noted that the maximum percentage of automated vehicles circulating in traffic is equal to 26.5%.
Mintsis et al. (2019) [29] modelled and calibrated the car following and lane change models implemented in SUMO for both automated and conventional vehicles. With reference to the lane change model only, a sensitivity analysis was carried out on four SUMO's parameters: `lcStrategic`, `lcKeepRight`, `lcSpeedGain` and `lcAssertive`. The following output were considered as relevant:

- Safe longitudinal gap to leading vehicle in the ego lane;
- Safe longitudinal gap to leading vehicle in the target lane;
- Safe longitudinal gap to following vehicle in the target lane.

Table 1.4: Lane change model parameters by Mintsis et al. (2019) [29]

Parameter	Conventional Vehicles	Automated Vehicles		
		Conservative behaviour	Moderate behaviour	Aggressive behaviour
`lcAssertive`	1.3	normc(0.5, 0.1, 0.5, 0.6)	normc(0.7, 0.1, 0.6, 0.8)	normc(0.9, 0.1, 0.8, 1.0)

From the sensitivity analysis conducted it emerges that the `lcStrategic` parameter has a limited influence on the output. The parameters `lcKeepRight` and `lcSpeedGain` affect the safe longitudinal gap between the leading vehicle in the target lane and ego vehicle and the gap to leading vehicle on the target lane, respectively. The parameter that affects all outputs is `lcAssertive`. Therefore, only this parameter was explicitly modified for the parameterization of the lane change model, while all other values were left by default.
Assuming that different car manufaturers design different automated vehicles, the behavior of lane change varies according to the vehicle considered. Data from the Hyundai Motor Europe Technical Center were used in the study for the calibration of the `lcAssertive` parameter. Based on the behavior of the test vehicles, the OEM provided gap data accepted by the automated vehicle for two distinct speed ranges: from 0 to 30 km/h and from 30 to 60 km/h. It has been observed that, as the speed increases, the accepted gap grows linearly. Furthermore, a distinction was made between different behaviors: aggressive, moderate and conservative. High values of `lcAssertive` indicate a more aggressive behavior as the vehicle-driver will find itself accepting gradually smaller gaps, while low values of `lcAssertive` indicate a more conservative behavior. Furthermore, it was observed that higher gap values have a positive effect on safety but a negative effect on traffic flow. Table 1.4 shows the values of the `lcAssertive` parameter for both automated and conventional vehicles. The value for modeling conventional vehicles derives from the experience gained by DLR, the Institute of Transportation System at German Aerospace Center.
The parameterized model was applied in eight different scenarios, with different simulation runs that provided simultaneous presence of automated and conventional vehicles for different penetration rates. In some simulations heavy vehicles were included. Final considerations were made in relation to the following SUMO outputs: travel time, mean speed for selected cross section, mean flow for selected cross section, vehicle trajectory, number of lane changes, CO_2 emissions.
Regarding the lane change behavior, it was noted that automated vehicles have a more prudent behavior than conventional vehicles. Since the scenarios considered are limited in scope, no particular relationships could be observed between the different lane change behavior of the vehicles and traffic efficiency.
Mintsis et al. (2019) [29] work, co-financed by the European Union, is taken as a reference by many other publications both in terms of the methodology used and in terms of the values of the calibrated parameters.

Lu et al. (2020) [25] investigated the impact of automated vehicles on the capacity of an urban network through the use of the MFD. Two different scenarios were modeled within the SUMO microsimulation software: a virtual grid network and a real-world road system in Budapest. The virtual grid was built to simulate a network with characteristics similar to the American urban centers, while the Budapest network was used as an application of the theoretical foundations in a real case. Authors decided to evaluate the impact of automated vehicles on the capacity of the networks presented by increasing their penetration rate by 10% at each subsequent configuration.
Automated vehicles were modeled using the previously described Lackey and Kavas parameters, while conventional vehicles were modeled using SUMO's default parameters. The demand was loaded into the network through the use of an O/D matrix, while the choice of the path was left to the software. To view all states of outflow, from the free flow conditions to jam, the demand was increased linearly with increasing time. Once the state of network congestion is reached, the demand is decreased linearly.
The MFDs were built starting from the Equation 1.8, 1.9 and 1.10, while the polynomial type was adopted as functional form for the representation of the MFDs. The output data considered are edge-based, i.e. density, flows and average speeds of a single link. The MFD was obtained by interpolating the SUMO output data through a polynomial. The authors reported the MFDs relating to the situation of 0% and 100% of automated vehicles in circulation, and the results of capacity and critical density for each penetration rate. The authors observed an increase in the capacity of the entire network equal to 16% compared to the situation of only automated vehicles in circulation, with a linear increase in capacity as the penetration rate increases. This benefit was due to shorter headway and less reaction time of automated vehicle. Benefits, even though minor, were obtained even with low percentages of automated vehicles in circulation. An increase in network capacity was already achieved with a penetration rate of 40%. Benefits were also observed as regards the critical density, with an increase of 48% of its value compared to the case of automated vehicles only in circulation.
Nippold et al. [31] evaluated the effects of automated vehicles in interrupted flow conditions. Therefore, the urban network of Dusseldorf was modeled within SUMO, with particular attention to the correct modeling of signal-controlled intersections. In the second part of the work, the authors investigated the effects of automated vehicles within a portion of the freeway to see their effect in the case of uninterrupted flow. The results were based on the penetration rate of automated vehicles, which ranges from 0% to 100%, with an increase of 10% for each scenario. The initial scenario was provided by the presence of only conventional vehicles, while the final scenario provided for the exclusive presence of automated vehicles. The authors evaluated how the capacity at intersections and the flows in the freeway vary as the penetration rate of automated vehicles increases.
The default parameters value of the SUMO software were adopted for modeling conventional vehicles, while adapted parameters were used for modeling automated vehicles. The authors decided to explicitly modify the acceleration and deceleration parameters of the vehicles and parameters related to the car following model, without modifying any parameters related to the lane change model.
As for the traffic light intersections, the authors observed a decrease in the capacity of the intersection as the penetration rate of automated vehicles increases. A 10% decrease

Table 1.5: Lane change model parameters by Berrazouane (2019) [6]

Parameters	Original SUMO value	Conventional Vehicles
`speedFactor`	1.0	1.193
`speedDev`	0.1	0.091
`lcSpeedGain`	1.0	0.887
`lcKeepRight`	1.0	0.835
`lcAssertive`	1.0	1.616

in capacity was observed compared to the case of conventional vehicles only.
Berrazouane et al. (2019) [6] aim was to compare traffic characteristics by analyzing different scenarios. Two scenarios required the existence of homogeneous traffic, consisting of only conventional vehicles or only automated vehicles, while the remaining scenarios required conventional vehicles and automated vehicles to coexist in different percentages. As regards the calibration of the lane change model for conventional vehicles, direct measurements from an Austrian motorway were used. Flows, speeds, occupancy, net time gaps and vehicle travel time between two consecutive motorway sections were detected.
To calibrate the model parameters, a sensitivity analysis was carried out to understand which parameters influence the lane change behavior the most. It has been observed that the `lcAssertive` parameter influences its behavior more, with less contribution from the `lcSpeedGain` parameter. The calibration was then performed on the travel time value using the root mean square as measure of proximity, a procedure repeated at each iteration until convergence. Table 1.5 shows the values of the parameters of the lane change model referring to the behavior of conventional vehicles.
Regarding the modeling of automated vehicles, the authors used the calibrated values from Mintsis et al.
The results were based on the automated vehicles' penetration rate, which go from 0%, existence of conventional vehicles only, to 100%, presence of automated vehicles only, with an increase rate of 10% for every scenario. Having built the fundamental flow-density diagram for each scenario, authors noted that automated vehicles have a more conservative behavior than conventional vehicles. In fact, the results show a deterioration in terms of maximum flow as the number of automated vehicles on the road increases. This result, which seems to contradict what the literature states, is due to the different modelling methodology for automated vehicles and the use of an ad hoc calibration for conventional vehicles. These considerations are valid in the motorway scenario investigated by Berrazouane.
Andreotti et al. (2021) [3] published a study on the impacts that automated vehicles will have on urban mobility. In order to do that, they used real traffic data of Gothenburg city and they insert an increasing percentage of automated vehicles on the road using a microsimulation software. SUMO was chosen as microsimulation software, in which authors modified various car following and lane change parameters to model different behaviors of automated and conventional vehicles. Authors used the parameters

available in the literature to model the different types of vehicles. Automated vehicles have been modeled to have a shorter reaction time and faster speed than conventional vehicles. Authors investigated the effects of the introduction of automated vehicles in three different outputs: fundamental diagrams, number of lane changes, number of conflicts.
As for the fundamental diagrams, the authors noted an improvement in the efficiency of traffic flow, as vehicles drive faster on average as the penetration rate of automated vehicles increase. Within the study, the authors considered the number of lane changes carried out as a measure of dissatisfaction in free flow condition. In fact, being able to change lanes means having the ability to reach the desired speed, something that only uncongested traffic states could allow. Authors noted a greater number of lane changes performed by automated vehicles as the penetration rate increases, due to a significantly higher `lcStrategic` value for automated vehicles than conventional vehicles. As for conflicts, 1% of vehicles were equipped with an SSM device. The thresholds considered for recording the conflict were the same as suggested by SUMO, i.e. TTC lower than 3.0 s, PET lower than 2.0 s and DRAC greater than 3.0 m/s^2. Authors identified `lcStrategic` as the parameter that most influences the number of conflicts, therefore they made evaluations in two different cases: constant parameter and parameter that distributes according to normal distribution. In the first case they observed a decrease in the number of conflicts and a better interaction between automated and conventional vehicles in case of low values of the parameter. In the second case, no significant differences are observed in the number of conflicts only for high penetration rates of automated vehicles.
Authors concluded that, while the introduction of automated vehicles within the urban traffic flow leads to an improvement in traffic efficiency, their introduction also leads to an increase in conflicts between vehicles. A final consideration was made regarding the parameters: the parameter that most affects traffic efficiency is `tau`, while the one that most affects security is `lcStrategic`.

1.6 Aim of the Study

Some considerations can be made from the analysis of the available literature. Few publications focus on the impacts of automated vehicles within an urban scenario and, among these, no publication investigates the variation of the flow characteristics by analyzing the automated vehicles' lane change behavior. In other words, there are no available publications that link the variation of the behavior of lane change with the variation of the characteristics of the outflow.
The aim of this study is to close this gap. From the parameters found in the literature, different lane change behaviors of both automated and conventional vehicles are modelled. These vehicles will then be placed in a real-world urban scenario, a portion of the network Hannover city. The results of the study will be shown in terms of system efficiency and safety. The results will be based on the penetration rate of automated vehicles, which ranges from 0% to 100%, with 10% progressive increment for each scenario.

Chapter 2

Methodology

2.1 SUMO Software

Investigating the effects of automated vehicles on the system performance in urban areas would involve carrying out field measurements but, given the low number of such vehicles in circulation, a simulation model is used. Simulation models are widely used in literature as a substitute or when field tests are difficult to implement. Furthermore, the use of a simulation model is very often chosen as it is considered less expensive and faster than field implementation and testing.
There are three types of simulation models, which differ according to the level of detail they represent the transport system with:

- Macroscopic models: average vehicle dynamics like traffic density are simulated;
- Microscopic models: each vehicle and its dynamics are modeled individually;
- Mesoscopic models: a mixture of macroscopic and microscopic model.

The advantage of macroscopic models lies in the speed of execution, while microscopic models lies in precision. For the purposes of the thesis, we will focus on microscopic simulation models.
Various simulation software are available to support model makers for research purposes. Many of these software are commercial, i.e. available by purchasing a license, such as Vissim and Paramics. Other software are open source, i.e. freely available on the internet, such as MATSim and SUMO. The latter was used within this thesis.
SUMO (Simulation of Urban Mobility) is an open source software developed by the Institute of Transportation Systems at German Aerospace Center (DLR in German) [1]. It is one of the most widely used microsimulation software in the research community, with more than one hundred scientific papers referring to it.
In order to correctly simulate the traffic, the software requires the following items. These three elements form a simulation scenario.

- Network data, i.e. data relating to the links and nodes that make up the road network, including signs and traffic lights;
- Vehicles data, i.e. behavioral data of vehicles in circulation;

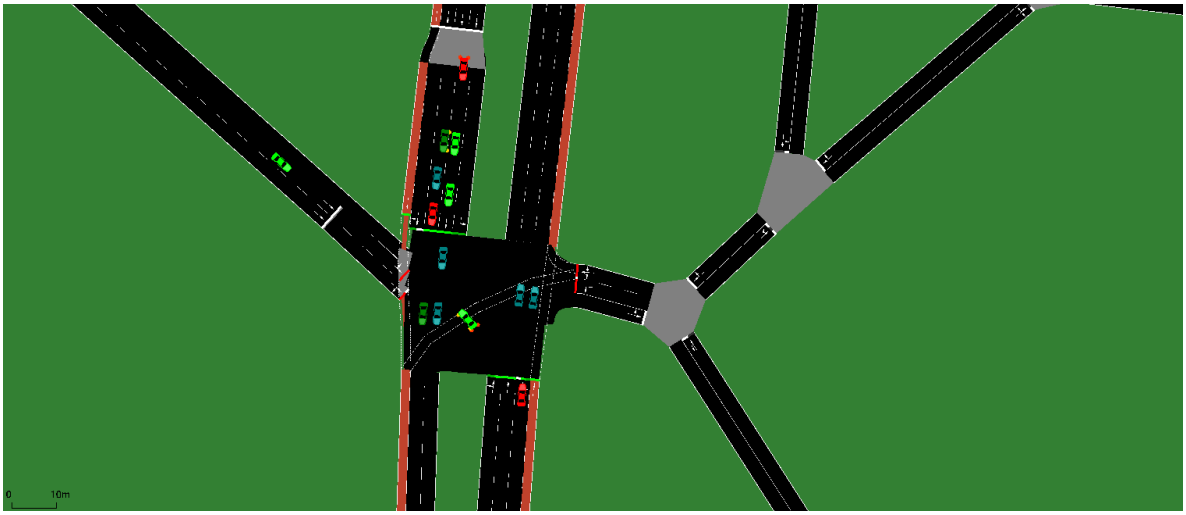

Figure 2.1: Screenshot of SUMO traffic simulator

- Traffic demand, or the quantity of vehicles circulating over time.

SUMO network is made up of nodes and edges. The edges are unidirectional links that connect two different nodes. Each link can represent a road, a cycle path, a pedestrian path, a public transport line etc. Characteristics, such as speed limits, widths, types of vehicles allowed are assigned to the road type links. Links with common characteristics can be grouped within categories. Each node can represent a road intersection, a stop of the public transport lines, or it can represent a fictitious point that separates two links with different charateristics. Regarding an intersection, information about allowed and prohibited maneuvers are assigned to the node. In the case of a signalized intersection it is necessary to provide the software with the traffic lights. The network can be generated from OpenStreetMap and converted into a file readable by SUMO using the Netconvert tool. In case of discrepancies with the real network, the resulting network can be further modified by hand through the use of Netedit.
SUMO allows the definition of different types of vehicles, by modifying numerous parameters for each vehicle type. The parameters are attributes of `vType` and are described in the Table 2.1, with particular reference to the lane change parameters. It is possible to notice how the parameters affect both the performance of the vehicles and the behavior of the drivers. For this reason, the term *vehicle-driver combination* is used in the literature. The software, upon insertion of a vehicle into the network, randomly assigns the characteristics of the vehicle. A vehicle type distribution can also be defined, which allows the modeler to generate a vehicle of a given type while respecting the probability distribution.
The SUMO demand can be generated via trips, flows and routes. The first type involves defining each individual movement by specifying the time of departure, the beginning and end link of the trip and any intermediate links. The second type involves defining a set of flows for a given source and destination node. The last type provides for the explicit definition of the path that must be followed. For each type it is possible to define the vehicle type explicitly or leaving the choice to SUMO, as described above. The choice of the route, where possible, can be done through different assignment models:

Table 2.1: SUMO parameters [8]

Parameters	Default value	Description
`id`		Name of the vehicle type
`accel`	2.6 m/s^2	The acceleration ability of the vehicles of this type (in m/s^2)
`decel`	4.5 m/s^2	The deceleration ability of the vehicles of this type (in m/s^2)
`length`	5.0 m	The length of the vehicles of this type (in m)
`minGap`	2.5 m	Empty space after leader vehicle in a jam (in m)
`maxSpeed`	55.55 m/s	The maximum speed of the vehicles of this type (in m/s)
`speedFactor`	1.0	The multiplying factor of the maximum speed
`lcStrategic`	1.0, range $]0, +\infty]$	Eagerness for performing strategic lane changes, with higher values resulting in earlier lane-changing actions
`lcCooperative`	1.0, range $]0, +\infty]$	Willingness to perform cooperative lane changes, with low values indicating reduced cooperation
`lcSpeedGain`	1.0, range $]0, +\infty]$	Eagerness to make lane changes with the sole purpose of gaining speed, with high values indicating a greater predisposition to lane change
`lcKeepRight`	1.0, range $]0, +\infty]$	Eagerness for following the obligation to keep right, with higher values resulting in earlier lane-changing actions
`lcAssertive`	1.0, range $]0, +\infty]$	Willingness to accept reduced front and rear gaps on the destination lane
`lcOpposite`	1.0, range $]0, +\infty]$	Desire to overtake using the oncoming lane, with higher values resulting in more lane-changing actions
`lcLookAheadLeft`	2.0, range $]0, +\infty]$	Probability of overtaking on the right in a carriageway with multiple lanes in each direction, with higher values resulting in more lane-changing actions
`lcSpeedGainRight`	0.1, range $]0, +\infty]$	Look ahead distance in vehicle's left lane to determine when to change lanes

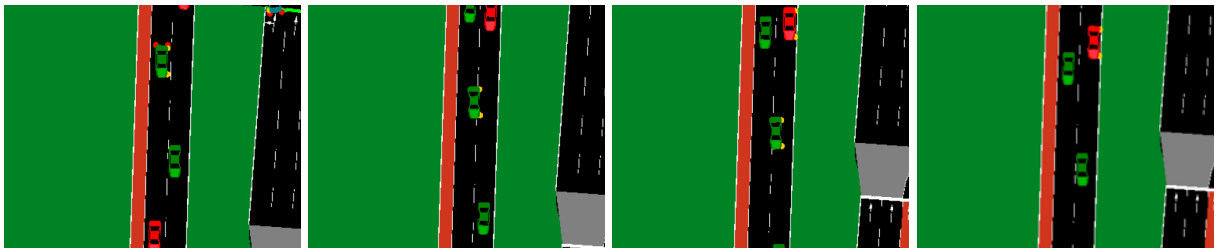

Figure 2.2: Screenshot of continuous lane changing

user equilibrium, stochastic user equilibrium or the fastest route at a given departure time.
Once all the necessary inputs have been defined, it is possible to start the simulation. As shown in Figure 2.1, the software allows the visualization of vehicles and their movements within the network, allowing the modeler to identify abnormal vehicle behavior. SUMO allows two different views of the lane changing model: discrete and continuous lane changing. Discrete lane changing occurs when a vehicle, during the lane change maneuver, instantaneously disappears from the former lane to appear on the desired lane. This leads to an untrue representation of the real behavior of the vehicles. To solve the problem, a continuous lane changing approach has been implemented which allows to animate the translation between one lane and the adjacent lane, as shown in Figure 2.2. This translation movement is linear and performed in one second.
To evaluate the simulation from a quantitative point of view, SUMO allows to generate numerous outputs, which can be divided as follows:

- Traffic data collected from modeled detectors;
- Traffic data collected from the single vehicle, such as lane change, surrogate safety measures, emissions, etc;
- Traffic data aggregated over edges (edge-based output);
- Traffic data aggregated over the whole trip of a vehicle.

These output files can then be analyzed using third parts applications, such as Python or Matlab, or tools provided by SUMO developers.

2.2 Network Setup

The network is part of the road system in the Vahrenwald-List neighborhood of the Hannover city, the capital of the Land Niedersachsen in Germany. The neighborhood is located northeast of the center of Hannover and is made up of the districts Vahrenwald, which occupies the west part, and List, which occupies the east part. With 71,173 inhabitants, the Vahrenwald-List neighborhood is the most populous district of Hannover [45].
The Vahrenwald district is crossed by the Vahrenwalder Straße, one of the largest traffic

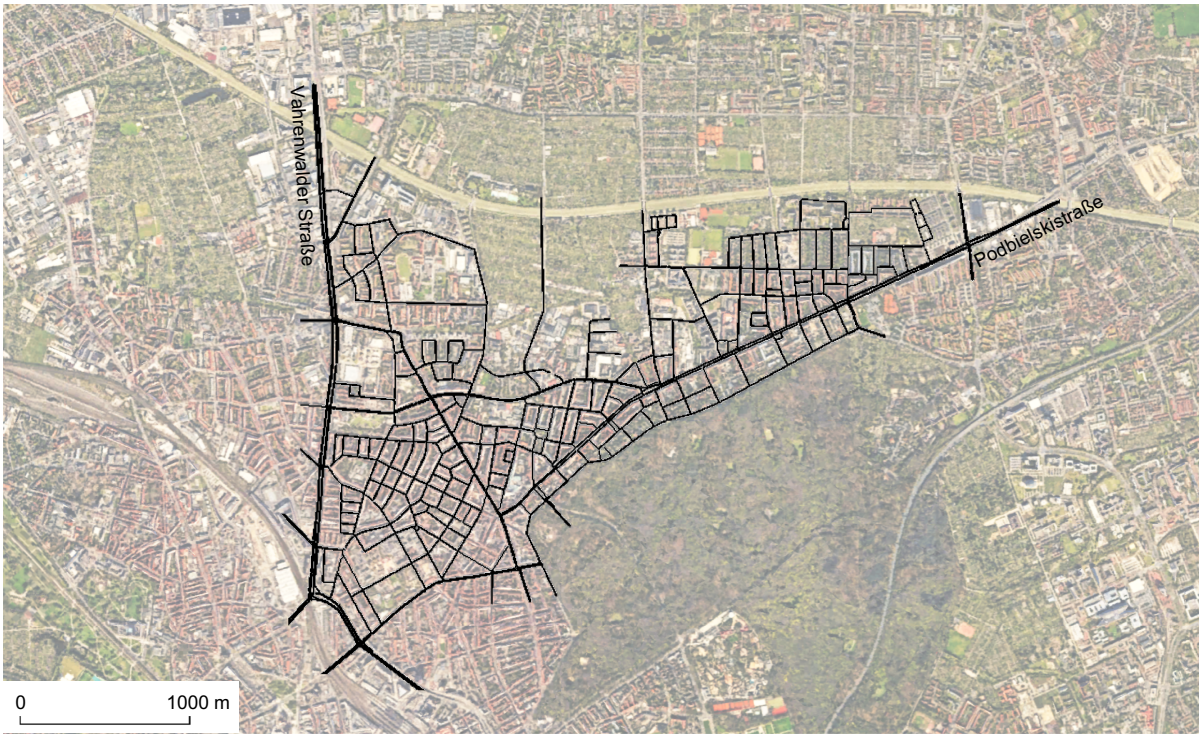

Figure 2.3: Real world Hannover Vahrenwald-List traffic network

Table 2.2: SUMO network charateristics

Description	Value
Area	5.88 km^2
Total length of the links	117.45 km
Number of signalized intersections	46

axes in the city of Hannover. It is a street made up of two to three lanes in each direction with a limit of 50 km/h. This street acts as a link between the city center and the A2 motorway. The Continental and ContiTech companies, respectively manufacturers of tires, plastic and rubber products, face this road.
The List district is crossed by Podbielskistraße, another major street with a speed limit of 50 km/h formed for most of its development by two lanes in each direction. It connects the city center with the neighborhoods located in the northeast area.
The streets Hamburger Allee, Celler Straße, Wedekindstraße and Bodekerstraße, located to the south, connect the two main arteries first mentioned.
There are also two other main streets within the district, Lister Kirchweg, Ferdinand-Wallbrecht-Straße and Niedersachsenring. These are roads with a speed limit of 50 km/h and one lane in each direction. Near the intersections they have specialized lanes for turns. The minor roads are local arteries with a speed limit of 50 km/h and one lane in each direction. Local roads with a speed limit of 30 km/h may also be encountered.
Figure 2.3 shows the network schematized in SUMO and superimposed on a satellite image of the Vahrenwald-List neighborhood, while Figure 2.4 shows the number of lanes

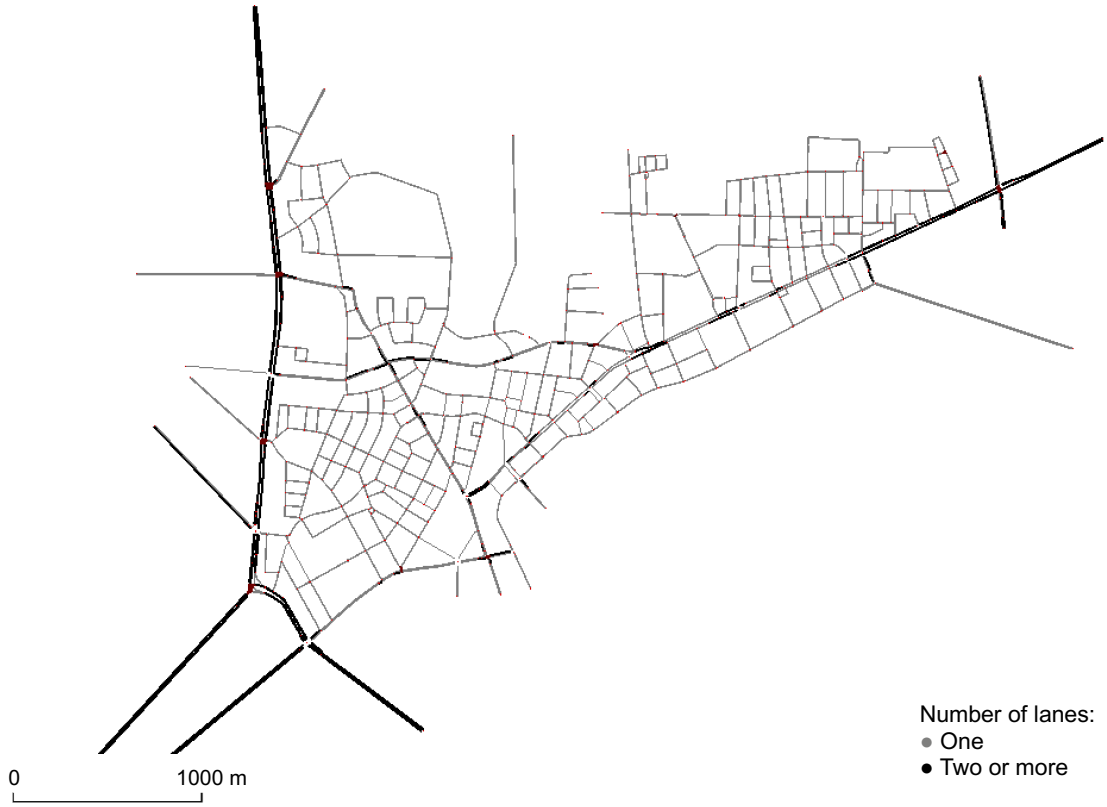

Figure 2.4: Number of lanes in the real world Hannover Vahrenwald-List traffic network

of the neighborhood streets. The network has an area of 5.88 km^2 and consists of 189 links, for a total length of 117.45 km. The total number of nodes is 84 and, among these, the total number of traffic light intersections is 46. The city of Hannover provided the data to define the traffic light plans. Table 2.2 summarizes the main characteristics of the network used in SUMO.

2.3 Vehicles Modeling

This paragraph describes the reasons for choosing the parameters for modeling both automated and conventional vehicles. The vehicle type distribution is used to define the percentage of automated vehicles. The penetration rate of automated vehicles is indicated through the parameter `probability`. The generation of a vehicle with certain characteristics is then left to SUMO in accordance with the indicated probability parameter.

2.3.1 Automated Vehicles

Definitions and standards concerning automated driving vehicles are provided by the Society of Automotive Engineers (SAE), an organization that deals with enacting technical standards for motorized vehicles of any category. SAE defines automated vehicle

as a "vehicle equipped with automated driving systems that perform part or all of the dynamic driving task" [5]. Two main actors contribute to the description of the automated aehicles: human user and ADS. SAE defines six automation levels, from level 0 (no driving automation) to level 5 (full driving automation), based on the roles of the two actors. Through these levels it is possible to describe all the automation ranges present in the motor vehicles. From level 0 to level 2 the vehicles are called "traditional", as driving is entirely controlled by the driver. From level 3 the guide begins to be partialy or totally performed by the vehicle. The culmination of automation is achieved with level 5, in which the vehicle can drive autonomously on any type of road, at any speed and for any environmental condition.
Automated Driving Systems (ADS) are the set of hardware and software that are able to perform the entire DDT. The term ADS is mainly used in the description of level 3, 4 and 5 automated vehicles. Dynamic Driving Task (DDT) are all those real time operational and tactical functions required to conduct a vehicle within the vehicular traffic. Note that strategic functions, such as route destination timing and selection, are not included within the definition. As regarding the operational functions, DDT include:

- Lateral vehicle motion control via steering;
- Longitudinal vehicle motion control via acceleration and deceleration;
- Monitoring the driving environmant via object and event detection and response preparation (OEDR).

As regarding the tactical functions, DDT include:

- Object and event response execution;
- Maneuver planning;
- Enhancing conspicuity via lighting, signaling and gesturing.

Figure 2.5 shows the schematic view of driving task showing DDT portion. As for DDT performance, level 1 and 2 vehicles incorporate partly or all of the functionality of the innermost loop, while the level 3, 4 and 5 encompass automation of both inner loops.
In case of request for intervention by the system, i.e. because of a mechanical failure, the driver can take control of the vehicle. This possibility is defined as DDT fallback. While in the lowest automation levels the intervention of the human driver is required, at levels 4 and 5, the ADS must be capable of performing the DDT fallback and achieving a minimal risk condition.
According to the definitions, SAE defines six levels of automation based on respective roles of the human driver and the ADS in relation to each other. Level 0 refer to cases in which the human driver performs the entire DDT. A Level 0 automated vehicle is called conventional vehicle, as it is designed to be operated by a human driver during part or all of every trip. Level 1 and level 2 automated vehicles refer to cases in which the human driver continues to perform part of DDT while the ADS is engaged. The term driver support system is used for these two automation levels as the autonomous driving equipment support, without replacing, the driver. Level 3 automated vehicles

Table 2.3: Automation levels [5]

SAE level	Name	Narrative definition	Lateral and longitudinal vehicle motion	OEDR	DDT fallback
0	No automation	The performance by the driver of the entire DDT, even when enhanced by active safety systems	Human driver	Human driver	Human driver
1	Driver assistance	The sustained and ODD-specific execution by a driving automation system of either the lateral or the longitudinal vehicle motion control subtask of the DDT (but not both simultaneously) with the expectation that the driver performs the remainder of the DDT	Human driver and system	Human driver	Human driver
2	Partial automation	The sustained and ODD-specific execution by a driving automation system of both the lateral and longitudinal vehicle motion control subtasks of the DDT with the expectation that the driver completes the OEDR subtask and supervises the driving automation system	System	Human driver	Human driver
3	Conditional automation	The sustained and ODD-specific performance by an ADS of the entire DDT with the expectation that the DDT fallback-ready user is receptive to ADS-issued requests to intervene, as well as to DDT performance-relevant system failures in other vehicle systems, and will respond appropriately	System	System	Human driver
4	High automation	The sustained and ODD-specific performance by an ADS of the entire DDT and DDT fallback without any expectation that a user will respond to a request to intervene	System	System	System
5	Full automation	The sustained and unconditional (i.e., not ODD-specific) performance by an ADS of the entire DDT and DDT fallback without any expectation that a user will respond to a request to intervene	System	System	System

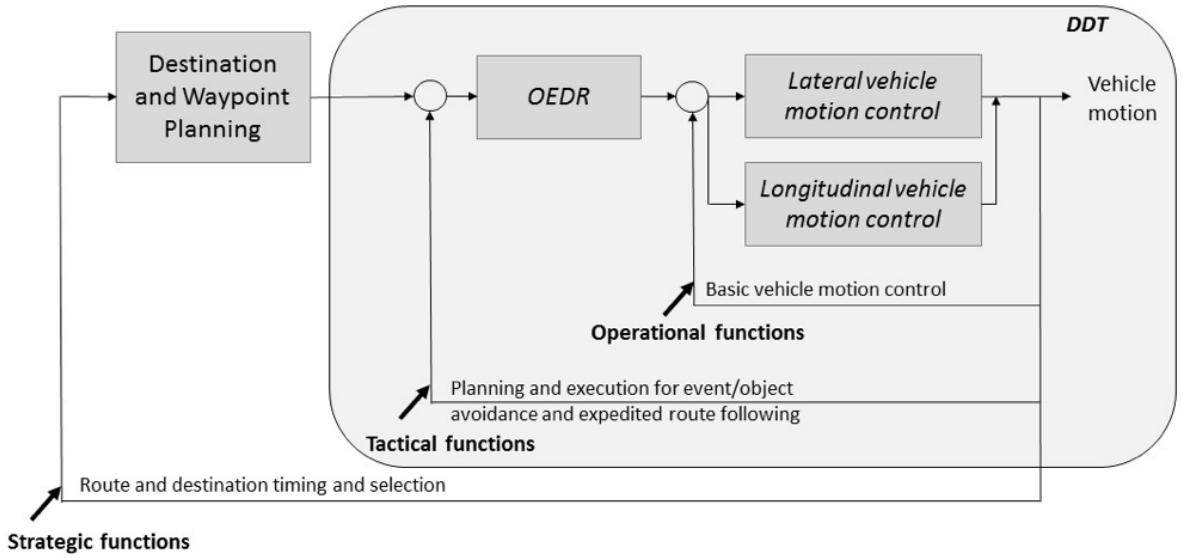

Figure 2.5: Schematic view of driving task showing DDT portion [5]

refer to cases in which the ADS performs the entire DDT. However, if a DDT fallback is expected to take over the DDT, then that user is expected to be receptive and able to resume DDT performance when alerted to the need to do so. Level 4 and 5 automated vehicles refer to cases in which ADS can perform the entire DDT and DDT fallback, and any users present in the vehicle while the ADS is engaged are passengers. Studies indicate that the introduction of automated level 5 vehicles may take place gradually in the time interval between 2025 and 2040 [27]. Table 2.3 shows the various levels of automation, with a detailed description of each of them.
Some considerations can be made regarding the introduction of automated vehicles in road traffic [27], [42].

- 90% of accidents occur as a result of human errors. With a high percentage of automated vehicles in circulation, a decrease in accidents is expected following the decrease in the possibility of human error occurring, up to a minimum value.
- With the introduction of automated vehicles, an improvement in road traffic is expected. Automated vehicles in fact have a more deterministic behavior and are prone to have fewer headways when compared with conventional vehicles.
- Driving license update for driving automated vehicles, as the driver will also need to know how the vehicle's on-board technology works, as well as knowing the rules of the road.
- Introduction of vehicles with a high level of automation requires specific legislation regarding civil and criminal liability in the event of an accident. It remains to be established whether any liability should fall on the driver or on the manufacturer of the vehicle that caused the accident. Many legislators are adjusting the laws in a view of introducing automated vehicles, even if automated vehicles of level 5 remain excluded from the most advanced legislation.

Table 2.4: Automated Vehicles sensors

	(1)	(2)	(3)	(4)	(5)
Camera	Yes	With low precision	Yes	Yes	Yes
Radar	Yes	Yes	No	No	No
Ultrasonic	No	Only distances	No	No	No
Lidar	Yes	Yes	Yes	No	Only weather

(1) Can detect objects far away?
(2) Can quantify distances and speeds of objects?
(3) Can classify different types of objects?
(4) Can interpret traffic signs and road markings?
(5) Is affected by light and weather conditions?

- Attention must be paid to security and privacy issues, which must also be protected following the introduction of automated vehicles. The right of users to maintain control over their data and the commitment of car manufacturers, software developers, authorities, etc. to protect data from hackers and terrorists are indisputable requirements.

Automated vehicles are equipped with numerous sensors for a correct real time survey of the surrounding environment. The sensors installed on all automated vehicles of higher level are LIDAR, cameras, radar and ultrasonic sensors, as shown in Table 2.4. LIDAR (Light Detection and Ranging) is a remote sensing technique that allows the vehicle to determine the distance to an object or surface using a laser pulse. The distance of the object is determined by measuring the time elapsed between the emission of an impulse and the reception of the diffused signal. The LIDAR sensor is able to measure distances in all directions in order to create a three-dimensional map of the surrounding environment. The ultraviolet wavelengths allow the vehicle to locate and obtain information on very small objects and have the advantage of operating regardless of the lighting conditions. The LIDAR sensor is not able to recognize colors, therefore it is combined with a series of cameras for the recognition of road signs and lane markings. The sensor is very large, therefore it is usually installed on the roof of cars. Vehicles are also equipped with high resolution cameras, able to recognize colors and contrasts in order to read road signs even in rainy weather. In case of low visibility, i.e. in case of fog, the cameras could have problems in interpreting the signals correctly. Being small objects, they can be installed in any position of the vehicle. RADAR sensor uses electromagnetic waves that allow optimal operation even in adverse weather conditions, i.e. with the presence of fog, rain or snow. Due to their operation, RADAR sensors work well with metal surfaces, with pedestrians essentially invisible. RADAR sensors are widely used on automated vehicles due to their low cost and small size. Ultrasonic sensors are able to recognize an object regardless of the material and are not affected by weather and visibility conditions. However, they have a low range and cannot recognize colors.
As described, the DDT cannot be performed using information from a single sensor.

Figure 2.6: Level 5 Automated Vehicle sensors

The sensors are coupled and synchronized with each other in order to use all the advantages. As an example, the Level 5 autonomous vehicles used by Lyft are equipped with 3 LIDARs, 5 RADARs and 7 cameras [17]. As shown in Figure 2.6, one LIDAR is on the roof of the vehicle and two of them are on the front bumper. Four RADARs are installed on the roof and one RADAR is placed on the front bumper.
To obtain information on the behavior of automated vehicles, numerous datasets are available online. Two of the available datasets were analyzed: Level 5 dataset and Argoverse dataset.
Level 5 dataset is a dataset detected from a fleet of level 5 vehicles on a suburban location in Palo Alto, California. The dataset is divided into two parts: a static part, consisting of the semantic map and the aerial map, and a dynamic part, consisting of driving data. The semantic map was created manually and contains useful information for driving, including number and width of lanes, speed limits, position of signs and traffic lights. The very high definition aerial map captures the area of Palo Alto. The driving data consists of frames, scenes, agents and traffic light faces. Each frame contains the timestrap, information on traffic lights, the indices of each agent and the position and direction of the ego vehicle. A scene consists of several frames, it contains information about the frames and the start and end time. Argoverse dataset is a dataset collected from a fleet of level 4 automated vehicles in the American cities of Miami and Pittsburgh, chosen because they differ in their different local driving habits. The dataset consists of two main parts: a static part and a dynamic part. The static part consists of the semantic vector map, which contains useful information on lanes, as lane centerlines, traffic direction, and intersection annotations. The dynamic part is made up of driving data, which can be viewed as vehicle trajectories superimposed on the semantic vector map. Figure 2.7 shows the graphic display of a scene for the (a) Level 5 and (b) Argoverse dataset.
Analyzing the scenes extracted from the Level 5 dataset it emerged that no lane change behavior occurs in any case. However detailed and complete, the analysis and use of this dataset becomes useless for the purposes of this thesis. As regards the use of the Argoverse dataset, it was observed that the data relating to lane change were difficult to extract and difficult to process. As useful as it is, it was decided not to analyze this dataset as it is complicated.
Given the impossibility of using the datasets as sources for an ad hoc parameter calibration, it was decided to use the parameter values found in the literature [19], [23], [29],

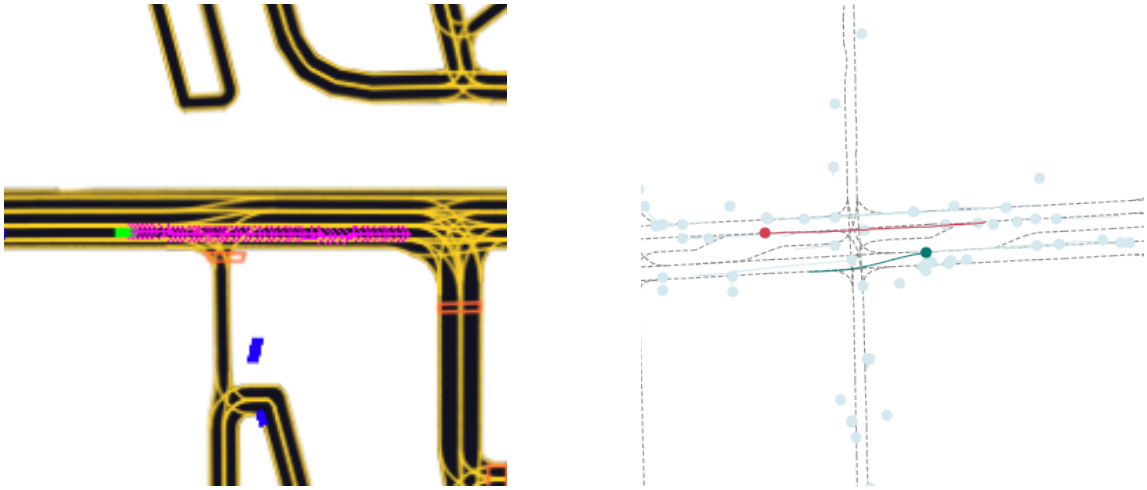

Figure 2.7: Scene for the (a) Level 5 and (b) Argoverse dataset

Table 2.5: Parameter set for modeling Automated Vehicles

Parameter	Value		
	Conservative	Moderate	Aggressive
`lcStrategic`	3.0	3.0	3.0
`lcCooperative`	1.0	1.0	1.0
`lcSpeedGain`	5.0	5.0	5.0
`lcKeepRight`	1.2	1.2	1.2
`lcAssertive`	0.5	0.7	0.9

and described in the paragraph 1.5. Table 2.5 shows the parameters used to describe the lane change behavior of automated vehicles. Default values have been left for the parameters that do not appear in the Table. By comparing the values used with the default values shown in the Table 2.1, some considerations can be made.

- Higher values of the `lcStrategic` parameter result in an earlier lane change. This means that compared to the default values, automated vehicles change lanes in advance of the dead-end point.
- Higher values of the `lcSpeedGain` parameter result in more lane changes. This means that compared to the default values automated vehicles have a lower threshold value that will make them change lanes more often to obtain a speed gain.
- Higher values of the `lcKeepRight` parameter result in an early lane change. This means that compared to the default values, automated vehicles have a lower threshold value that will make their lane change early with the aim of leaving the fast lane free.

Table 2.6: Parameter set for modeling Conventional Vehicles

Parameter	Value		
	Conservative	Moderate	Aggressive
`lcStrategic`	1.0	1.0	1.0
`lcCooperative`	1.0	1.0	1.0
`lcSpeedGain`	1.0	1.0	1.0
`lcKeepRight`	1.0	1.0	1.0
`lcAssertive`	1.0	1.3	1.6

- Lower values of the `lcAssertive` parameter result in an increase in the accepted gap value on the destination lane. This means more prudent behavior of automated vehicles than the default values.

The different values of the `lcAssertive` parameter aim to describe the behavior of automated vehicles of different car manufacturers. It is realistic to think that the traffic is made up of automated vehicles of different brands.

2.3.2 Conventional Vehicles

A conventional vehicle is "a vehicle designed to be operated by a conventional driver during part or all of every trip" [5]. A conventional vehicle corresponds to level 0 of the classification proposed by SAE. To model conventional vehicles, the software default parameters are used. The SUMO default parameters are calibrated by software developers on the basis of their experience. Default parameters are well suited to the most common scenarios. This choice is made in accordance with the available literature, in which the authors who modify the parameters do so for a motorway scenario. Exception is for the `lcAssertive` parameter, which has an explicit parameterization available in the literature [29]. Table 2.6 shows the parameters used to describe the lane change behavior of conventional vehicles.
Considerations can only be made regarding the `lcAssertive` parameter. The increasing values of the parameter indicate a greater predisposition to accept lower gaps on the destination lane by the drivers. Higher values of this parameter lead to more aggressive behavior of drivers. The three values considered aim to describe the behavior of different types of drivers: aggressive, conservative or moderate behavior.

2.4 Demand Modeling

For the purposes of this thesis, two demand profiles are evaluated. The first profile, called *real traffic flow*, is derived from actual traffic counts provided by the City of Hannover Traffic Management Center. The second profile, called *intensified flow*, is created to observe the network in congested conditions and it is obtained by gradually increasing the demand.

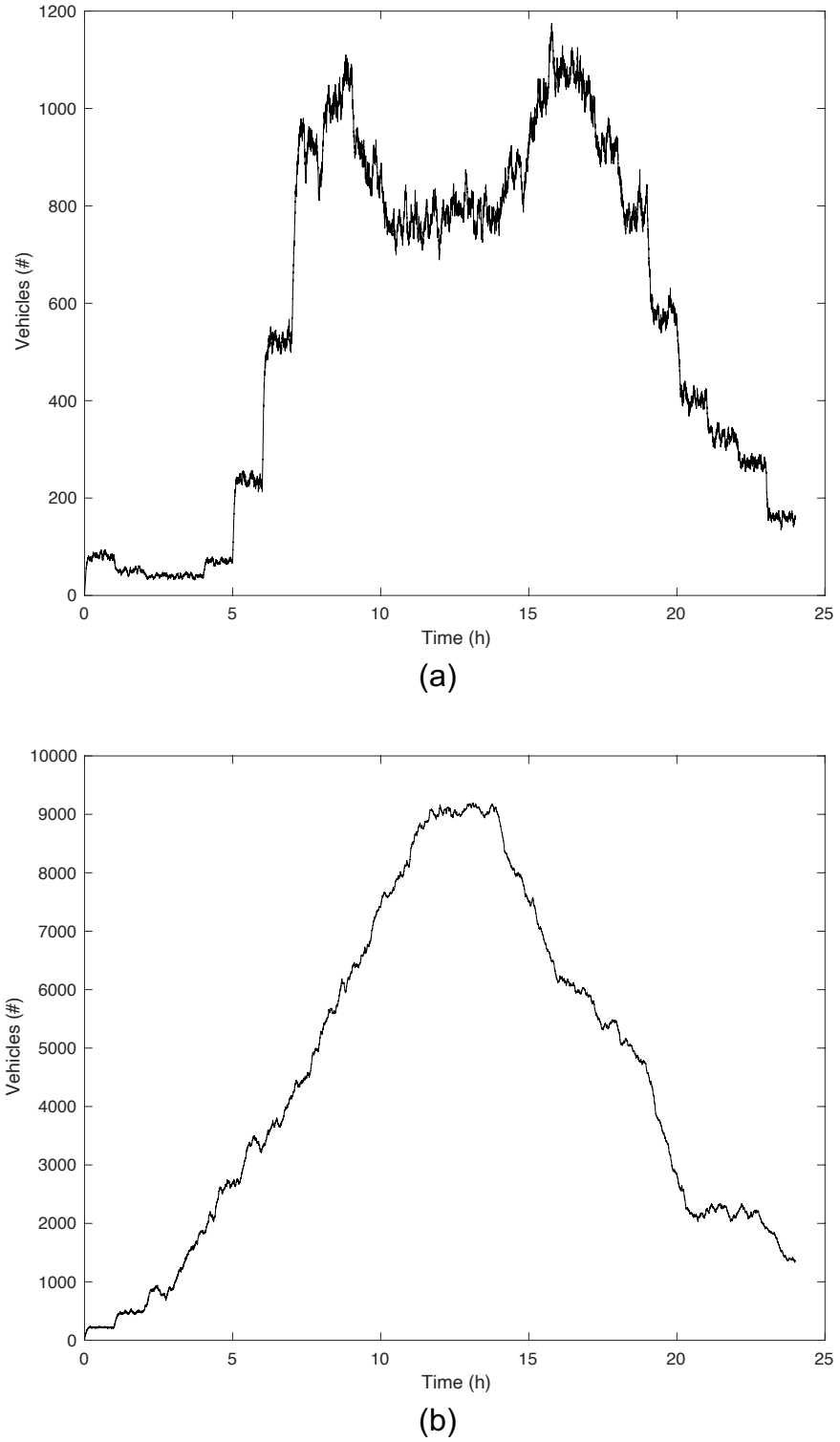

Figure 2.8: Demand profile: (a) real traffic flow and (b) intensified flow

Figure 2.8 (a) shows the demand profile obtained from real traffic counts. Data from the detector counts are used for the calibration of traffic demand. The the City of Hannover Traffic Management Center has made traffic counts available for the period from the beginning of 2018 to February 2020. It is of interest to obtain the representative demand of a typical working day, therefore, only the days Tuesday to Thursday are considered in the preparation of the data, as Monday and Friday have different traffic patterns due to weekend commuters. Furthermore, public holidays are not considered. The demand patterns thus filtered were then grouped to obtain the real traffic demand. Within the demand profile, an initial peak in demand can be seen within the time slot from 8 to 9 am time slot. In the late morning and early afternoon there is a decrease in demand. The second peack time is reached between 6 and 7 pm. Both peaks are due to the effect of home-to-work or home-to-school commuting. Demand remains at a low level at night.
The routing of vehicles takes place using the SUMO trip file to form the traveling demand. For each trip, the start time, the source and destination link of the movement are defined. An entire list of links to be followed is not provided, but the software calculates the fastest route in accordance with the surrounding traffic conditions through the use of the A* algorithm.
Figure 2.8 (b) shows the intensified demand profile obtained by varying the demand level, including situations from the free flow to the rush hours flow. This demand profile is created for the purpose of MFD estimation only. At the beginning of the simulation, the level of demand is kept low and made to grow by adding each time an increasing number of vehicles in the network in order to arrive at a congested situation. Upon reaching saturation, the demand profile started to progressively decrease.
The routing of vehicles takes place through the use of flow to form the traveling demand. The network has been divided into five zones, which generate and attract vehicles. For each hour, the number of generated vehicles, the start and the end flow's zones are defined. The departure and arrival links, as well as the path to be followed within the network, are left to the software. The calculated route is the fastest route in accordance with traffic conditions calculated through the A* algorithm. Both demand profiles have a 24 hours duration.
A* is a graph-based routing and optimization algorithm. In the application to transport networks, given an origin and a destination point, the algorithm is used to determine the shortest path [47]. The shortest path is the minimum cost path formed by all the links that connect the origin with the destination point. It uses travel time as primary measurement and the lower bound is given by the air distance between the origin and the destination point divided by the maximum achievable speed in the network. The maximum speed depends on the maximum vehicle's speed or on the speed factor of a given vehicle type.
The assignment of vehicles to the network is dynamic. The dynamic routing assignment was chosen for two main reasons.

- No enough time to wait for the dynamic user equilibrium;
- Vehicles need to adapt their route while running.

All vehicles have been equipped to be able to re-compute the route periodically. The travel time is defined as the weight of the edges and is collected for each edge during

Table 2.7: Minimum number of runs [10]

Desired range $\frac{CI}{\sigma}$	Desired confidence $1-\alpha$	Number of runs N
0.5	99%	130
0.5	95%	83
0.5	90%	64
1.0	99%	36
1.0	95%	23
1.0	90%	18
1.5	99%	18
1.5	95%	12
1.5	90%	9
2.0	99%	12
2.0	95%	8
2.0	90%	6

the simulation. If a vehicle needs to be rerouted, then it will choose the fastest route based on present travel times. The updating of the weights of each link is not carried out simply by overwriting the old value, but by making a weighted average of the last measured values. Since updating the weights of edges requires a significant computational effort, the greater the number of vehicles in circulation, the slower the simulation will be.

2.5 Simulation Runs

The simulation is carried out by executing several simulation runs using the parameters described above. Each simulation run is characterized by a random number, called *seed*, which is responsible for vehicles generation process, their followed path and their behavior within the network. Between two consecutive runs, the type of vehicle generated may vary. Consequently, its aggressiveness and the followed path vary. The final result of the simulation depends on these choices and it is not possible to completely describe all the field conditions through a single simulation run. Evaluating the model on the basis of a single simulation run would be wrong since two simulation runs with two different seeds can lead to results that differ from each other by up to 25% [10].
The number of repetitions is determined by the iterative procedure based on statistical considerations proposed by the Federal Highway Administration (FHWA) [10]. Figure 2.9 shows the general procedure to determine the minimum number of simulation runs. The procedure begins with the execution of four model runs repetition, each using a different seed. Once the indicator used to evaluate the goodness of the model has been chosen, it is possible to determine the standard deviation between the subsequent runs.

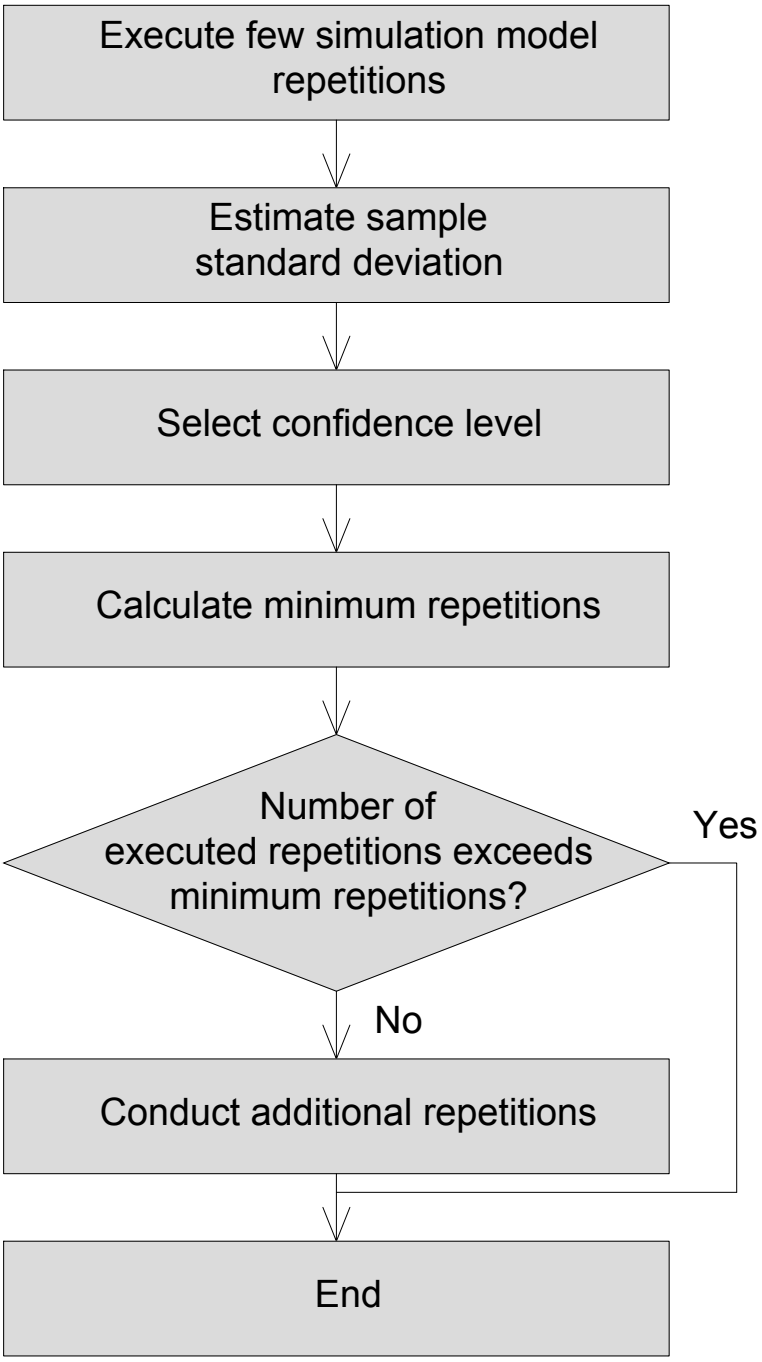

Figure 2.9: Number of run of the simulation model, adapted from [10]

Table 2.8: Number of runs per each scenario

Automated vehicles penetration rate	Number of runs	
	Real traffic flow	Intensified flow
0% *Scenario 0*	20	25
10%	20	25
20%	20	25
30%	20	25
40%	20	25
50%	20	25
60%	20	25
70%	20	25
80%	20	25
90%	20	25
100%	20	25

$$\sigma^2 = \frac{\sum_{m=1}^{N}(x_m - \bar{x})^2}{N-1} \tag{2.1}$$

Where:

- x_m is the output value for each simulation run m;
- $\bar{x}$ is the average output value for all runs;
- N is the number of runs.

Initially, the analyst must choose the desired confidence level $(1-\alpha)$, i.e. the probability that the true mean lies within the target confidence interval. Usually a 95% confidence level value is used, i.e. it is possible to be 95% sure that each given repetition produces an interval that contains the true value of the indicator. Values greater than the confidence level require the execution of a greater number of runs. The analyst must also choose the value of the confidence interval length (CI), i.e. the range of values within which the true mean value may lie. The length of the interval is at the discretion of the analyst and may vary according to the purposes for which the results will be used. Values smaller than the confidence level require the execution of a greater number of runs. The number of simulation runs required is calculated as follows.

$$N = \left(\frac{2 \cdot t_{1-\frac{\alpha}{2},N-1} \cdot \sigma}{CI_{1-\alpha}}\right)^2 \tag{2.2}$$

Where:

- $t_{1-\frac{\alpha}{2},N-1}$ is a parameter of the Student distribution that allows calculating the confidence interval of the mean value of a sample within which the mean of the total population will be distributed. Its value depends on α and on the $N-1$ degrees of freedom;

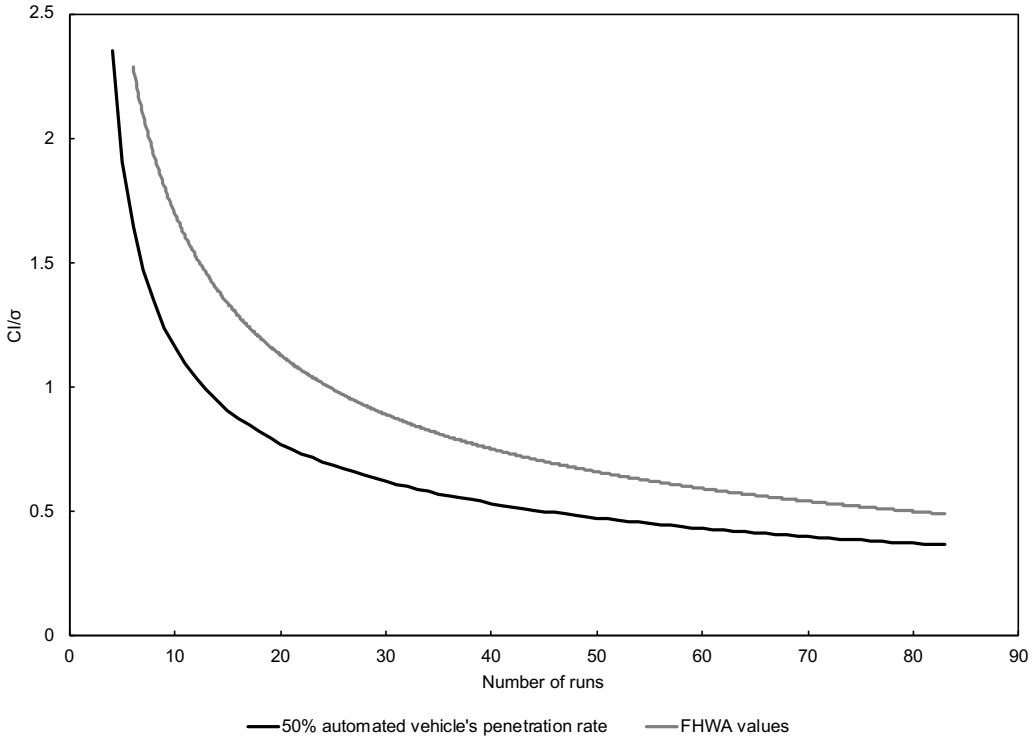

Figure 2.10: Desired range vs number of runs

- σ is the standard deviation;
- $CI_{1-\alpha}$ is the confidence interval for the true mean, where α equals the probability of the true mean not lying within the confidence interval.

The use of the formulas described leads to an iterative process. The number of runs resulting from the Equation 2.2 must be less than, or at the same limit, the number of runs actually performed and used for the calculation of the standard deviation. Otherwise, a new run must be performed until convergence is achieved.
Table 2.7 shows the solutions to the above Equation in terms of the minimum number of repetitions for various desired confidence intervals and desired degrees of confidence. The Table can be read in the following way, taking into consideration the average delay as indicator with which to evaluate the goodness of the model. Having chosen a confidence interval of 3.0 s, if the analyst obtains a standard deviation equal to 1.5 s with a confidence level of 95%, then it is possible to perform 8 simulation runs to obtain the average delay with a error of ± 1.5 s.
This thesis focuses on 11 different scenarios, each of which is characterized by a different penetration rate of automated vehicles within the network. The initial situation in which the traffic is composed of conventional vehicles only is defined *Scenario 0* and is taken as a reference to understand whether the different behavior of lane change of automated vehicles brings beneficial or non-beneficial effects on traffic. For each subsequent scenario there is an increase of 10% of automated vehicles in circulation. The number of vehicles circulating in each scenario is the same and reflects what is reported in paragraph 2.4, the changes lie in the type of vehicles involved, as reported in the

paragraph 2.3. Table 2.8 shows the different scenarios analyzed and the corresponding number of runs.
The average speed parameter is chosen as indicator to evaluate the goodness of the model. As for the real traffic flow, 20 runs are performed for each scenario, modifying the seed associated with the simulation. With 20 runs we get a desired range of 0.77. In the most stringent scenario, i.e. the scenario corresponding to a penetration rate of 90%, with a confidence level of 95% and a standard deviation of 0.20 km/h, a confidence interval of 0.15 km/h is obtained to get the average speed with an error of ± 0.08 km/h ($\pm 0.25\%$). As regards the enhanced flow, we decide to use a lower confidence interval to have greater precision in the determination of MFD. Therefore, 25 runs are performed for each scenario, with a desired range of 0.67. Considering all the scenarios analyzed, a total of 475 simulation runs are conducted.
Considering the 50% automated vehicle penetration rate scenario, a sensitivity analysis on the number of runs is conducted. In this regard, a total of 83 simulation runs have been created for this scenario. The sensitivity analysis, the results of which are shown in Figure 2.10, aims to observe how the desired range varies as the number of runs increases with our values, similar to what the FHWA did. It is observed that the results obtained with our values allow to perform a lower number of runs to obtain the same desired range than the FHWA method. That is, once a desired range has been set, in this thesis work it is possible to perform a lower number of runs compared to the general method of the FHWA.

Chapter 3

Results

Within this chapter, the results of the simulations carried out and described in the previous chapters will be presented. As mentioned in paragraph 1.6, the final goal of the thesis is to observe how the different lane change vehicle's microscopic behavior impacts on traffic efficiency and safety. Initially, the results relating to the lane change maneuvers are presented. The results are then presented in terms of efficiency and safety of the system. Within the chapter, the methodologies adopted to obtain the results are also shown. As for efficiency, the travel time, speed and MFD analysis will be shown. As for safety, the analysis of conflicts based on SSM will be shown.
As previously reported, *Scenario 0* is defined as the scenario in which only conventional vehicles circulate in the network. For each subsequent scenario, the automated vehicles in circulation increase by 10%, until reaching a penetration rate of 100%. The assessments in terms of efficiency and safety are carried out by comparing each scenario with Scenario 0, taken as a reference for the analyses.

Table 3.1: Number of inserted vehicles for the real traffic flow demand profile

Automated vehicles penetration rate	Conventional vehicles	Automated vehicles	Total number
0 %	152403	0	152403
10 %	137163	15240	152403
20 %	121922	30481	152403
30 %	106682	45721	152403
40 %	91442	60961	152403
50 %	76202	76202	152403
60 %	60961	91442	152403
70 %	45721	106682	152403
80 %	30481	121922	152403
90 %	15240	137163	152403
100 %	0	152403	152403

Table 3.2: SUMO lane change measures

Output name	Unit of measure	Description
`id`		Name of the vehicle involved
`vType`		Type of vehicle involved
`time`	s	The simulation time at which the lane change took place
`pos`	m	The position at which the lane change took place
`reason`		The reason for changing lane
`speed`	m/s	The speed at which the lane change took place
`leaderGap`	m	The gap between the ego and the leader vehicle in the target lane
`followerGap`	m	The gap between the ego and the follower vehicle in the target lane
`origLeaderGap`	m	The gap between the ego and the leader vehicle in the current lane

3.1 About Lane Changes

SUMO lane change output was collected in order to count and identify the lane change maneuvers carried out by the vehicles. In this regard, the number of vehicles inserted within the simulation for each scenario are shown in Table 3.1 and the results obtained from the analysis of the lane change outputs are presented below.
A lane change event is recorded when a vehicle moves sideways from the current lane to the adjacent lane. As reported in Table 3.2, the output generated by SUMO allows to identify the type of vehicle involved, i.e. whether conventional or automated vehicle, and its behavior, i.e. whether conservative, moderate or aggressive vehicle. For each registered lane change maneuver, it is possible to obtain information on the motivation behind the maneuver, as reported in the paragraph 1.2. The reasons for a lane change maneuver are:

- Speed gain, in order to allow the ego vehicle to gain speed;
- Strategic, in order to avoid a dead-end lane;
- Cooperative, in order to allow another vehicle to make a mandatory lane change;
- Keep right, in order to clear the left lane used to overtake a vehicle.

As reported in paragraph 2.1, a continuous lane change is implemented. This means that the vehicle performs a continuous lane change maneuver from one lane to the adjacent one instead of disappearing from the current lane and reappearing in the adjacent lane.
Table 3.3 shows the number of lane changes made by conventional and automated vehicles. A high number of lane changes indicates greater freedom of movement by vehicles as it allows, for example, to reach the desired speed without being blocked by a slower vehicle. On the other hand, a high number of lane changes cause greater situations of

Table 3.3: Number of lane change maneuver

Automated vehicles penetration rate	Conventional vehicles	Automated vehicles	Total number	Change in number of lane change from Scenario 0
0 %	355025	0	355025	0.0 %
10 %	306360	30835	337194	−5.0 %
20 %	280586	51938	332524	−6.3 %
30 %	245761	77402	323163	−9.0 %
40 %	213406	103462	316869	−10.7 %
50 %	179409	134324	313733	−11.6 %
60 %	144942	155051	299993	−15.5 %
70 %	109960	181071	291031	−18.0 %
80 %	73640	207118	280758	−20.9 %
90 %	37124	233142	270266	−23.9 %
100 %	0	259528	259528	−26.9 %

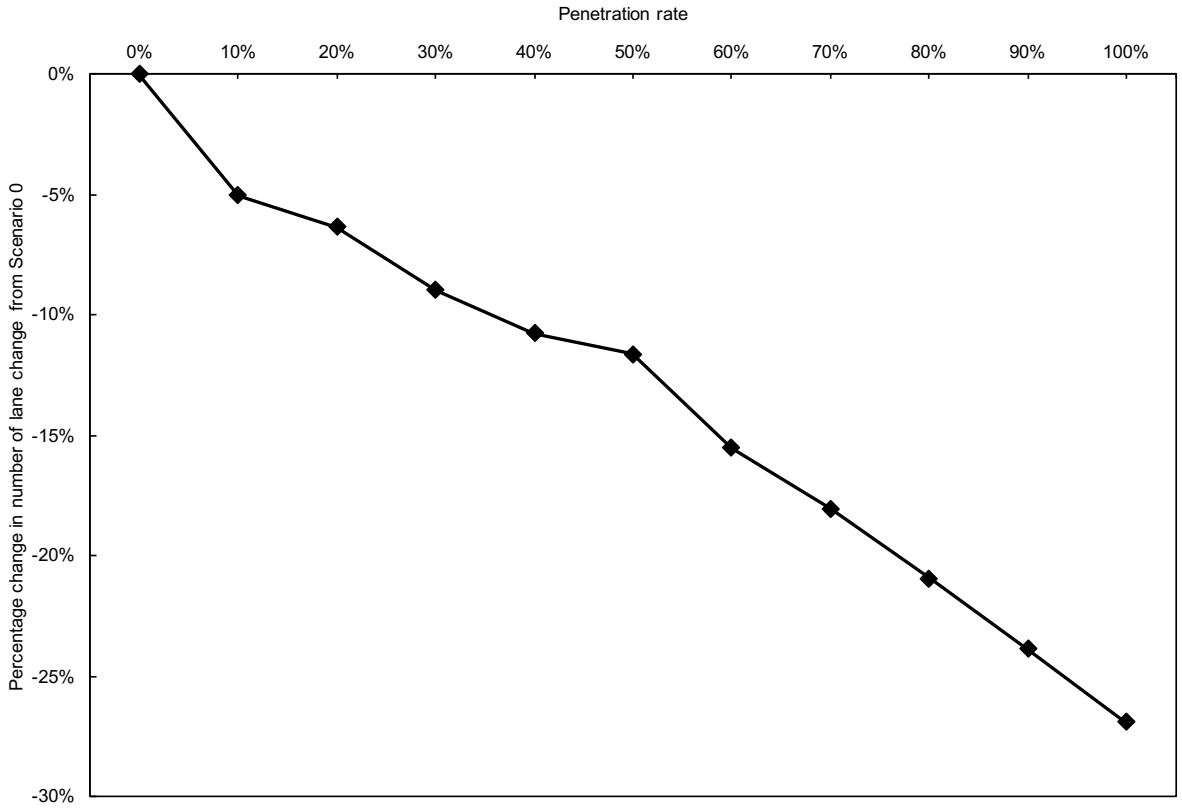

Figure 3.1: Change in number of lane change maneuver from Scenario 0

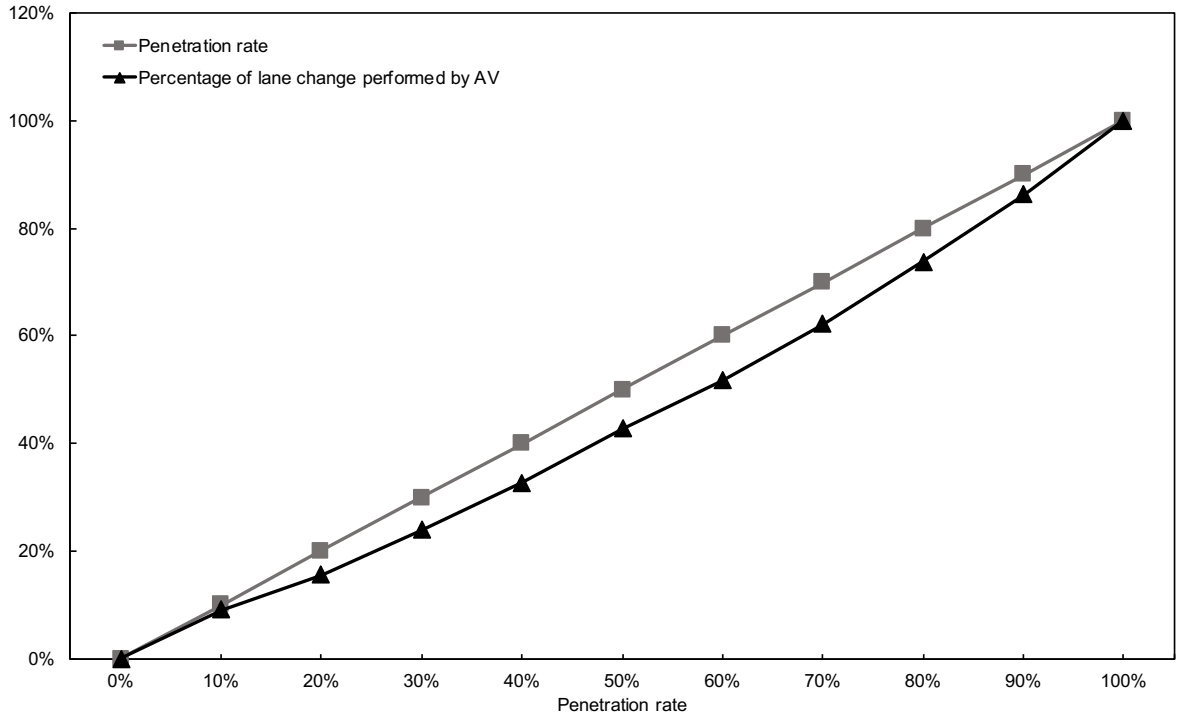

Figure 3.2: Automated vehicle's lane change maneuver

conflict between vehicles, which can lead to a greater probability of crash. The graph shown in Figure 3.1 represents the percentage change in the number of total lane change maneuvers from Scenario 0, taken as reference. It is noted how the total number of maneuvers decreases as the automated vehicles penetration rate increases, up to a decrease of 26.9 %.
For each scenario, the graph in Figure 3.2 shows the percentage of automated vehicles in circulation and the percentage of lane change maneuvers performed by automated vehicles. The line relating to the percentage of automated vehicles is arranged on the diagonal of the graph, while the line relating to the lane change maneuvers performed by automated vehicles follows another trend. For example, considering a penetration rate of 50 % it results that the lane change maneuvers carried out by automated vehicles are only 42.8 %, while the remaining 57.2 % of the maneuvers are carried out by conventional vehicles. That is, for each penetration rate, it appears that automated vehicles proportionally perform fewer lane change maneuvers than conventional vehicles. From the two graphs described, it can be deducted that the `lcAssertive` parameter is the one that most influences the lane change maneuvers, determining for automated vehicles a more precautionary behavior in lane change maneuvers. The decreasing number of maneuvers performed could be therefore attributable to a smaller gap accepted by automated vehicles.

Table 3.4: SUMO edge-based measures

Output name	Unit of measure	Description
`period`	s	Measurement aggregation period
Edge `id`		Name of the reported link
`entered`		The number of vehicles that entered the link within the reported period
`sampledSeconds`	s	The sum of the travel times required by the vehicles to travel the generic link within the reported period
`speed`	m/s	Average space speed in the generic link within the reported period. The average velocity in space is then averaged over time, so it is defined as *space-mean-speed*
`laneDensity`	$veh/km/ln$	Density of vehicles in the generic link per lane within the reported period

3.2 About Travel Time and Speed

SUMO edge-based measures were collected to determine the travel time and the average speed of vehicles within the network. Referring to the SUMO output values described in Table 3.4, the description of the procedure adopted for the calculation of travel times and average speeds is presented. Results concerning mean travel time and speed are made at the network level. Therefore, it will be necessary to analyse network variables by aggregating the edge-based outputs from the simulation. As presented in the literature review section, many authors aggregate edge variables to obtain network measures. Examples of this are the works of Geroliminis and Daganzo (2007) [9] and Lu et al. (2020) [25], in which procedures for obtaining network measurements from edge outputs are presented.
The edge-based values are recorded for each fixed period for each link. It was decided to use a fixed interval equal to 15 minutes, that is the period that guarantees the validity of the stationary flow conditions [32].
Travel time is defined as the total time that vehicles spend within the network. This value is obtained by adding all the values of `sampledSeconds`. The average travel time that a vehicle spends within the network is then obtained by dividing the total time by the total number of vehicles. This data will be referred to below as *mean travel time*.

$$\bar{t} = \frac{\sum_{i=1}^{N} \texttt{sampledSeconds}}{N_v} \tag{3.1}$$

Where:

- $\bar{t}$ is the mean travel time that a vehicle spends within the network, in s;
- N is the total number of link i;
- $\sum_{i=1}^{N} \texttt{sampledSeconds}$ is the total time that vehicles spend within the network, in s;

- N_v is the total number of vehicles, in this case study equal to 152,403 veh.

Speed is defined as the average space speed in the network. It is calculated by dividing the total distance traveled by the total time of vehicles within the network, or calculated by weighting the average space speed of a link by the number of vehicles in circulation [25]. This data will be referred to below as *mean speed*.

$$\bar{v} = \frac{\sum_{i=1}^{N} N_i \cdot v_i}{\sum_{i=1}^{N} N_i} \cdot 3.6 \tag{3.2}$$

Where:

- $\bar{v}$ is the mean space speed in the network, in km/h;
- N is the total number of link i;
- v_i is the mean space speed in the generic link i, in m/s;
- N_i is the number of circulating vehicles in the generic link i.

The number of vehicles circulating in the generic link i is not an output data of the software, but it can be indirectly calculated by dividing the `sampledSeconds` attribute by the `period` attribute.

$$N_i = \frac{\texttt{sampledSeconds}}{\texttt{period}} \tag{3.3}$$

Where `period` is the time interval chosen to collect the output, equal to 15 min (900 s). Using this definition, it is possible to write the Equation 3.2 as follow.

$$\bar{v} = \frac{\sum_{i=1}^{N} \texttt{speed} \cdot \texttt{sampledSeconds}}{\sum_{i=1}^{N} \texttt{sampledSeconds}} \cdot 3.6 \tag{3.4}$$

The equation obtained represents average weighted space speed in the network and is equivalent to the Equation 1.9 expressed through the outputs of the SUMO software.
For each data presented, the associated error is also calculated, as described in the paragraph 2.5.
The results are presented in terms of percentage change from the Scenario 0, taken as reference. Tables 3.5 and 3.6 show the results of mean travel time and mean speed for all vehicles in circulation, while Tables 3.7 and 3.8 show the same results divided by conventional vehicles and automated vehicles. The graphs relating to the tables shown in Figure 3.3 and 3.4.
Some partial considerations can be made in relation to mean travel time and mean speed. As regarding the mean travel time, it can be observed how, in each scenario considered, automated vehicles show a mean travel time that is always higher than conventional vehicles. Furthermore, as the penetration rate of automated vehicles increases, the mean travel time increases more and more, up to an increase of 7.35 % compared to Scenario 0. Specularly, as regarding the mean speed, it can be observed how, in each scenario considered, automated vehicles travel with an average speed lower than conventional vehicles. There is also a decrease in the average travel speed as the penetration rate of automated vehicles increases, up to a decrease of 6.17 % average speed compared to Scenario 0.

Table 3.5: Change in mean travel time from Scenario 0 for all vehicles

Automated vehicles penetration rate	Mean travel time (s)	Change in mean travel time from Scenario 0
0 %	297	0.00 % ± 0.15 %
10 %	299	0.79 % ± 0.12 %
20 %	301	1.47 % ± 0.16 %
30 %	302	1.59 % ± 0.16 %
40 %	304	2.32 % ± 0.14 %
50 %	308	3.73 % ± 0.24 %
60 %	310	4.41 % ± 0.13 %
70 %	312	5.22 % ± 0.17 %
80 %	314	5.79 % ± 0.17 %
90 %	316	6.61 % ± 0.27 %
100 %	319	7.35 % ± 0.26 %

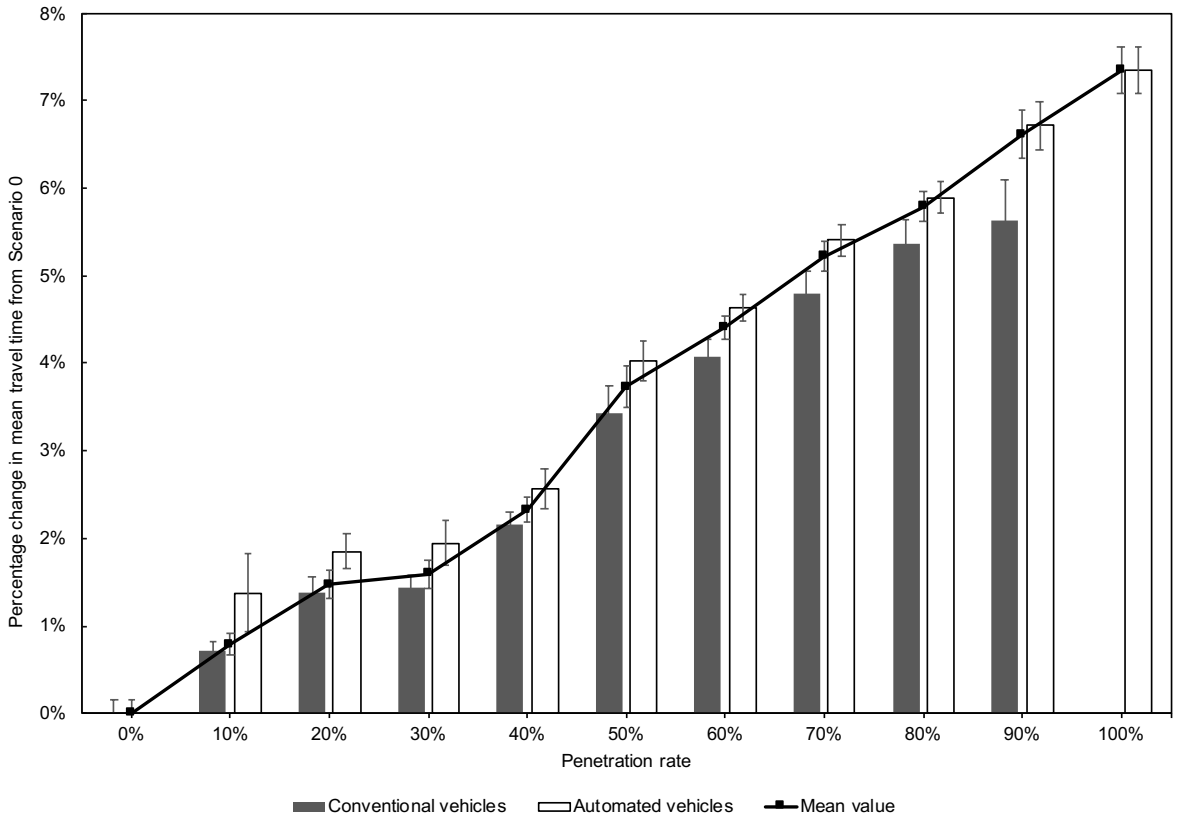

Figure 3.3: Change in mean travel time from Scenario 0

Table 3.6: Change in mean speed from Scenario 0 for all vehicles

Automated vehicles penetration rate	Mean speed (km/h)	Change in mean speed from Scenario 0
0 %	32.23	0.00 % ± 0.13 %
10 %	32.01	−0.67 % ± 0.11 %
20 %	31.83	−1.23 % ± 0.15 %
30 %	31.78	−1.37 % ± 0.15 %
40 %	31.58	−2.00 % ± 0.14 %
50 %	31.21	−3.15 % ± 0.23 %
60 %	31.03	−3.72 % ± 0.12 %
70 %	30.81	−4.41 % ± 0.16 %
80 %	30.66	−4.87 % ± 0.15 %
90 %	30.44	−5.54 % ± 0.25 %
100 %	30.24	−6.17 % ± 0.24 %

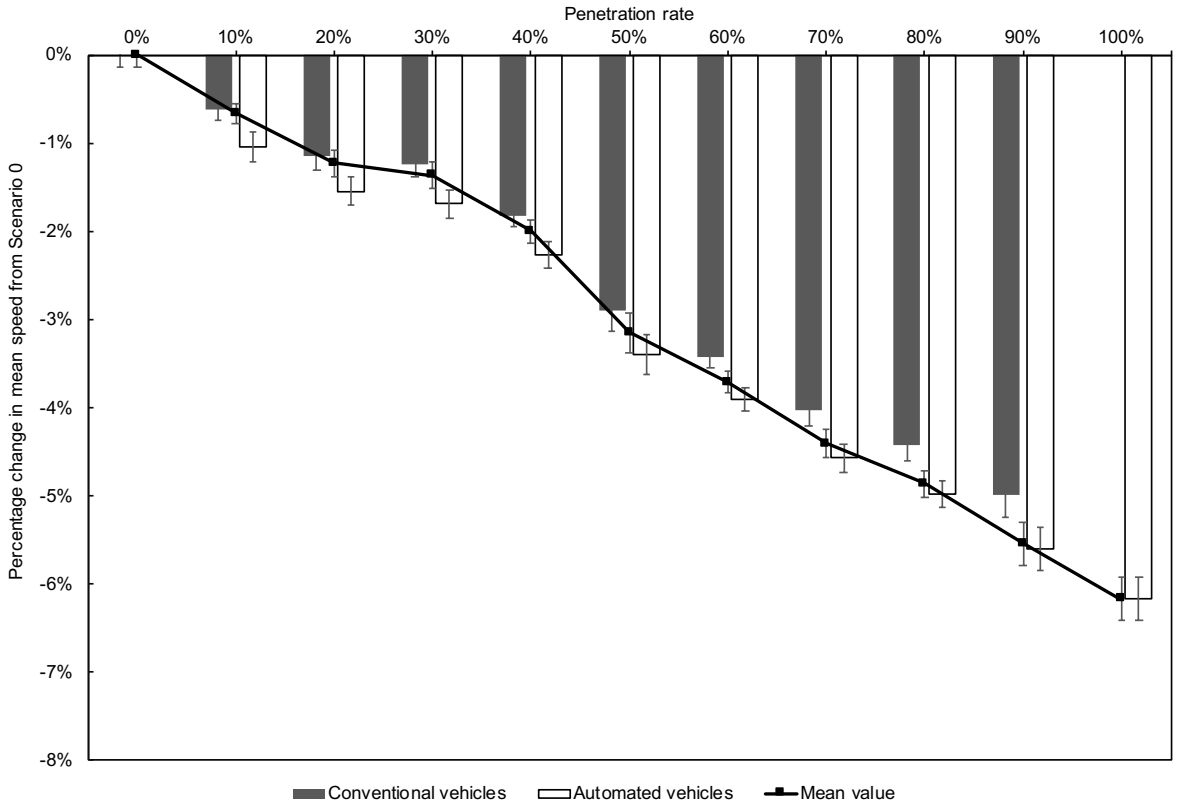

Figure 3.4: Change in mean speed from Scenario 0

Table 3.7: Change in mean travel time from Scenario 0 for conventional and automated vehicles

Automated vehicles penetration rate	Mean travel time (s)		Change in mean travel time from Scenario 0	
	Conventional vehicles	Automated vehicles	Conventional vehicles	Automated vehicles
0 %	297		0.00 % ± 0.15 %	
10 %	299	301	0.72 % ± 0.10 %	1.38 % ± 0.44 %
20 %	301	302	1.37 % ± 0.18 %	1.85 % ± 0.20 %
30 %	301	303	1.44 % ± 0.15 %	1.95 % ± 0.26 %
40 %	303	304	2.16 % ± 0.14 %	2.57 % ± 0.23 %
50 %	307	309	3.44 % ± 0.30 %	4.03 % ± 0.23 %
60 %	309	311	4.08 % ± 0.20 %	4.63 % ± 0.15 %
70 %	311	313	4.80 % ± 0.25 %	5.40 % ± 0.18 %
80 %	313	314	5.36 % ± 0.28 %	5.89 % ± 0.19 %
90 %	314	317	5.64 % ± 0.45 %	6.72 % ± 0.27 %
100 %		319		7.35 % ± 0.26 %

Table 3.8: Change in mean speed from Scenario 0 for conventional and automated vehicles

Automated vehicles penetration rate	Mean speed (km/h)		Change in mean speed from Scenario 0	
	Conventional vehicles	Automated vehicles	Conventional vehicles	Automated vehicles
0 %	32.23		0.00 % ± 0.13 %	
10 %	32.03	31.89	−0.62 % ± 0.11 %	−1.04 % ± 0.18 %
20 %	31.86	31.73	−1.15 % ± 0.15 %	−1.55 % ± 0.16 %
30 %	31.83	31.68	−1.24 % ± 0.15 %	−1.69 % ± 0.16 %
40 %	31.64	31.50	−1.82 % ± 0.14 %	−2.27 % ± 0.15 %
50 %	31.29	31.13	−2.90 % ± 0.23 %	−3.40 % ± 0.23 %
60 %	31.12	30.97	−3.43 % ± 0.13 %	−3.90 % ± 0.13 %
70 %	30.93	30.75	−4.04 % ± 0.16 %	−4.57 % ± 0.16 %
80 %	30.80	30.62	−4.43 % ± 0.17 %	−4.98 % ± 0.15 %
90 %	30.62	30.42	−4.99 % ± 0.25 %	−5.60 % ± 0.25 %
100 %		30.24		−6.17 % ± 0.24 %

3.3 About Macroscopic Fundamental Diagram

SUMO edge-based measures were collected to obtain speed, flow, and link density measurements, as reported in Table 3.4. To build the fundamental network diagrams, it is necessary to have network measurements instead of edge measurements. It will be necessary to aggregate the edge measurements to obtain the network data of speed, flow and density. The procedure for calculating these values and constructing the MFD is described in paragraph 1.3.
The edge-based values are recorded for each fixed period for each link. As reported in the previous paragraph, a period of 15 *min* was chosen, within which the stationary flow conditions apply. Under stationarity flow conditions, the fundamental law of traffic flow applies [32].

$$q_i = k_i \cdot v_i \tag{3.5}$$

Where:

- i represents the generic link of the network;
- q_i is the flow, number of vehicles passing through a lane section in a given time;
- k_i is the density, attribute `laneDensity`, number of vehicles that at a given instant are contained in a given lane length;
- v_i is the spatial average speed, attribute `speed`, spatial average of the instantaneous speeds of vehicles that are contained in a given lane length at instant of time.

Under the assumption of stationary flow conditions, the flow does not depend on position and the density does not depend on time.
As the flow is a value not directly recorded by SUMO, the fundamental law of traffic flow, Equation 3.5, is valid within the given period for each individual link in the network.
The aggregation of edge variables into network variables using the outputs of microsimulation software is described in the work of Lu et Al. (2020) [25]. Average network flow Q, density K and speed V can be determined with the following Equations.

$$K = \frac{\sum_{i=1}^{N} N_{vi}}{\sum_{i=1}^{N} l_i} \tag{3.6}$$

$$V = \frac{\sum_{i=1}^{N} v_i \cdot N_{vi}}{\sum_{i=1}^{N} N_{vi}} \cdot 3.6 \tag{3.7}$$

$$Q = \sum_{i=1}^{N} v_i \cdot k_i \cdot 3.6 \tag{3.8}$$

Where:

- K, V, Q are the average network density (in veh/km), speed (in km/h) and flow (in veh/h);

Table 3.9: MFD: maximum flow, optimum density and optimum speed

Automated vehicles penetration rate	Q_{max} $(veh/h/ln)$	K_0 (veh/km)	V_0 (km/h)
0%	392.98	15.96	24.81
10%	390.83	15.63	25.13
20%	385.55	16.00	24.22
30%	387.34	15.93	24.47
40%	388.98	15.76	24.76
50%	385.22	15.68	24.76
60%	383.13	16.10	23.98
70%	379.72	15.75	24.27
80%	378.86	15.75	24.18
90%	377.40	15.33	24.89
100%	378.62	15.64	24.46

- N is the total number of link i;
- N_{vi} is the total number of vehicles passing through the generic link i;
- l_i is the length of the generic link i, in km;
- v_i is the average space speed of the generic link i, in m/s;
- k_i is the density of the generic link i, in veh/km.

Using these formulas is equivalent to using the general Equations 1.8, 1.9 and 1.10 proposed by Geroliminis and Daganzo (2007).
Regarding the demand profile, using the real traffic flow profile no critical points appear in the MFD. Therefore, as reported in the paragraph 2.4, it was decided to use an intensified flow demand for the construction of the MFD, so that both the free flow area and the unstable area of the diagram are covered. In the intensified flow demand, flow increases initially, until the network congestion situation is reached, then the demand starts to decrease. The tern of points obtained from using the above Equations is inserted into the flow-density diagram. Figure 3.5 shows the MFD for a 50% penetration rate. Figure 3.5 (a) shows the experimental points obtained from a single run, corresponding to seed 1, while Figure 3.5 (b) shows the experimental points from all runs considered. There are no significant deviations in the shape of the fundamental diagram between one run and the following ones. The diagrams obtained show a considerable dispersion of values, especially in the congested part of the diagram. The presence of two sets of parallel points in the congested part of the diagram can be seen. The first set of points is located in the upper part of the diagram, while the second set of points is located in the lower part of the diagram, parallel to the first. To better investigate the cause of the phenomenon, it is decided to plot the points of the fundamental diagram in chronological order, as shown in Figure 3.6 (a). From the analysis of the Figure, the

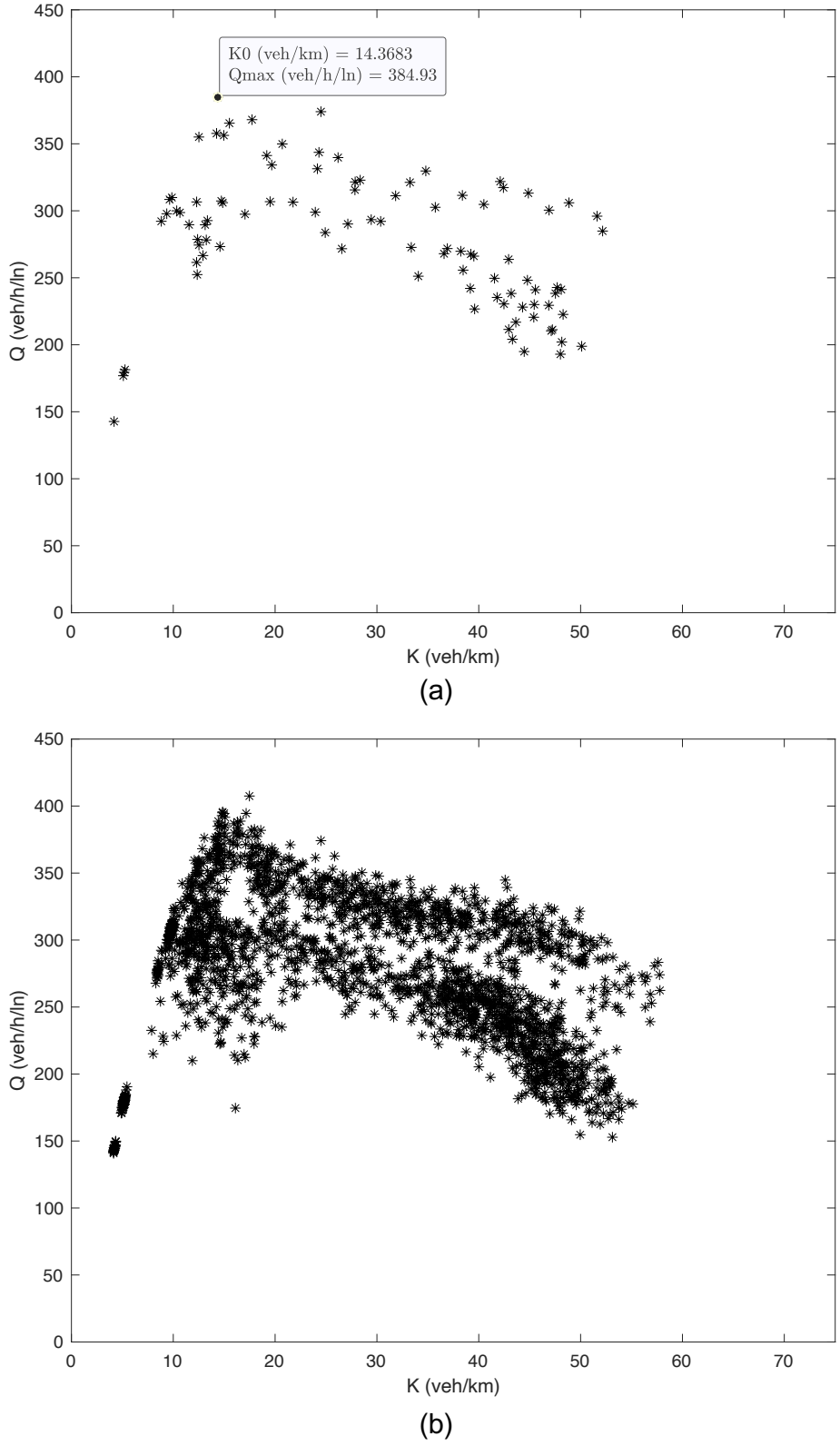

Figure 3.5: 50% penetration rate Macroscopic Fundamental Diagram. (a) Plot of the seed 1 simulation and (b) plot of all 25 seeds

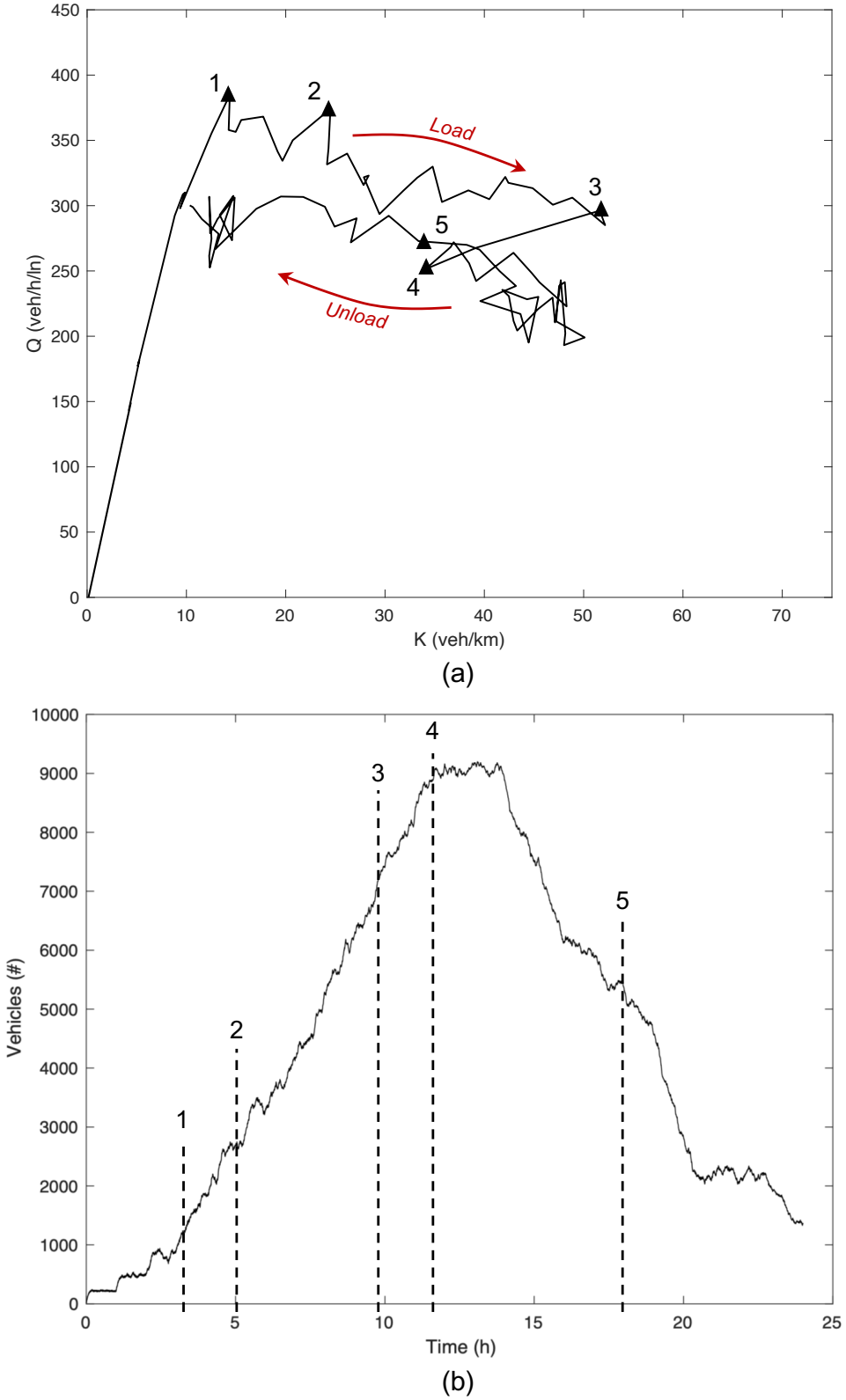

Figure 3.6: Hysteresis cycle in the seed 1 simulation, 50% penetration rate Macroscopic Fundamental Diagram. (a) Plot of the Macroscopic Fundamental Diagram and (b) demand profile

Table 3.10: MFD: linear regression analysis

	Q_{max}	K_0	V_0
t-test	−7.284	−1.203	−6.872 exp −15
p-value	<0.001	0.230	1.000

occurrence of a hysteresis loop within the unstable area of the diagram is evident.
In the presence of a hysteresis loop, a splitting of the curve is obtained: if travelled from left to right, one path is obtained; if travelled in the opposite direction, another path is obtained. Within the congested branch of the diagram, the congestion loading phase follows one path, while the congestion unloading phase follows another path. In particular, the congestion unloading branch occurs with a lower flow than the loading branch, at the same density. This can be explained by the non-homogeneity of the demand distribution within the network, i.e. by the fact that demand takes a certain amount of time to settle evenly. The result observed within the diagrams is in accordance with Geroliminis and Daganzo (2007) [9] and reported in Chapter 1, which predicted MFD with little scattered values in case of homogeneous conditions. The observation of a hysteresis loop within an MFD in the presence of spatially non-homogeneous density within the network is also due to Buisson and Ladier (2009) [7] and Zhang et Al. (2020) [48]. A weakly dispersed fundamental diagram could be obtained by dividing the network into uniformly congested parts, i.e. into parts where the spatial evolution of demand is similar. The uniform density condition requires all roads in the network to be either congested or in the low-density state. The observations made so far for the scenario corresponding to a 50% penetration rate are also valid for all other scenarios analyzed. This can be seen by observing the MFD for each analysed scenario, reported in the Appendix.
The MFD analysis is useful for determining the flow, density and speed parameters that identify the critical point of the diagram. The critical point is the weak point of the network, which divides the free flow condition from the congested condition. Several methods for determining these points were shown in Chapter 1: "method of cuts" [9] or Ambuhl's mathematical formula [2]. However, it was decided not to use the proposed methods, but to adopt an empirical procedure based on direct observation of the parameters of interest, as the aim is to estimate the values that characterize the critical point of the diagram rather than the entire function. Therefore, for each run of each scenario considered, the maximum flow value Q_{max} and the corresponding optimum density value K_0 are observed. Figure 3.5 (a) shows the values of maximum flow and optimal density (seed 1, 50% penetration rate). The optimum speed value $V_{free-flow}$ is obtained by applying the fundamental law of traffic flow, Equation 3.5. For each scenario the values of maximum flow, optimum density and optimum speed are obtained by averaging the values of each individual run, given in Table 3.9. The maximum flow measurements obtained are similar to those available in the literature for cities and contexts similar to the city of Hannover. In particular, a maximum flow value of 530 $veh/h/ln$ was observed in the cities of Marseille (France) and Zurich (Switzerland) [2]

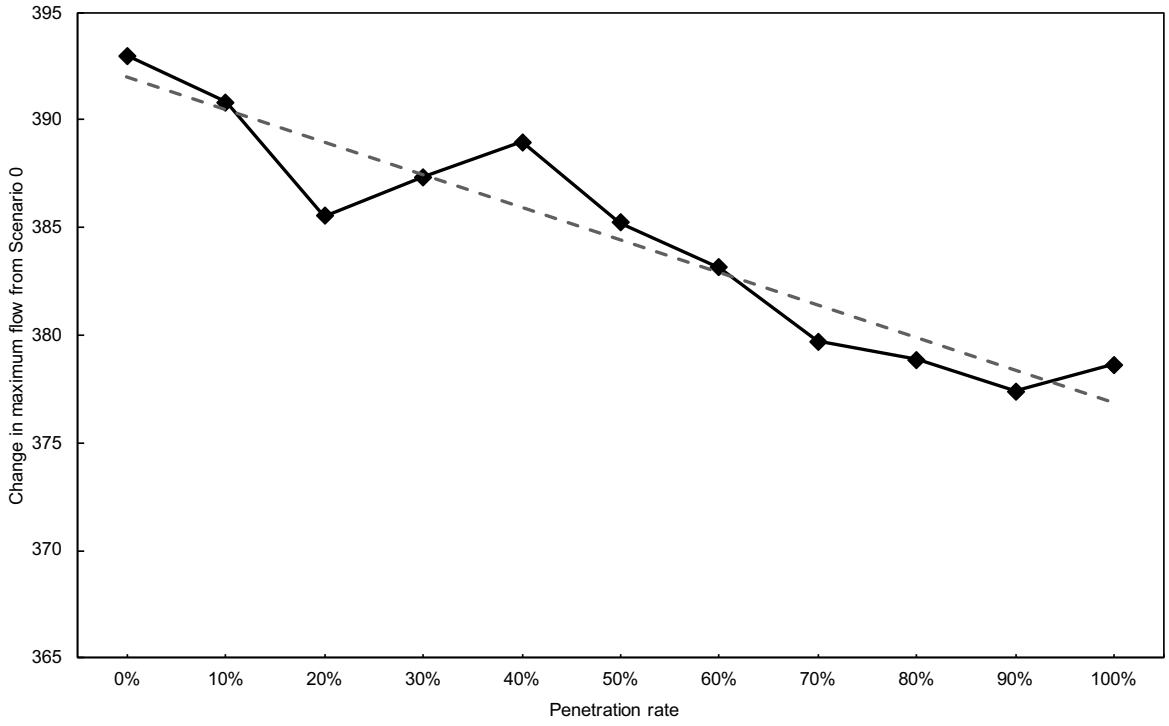

Figure 3.7: Change in maximum flow from Scenario 0

and a value of 600 $veh/km/ln$ was observed in the city of Toulouse (France) [7]. It can be seen that the authors used portions of the city involving the presence of suburban roads and highways, as well as urban roads.
In order to evaluate whether the observed parameters show a statistically significant variation from the Scenario 0, a linear regression analysis is performed. A confidence level of 95%, i.e. $\alpha = 5\%$, is defined and a linear regression analysis of the values of maximum flow, optimum density and optimum speed at varying penetration rates is performed. Table 3.10 shows the results of the statistical analysis performed. The *null hypothesis* states that the regrassion line coefficient is equal to zero, which, in physical terms, means that the penetration rate has no effects on the dependent variable analyzed. The *p-value* is the observed significance level, the lower its value the stronger its evidence against the null hypothesis. The *t-test* is a parameter of the Student distribution. The null hypothesis is rejected if p-value $< \alpha$, while it is not rejected otherwise.
From the results obtained, it is evident that the only value with a statistically significant variation is the maximum flow Q_{max}. The graph in Figure 3.7 shows how, as the penetration rate increases, a decrease in maximum flow is expected. The maximum flow value changes from 392.98 $veh/h/ln$ for an automated vehicles penetration rate of 0% to 378.62 $veh/h/ln$ for an automated vehicles penetration rate of 100%. The decrease in percentage terms is 3%.
The values of optimum density and optimum speed, on the other hand, show no statistically significant change as the penetration rate of automated vehicles increases. Despite this, graphs of the trend in optimum density and optimum speed as the number of autonomous vehicles on the road increases are shown in Figures 3.8 and 3.9.

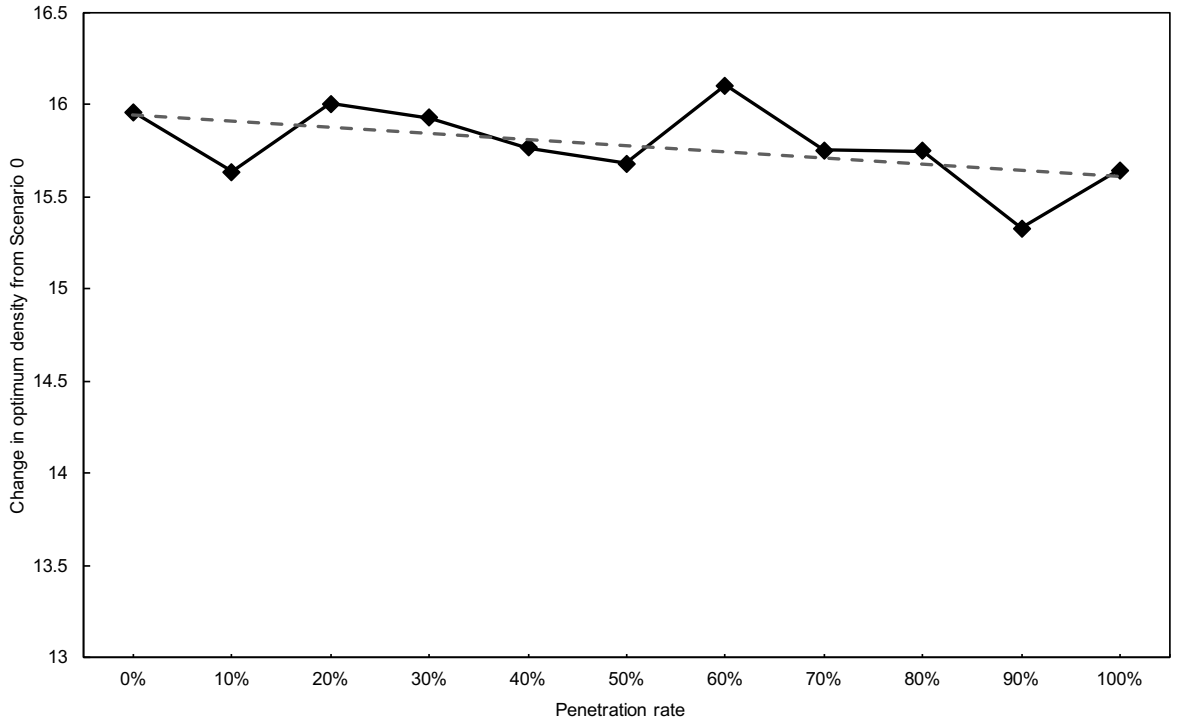

Figure 3.8: Change in optimum density from Scenario 0

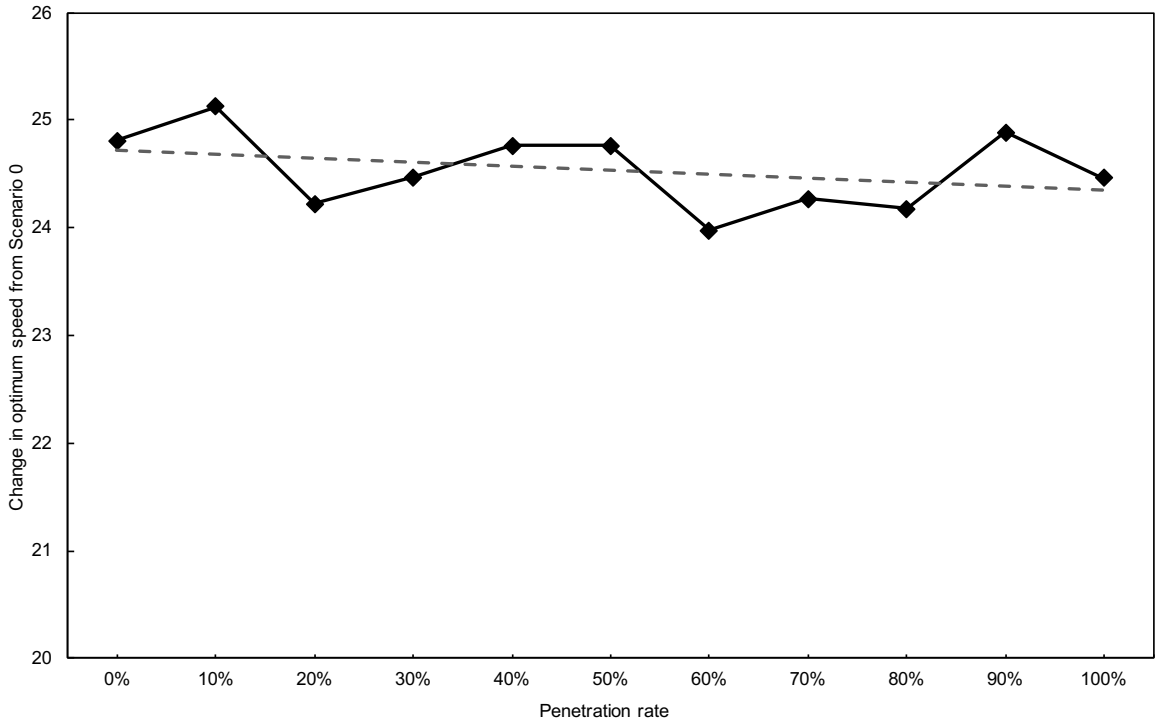

Figure 3.9: Change in optimum speed from Scenario 0

Table 3.11: SUMO SSM measures

Output name	Unit of measure	Description
`pos`	m	The position at which the lane change took place
`begin`	s	The simulation time at which the conflict begins
`end`	s	The simulation time at which the conflict end
`ego`		Name of the ego vehicle
`foe`		Name of the foe vehicle
DRAC `type`		Type code of the corresponding encounter type
DRAC `value`	m/s^2	The maximum value of DRAC measured within the conflict time interval
TTC `type`		Type code of the corresponding encounter type
TTC `value`	s	The minimum value of TTC measured within the conflict time interval
PET `type`		Type code of the corresponding encroachment type
PET `value`	s	The value of PET measured within the conflict time interval

3.4 About Surrogate Safety Measures

SUMO surrogate safety measures output was collected in order to count and identify the conflicts that occur between vehicles. The software allows a percentage of vehicles to be equipped with a device capable of obtaining information on conflicts, called the SSM device. It was decided to equip 10 % of vehicles with an SSM device. We therefore expect to obtain a number of conflicts equal to 1/10 compared to the real one. According to the software documentation, SUMO records a conflict if one of the following conditions is satisfied:

- TTC $< 3.0\ s$;
- PET $< 2.0\ s$;
- DRAC $> 3.0\ m/s^2$.

In accordance with the requirements of the FHWA, reported in paragraph 1.4, SUMO allows the modeler to identify three types of conflict: rear-end, crossing and merging/lane change conflict. In this case, conflict analysis focuses on the type of merging/lane change conflict, excluding the other types. The goal behind this choice is to analyze the impacts that the different lane change vehicle's microscopic behavior has on safety.
Merging/lane change conflicts involve only one of the security measures presented, the TTC. We choose to analyze conflicts that have a TTC value lower than 3.0 s. The chosen value, although very high, is supported by the relevant literature, reported in Chapter 1.
A further condition is set for the analysis of the results: the type of vehicles involved in a conflict situation. We decide to consider only the cases in which human error is

Table 3.12: Number of conflicts

AV penetration rate	Number of CV conflicts	Change in number of CV conflicts from Scenario 0	Number of mixed conflicts	Number of total conflicts
0 %	1832	100.00%	0	1832
10 %	1423	77.70%	193	1616
20 %	1180	64.41%	288	1467
30 %	901	49.20%	387	1288
40 %	670	36.59%	448	1118
50 %	466	25.45%	465	931
60 %	302	16.50%	450	752
70 %	174	9.50%	394	568
80 %	74	4.05%	299	373
90 %	18	1.00%	171	189
100 %	0	0.00%	0	0

possible, excluding the possibility of failure of automated vehicles, or assuming that automated vehicles are designed to fail as little as possible. As shown in the Table 3.11, the type of vehicle involved is not explicitly reported in the output file, while only the name is reported. To get the data of interest, we use the values generated by the trip output, which contains both the list of vehicles and the vehicle type associated. Conflicts are therefore considered between conventional vehicles and between conventional and automated vehicles, i.e. mixed vehicles conflicts, but only when the conventional vehicle has to react to a lane change maneuver of the automated vehicle, not vice versa. The remaining cases are excluded from the analysis.
A conflict thus described is shown in the Figure 3.10. The conflict occurs between the two purple vehicles, with the first vehicle, the leader vehicle, making a lane change maneuver to move into the leftmost lane (a). The second vehicle, the follower vehicle needs to perform the same maneuver as the leader vehicle and activates the direction indicators to move to the left lane (b). Realizing that it has a too small TTC, the follower vehicle brakes (c) and aborts the lane change (d), turning off the direction indicators and staying in the current lane. The maneuver will be completed by the follower vehicle at a later time (e), i.e. when there are safety conditions to carry out the maneuver. The minimum TTC value recorded during the encounter is the one relating to point (c). This value is compared with the TTC threshold value in order to verify the actual occurrence of a conflict.
Table 3.12 shows the number of conflicts between conventional vehicles and mixed vehicles as described above. The number of conflicts between conventional vehicles decreases as the penetration rate increases, while the number of conflicts increases as the penetration rate increases, up to 50 % of autonomous vehicles in circulation. From the 50 % penetration rate, the number of mixed conflicts begins to decrease as the number of conventional vehicles in circulation decreases. However, observing the total of conflicts,

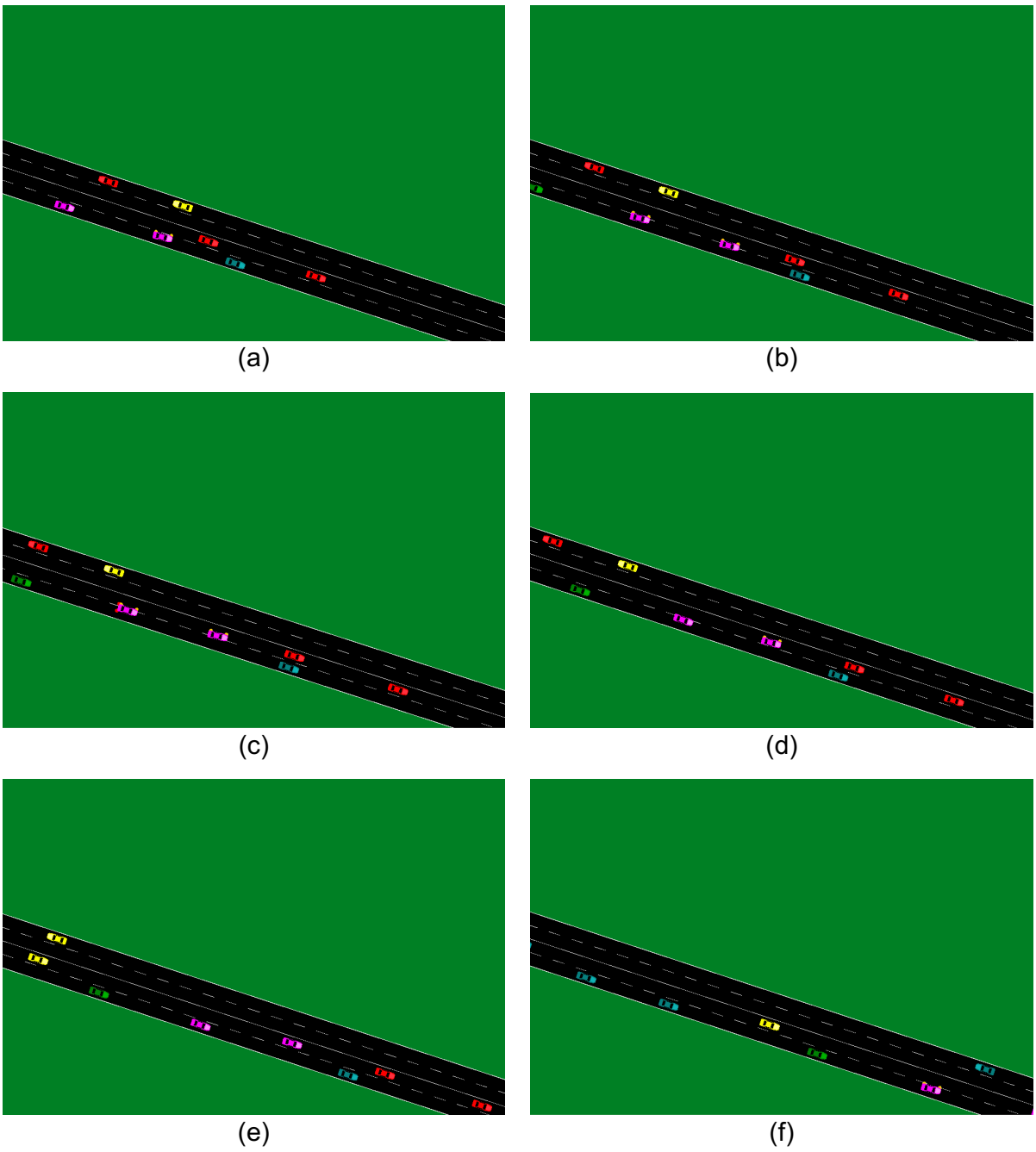

Figure 3.10: Screenshot of a lane change conflict between vehicles. The conflict occurs between the two purple vehicles: (a) The leader vehicle performs a lane change maneuver; (b) The follower vehicle needs to perform the same maneuver as the leader; (c) The follower vehicle has too small TTC value so it brakes; (d) The follower vehicle refuses changing lanes; (e) The follower vehicle changes lanes at a later time, safely.

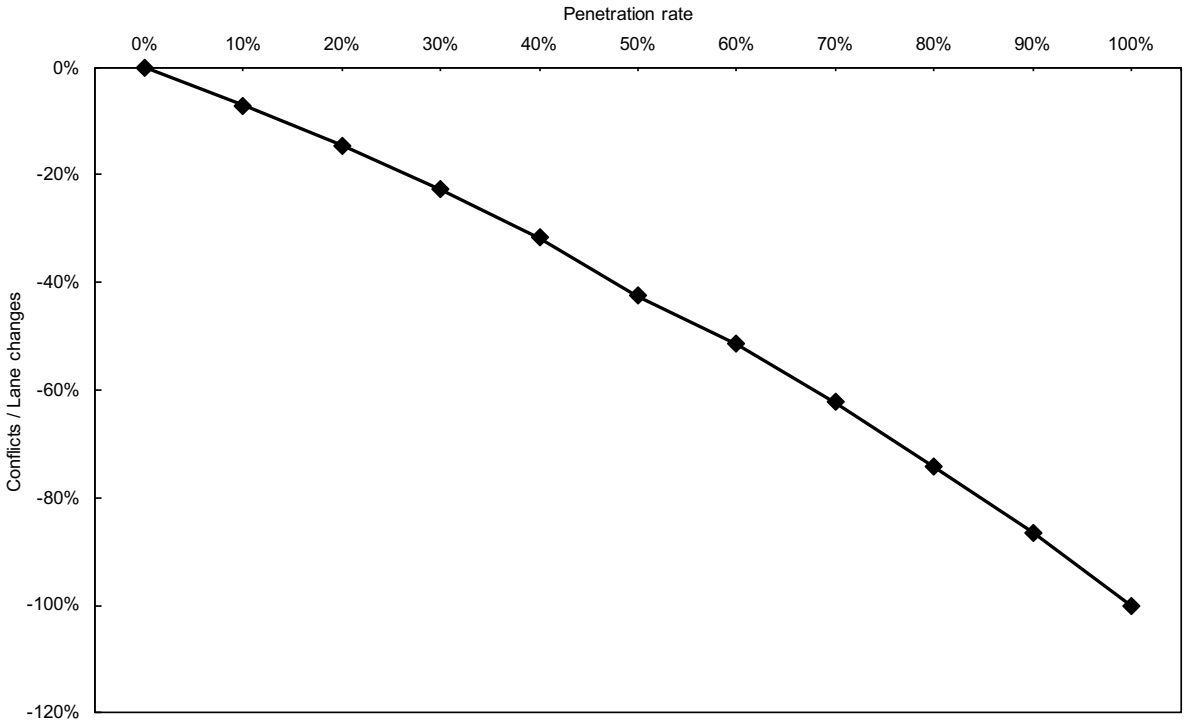

Figure 3.11: Change in the ratio conflicts/lane changes from Scenario 0

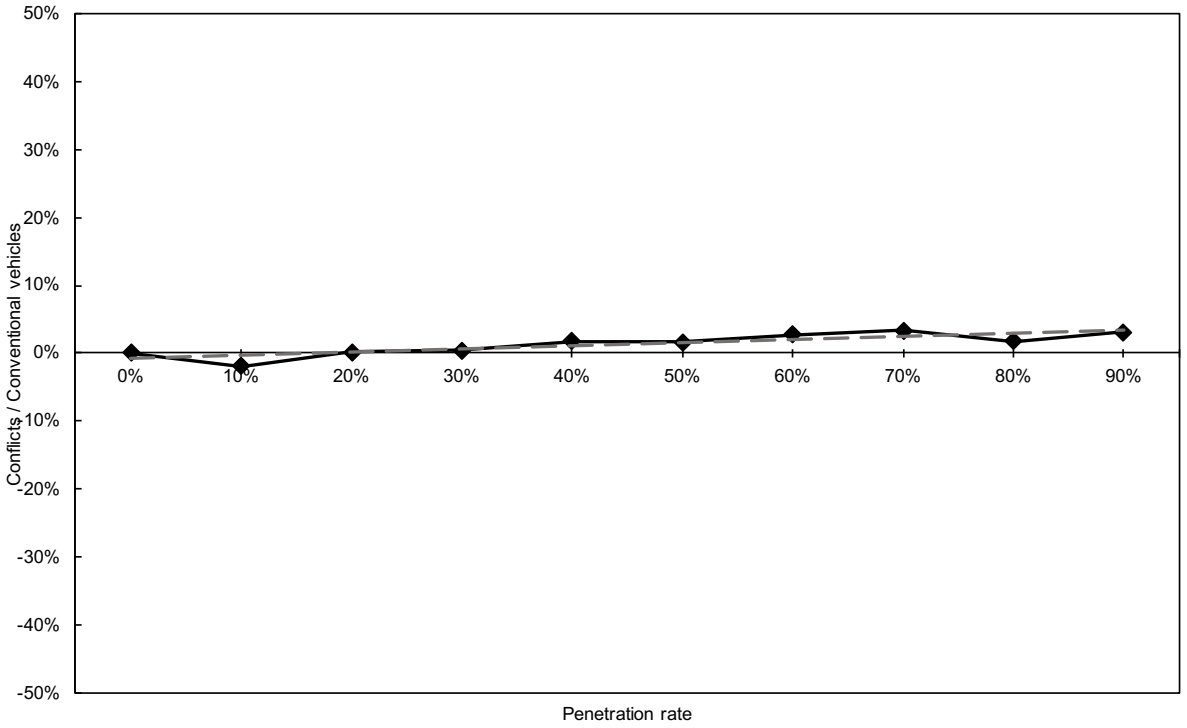

Figure 3.12: Change in the ratio conflicts/conventional vehicles from Scenario 0

Table 3.13: Change in number of conflicts from Scenario 0

Automated vehicles penetration rate	Change in the ratio conflicts/lane changes From Scenario 0	Change in the ratio conflicts/conventional vehicles From Scenario 0
0 %	0.00%	0.00%
10 %	−7.12%	−1.98%
20 %	−14.47%	0.14%
30 %	−22.74%	0.46%
40 %	−31.60%	1.74%
50 %	−42.47%	1.68%
60 %	−51.39%	2.69%
70 %	−62.19%	3.30%
80 %	−74.27%	1.73%
90 %	−86.46%	3.10%
100 %	−100.00%	

it can be seen that this also decreases as the penetration rate increases.
Making observations exclusively based on these results can lead to data interpretation errors, as conventional vehicles decrease as the penetration rate of automated vehicles increases, and therefore it is expected that the total number of conflicts decreases. To avoid wrong considerations, the following ratios have been calculated.

$$\frac{\text{Conflicts}}{\text{Lane changes}} \tag{3.9}$$

$$\frac{\text{Conflicts}}{\text{Conventional vehicles}} \tag{3.10}$$

The ratio 3.9 is visible in Table 3.13 and in the graph in Figure 3.11. The decreasing trend occurs despite both the numerator and the denominator of the fraction being decreasing. This means that conflicts decrease more than proportionally with respect to lane change maneuvers. Limited to lane change maneuvers, an increase in safety is therefore expected.
The ratio 3.10 is visible in Table 3.13 and in the graph in Figure 3.12. The increasing trend occurs despite the fact that both the numerator and the denominator of the fraction are decreasing. Limited to this ratio, to assess whether the variation with respect to Scenario 0 is statistically significant, a linear regression analysis is conducted. Defined at a confidence level of 95%, i.e. $\alpha = 5\%$, a linear regression analysis of the ratio 3.10 is performed as the penetration rate of automated vehicles increases. Table 3.14 shows the results of the statistical analysis performed. The null hypothesis requires the coefficient of the line to be 0, i.e. no statistically significant variation between the values. The observed p-value less than 0.001 leads to the rejection of the null hypothesis. The p-value is very small, which means that the inferential conclusion is very strong. It can be stated that the penetration rate has a statistically significant effect on the ratio

Table 3.14: Conflicts/conventional vehicles: linear regression analysis

	$\frac{\text{Conflicts}}{\text{Conventional vehicles}}$
t-test	3.895
p-value	<0.001

3.10.

The observed growing trend means that the conflicts attributed to a single conventional vehicle increase as the automated vehicle's penetration rate increases, i.e. as the number of conventional vehicles in circulation decreases. This leads to the observation of a worsening of safety conditions, although minimal and limited to a 3% compared to Scenario 0. The worsening is due to the fact that, as the penetration rate of autonomous vehicles increases, conventional vehicles are more likely to create conflict situations.

Chapter 4

Discussion and Future Outlook

This thesis investigates the impact that the introduction of automated vehicles in an urban network will have in terms of efficiency and safety in vehicle flow. In particular, the aim of the thesis is to analyse how the lane change behavior of different vehicles impacts on travel time, speed and safety. Few publications on the subject focus on urban scenarios, while much literature is available on the evaluation of impacts on highways, both with theoretical references and with analyses using micro and macro-simulation tools. Furthermore, there are no publications exclusively analysing the impacts of lane change behavior. The present work aims to close this gap in the literature.
To achieve this goal, the urban network of the city of Hannover (Germany) was modelled and two different demand profiles were loaded. The first demand profile, real traffic flow, relates to a typical working day, while the second profile considered, intensified flow, is a fictitious demand profile obtained by increasing traffic demand until a saturation is reached and decreasing it thereafter. Then, in order to include both conventional and automated vehicles within the vehicle traffic, a literature review was performed to identify the parameters that best describe the behavior of each type of vehicle. Scenario 0 is characterised by the presence of conventional vehicles only. Each subsequent scenario is created by increasing the percentage of automated vehicles on the road by 10%. For each scenario, multiple simulation runs are performed. The results are discussed by comparing the subsequent scenarios with the reference Scenario 0.

4.1 About Efficiency

As far as efficiency, the measurements of travel time and average speed were used, in addition to the use of macroscopic fundamental diagrams. Mean travel time is defined as the average time a vehicle takes within the network, while mean speed is defined as the average spatial speed within the network. Fundamental network diagrams were used to determine maximum flow, optimum density and optimum speed. From the analysis of the presented parameters, considerations are made regarding travel time, mean speed and maximum flow. As can be seen from the graph shown in Figure 4.1 and from the results shown in Table 3.9, a general worsening of the system's performance is observed as the automated vehicles penetration rate increases. The general deterioration in terms of efficiency is likely explainable by the more cautious behavior

of automated vehicles compared to conventional vehicles. The latter are inclined to accept smaller gaps to perform a lane change maneuver when compared to conventional vehicles. The parameter that most influences the behaviour of these vehicles is the one concerning gap acceptance theory. The fact that automated vehicles accept higher gap values than conventional vehicles makes them more cautious in their behaviour.
These conclusions contrast to what is observed in the literature, where a general improvement in performance is expected as the number of automated vehicles on the road increases. It should be noted that the authors modify both vehicle's behavioural parameters, i.e. headway held by vehicles and minimum space maintained by vehicles in jam conditions, and lane change and car following behavior. Lu et. Al [25] observed an improvement in maximum flow by 16% from the scenario with only conventional vehicles to the scenario with only automated vehicles, while Friedrich [13] observed an improvement in maximum flow by 40% from the same scenarios. The authors agree in attributing the improved performance of the lower headway observed between automated vehicles and the smaller gap that automated vehicles maintain in jam conditions. However, having modified both behavioural parameters, lane change and car following parameters, the effects of individual behaviours are not visible, but an overall effect is observed due to the sum of individual behaviours.
We can conclude that the lane change behavior of automated vehicles, performed in a more cautious way, lead to a reduction in system performance. The performance improvement found in the literature could be attributed to other models governing vehicle motion, such as the car following model, or to driver behavioural parameters, such as headways or gaps manteined in jam conditions. It has been shown that the parameters that most influence MFD are the headways held by vehicles and the minimum space maintained by vehicles in jam conditions, which are not the subject of analysis in this thesis. Observing only the lane change behavior, it can be seen that the car following model and the behavioural parameters lead to an improvement in performance that can absorb the deterioration due to lane change behavior.

4.2 About Safety

As far as safety is concerned, a conflict analysis was carried out through the use of surrogate safety measures. The 10% of the circulating vehicles were equipped with an SSM device, in order to record encounters and, consequently, conflicts by comparing the recorded SSM values with the corresponding threshold values. Analyses and considerations are made with regard to lane change maneuvers, only in the case where a conventional vehicle has to react to a maneuver of an automated vehicle. Indeed, it is assumed that automated vehicles are designed to fail as little as possible.
The analysis of conflict results is made with regard to lane change maneuvers and to the presence of conventional vehicles in the network. With regard to lane change maneuvers, an increase in safety is expected. Analysis of the data shows that conflicts decrease more than proportionally with respect to lane change manoeuvres as the penetration rate of automated vehicles increases. The expected decrease in the number of lane changes leads to a more than proportional decrease in the number of conflicts.
As far as the presence of conventional vehicles is concerned, their decrease does not lead to any apparent improvement in safety within the network. An analysis of the data

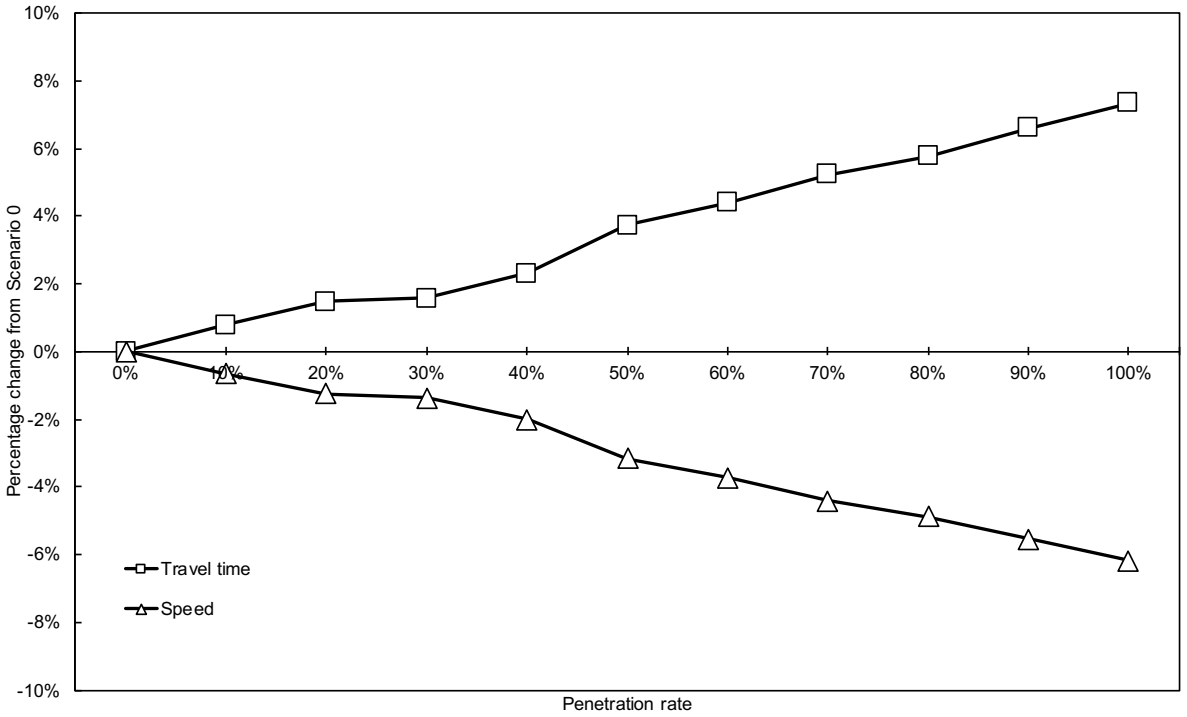

Figure 4.1: Change from the Scenario 0 of mean travel time and speed

shows that conventional vehicles show a greater propensity to generate conflicts as the penetration rate increases. The safety deterioration achieved, however, at 3%, is low. The final situation with a penetration rate of 90%, i.e. a circulation of 10% conventional vehicles, can be considered comparable to Scenario 0 in terms of the number of conflicts generated by conventional vehicles.
Studying the conflicts generated by the interaction between conventional and automated vehicles is important since automated vehicles will be circulating in increasing numbers in the near future. The results presented are aimed at closing this gap, limited to the analysis of lane change maneuvers.

4.3 Future Outlook

The results presented and discussed are based on models built and tested for conventional vehicles, i.e. the LC2013 model in SUMO. Furthermore, the parameters for conventional vehicles were assumed constant as the penetration rate increases, i.e. always assuming the same behavior of the drivers as the penetration rate increases. Future studies could close this gap by calibrating the parameters for conventional vehicles for each scenario. There could be an adjustment of the driving style of drivers of conventional vehicles to the driving style of automated vehicles, making conventional vehicles more prudent as the penetration rate increases.
One possible improvement of SUMO's models concerns the actual maneuvers of automated vehicles. The development of models specifically built on the behavior of

automated vehicles with dedicated parameters is expected. Such models should take into account both the different driving styles and the different equipment possessed by automated vehicles.
Further studies are needed within urban contexts other than the one considered, i.e. in cities other than European cities, as well as considering road networks composed of roads of different categories. In urban contexts, it is also necessary to study the effects of the introduction of automated vehicles on traffic by modifying all vehicle behavioral parameters.

Appendix A

Macroscopic Fundamental Diagram

Graphs of the Macroscopic Fundamental Diagrams for the different scenarios analised are given in this Appendix. Each scenario is is characterised by a different penetration rates of automated vehicles within traffic. The *Scenario 0* refers to a scenario where traffic is composed of conventional vehicles only. For each subsequent scenario there is an increase of 10% of automated vehicles in circulation, with the final scenario composed by only automated vehicles in circulation.

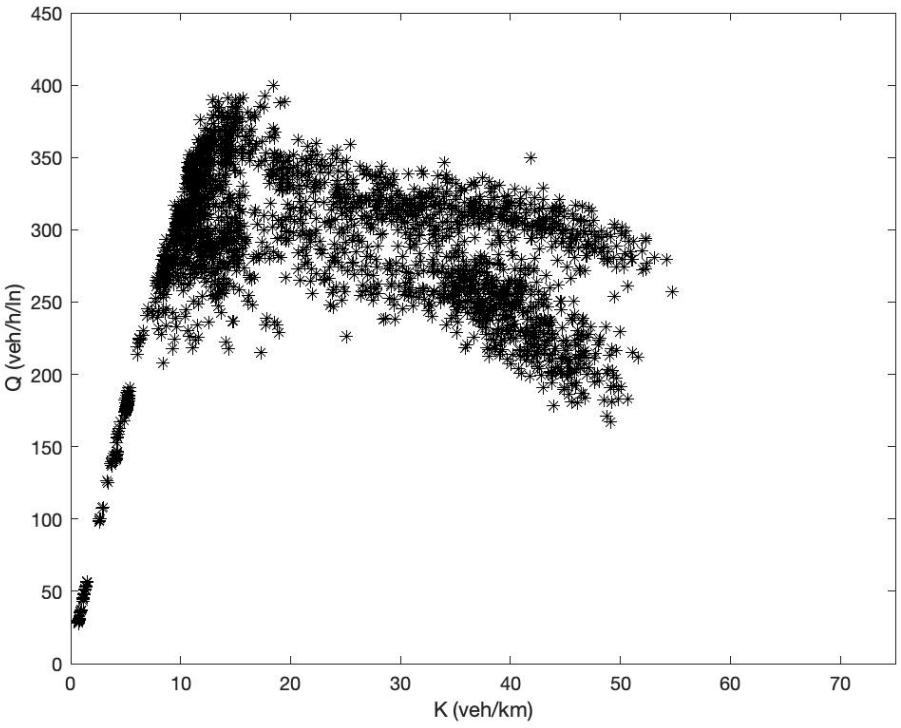

Figure A.1: MFD of the 0% automated vehicles penetration rate, *Scenario 0*

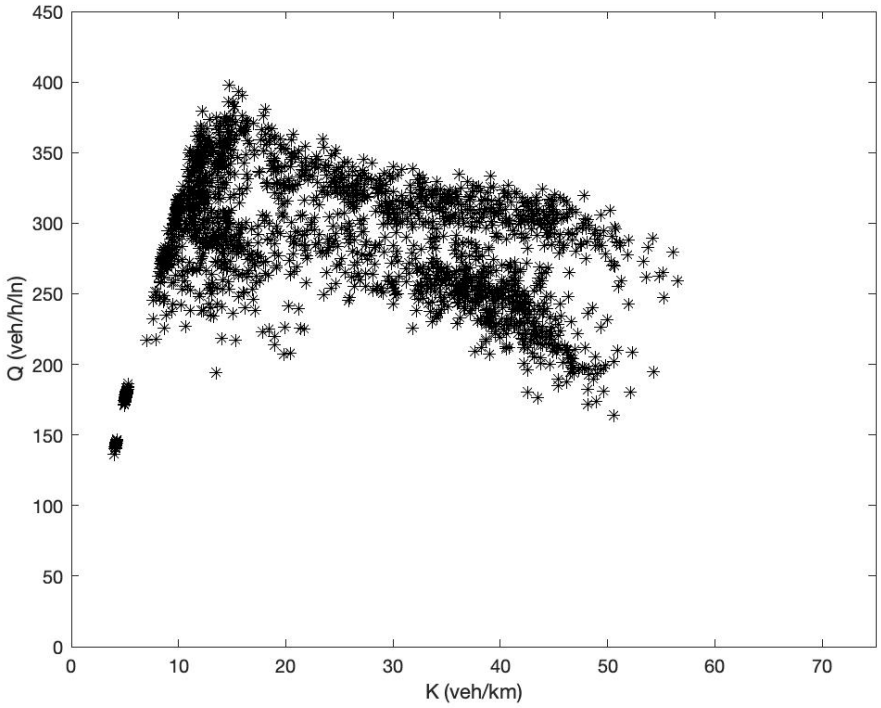

Figure A.2: MFD of the 10% automated vehicles penetration rate

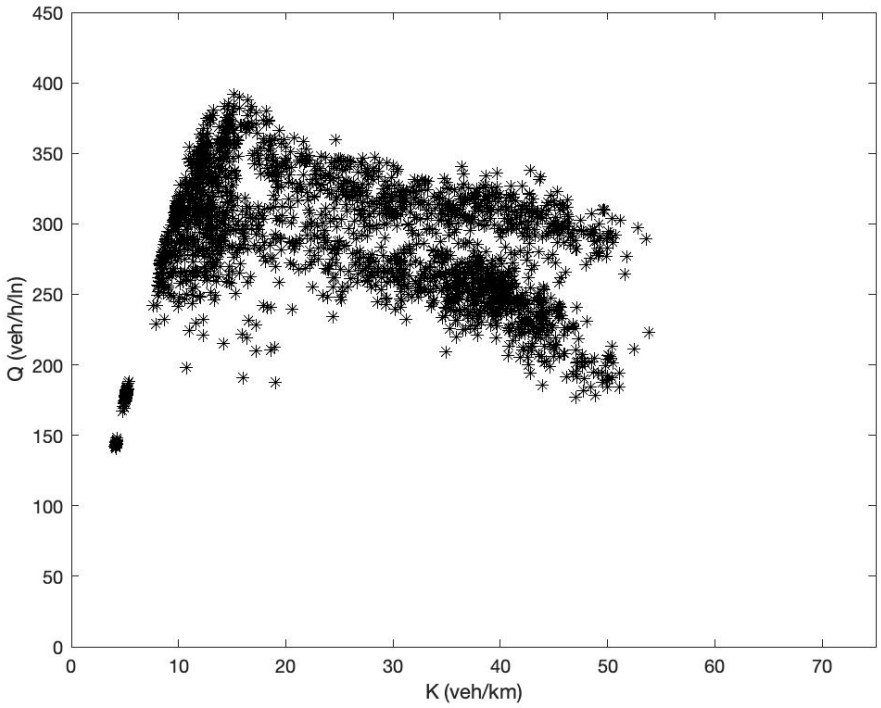

Figure A.3: MFD of the 20% automated vehicles penetration rate

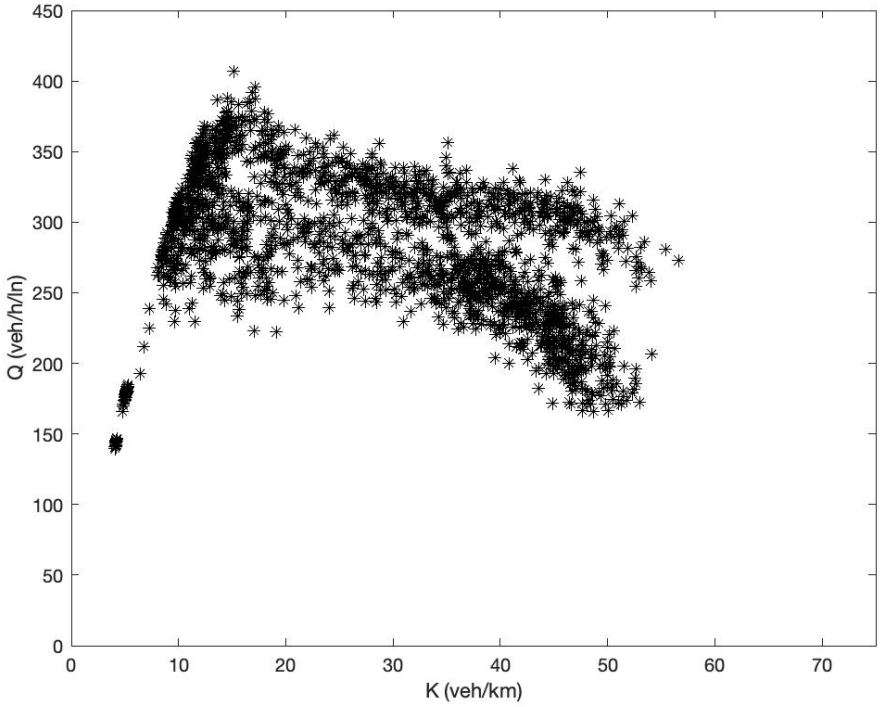

Figure A.4: MFD of the 30% automated vehicles penetration rate

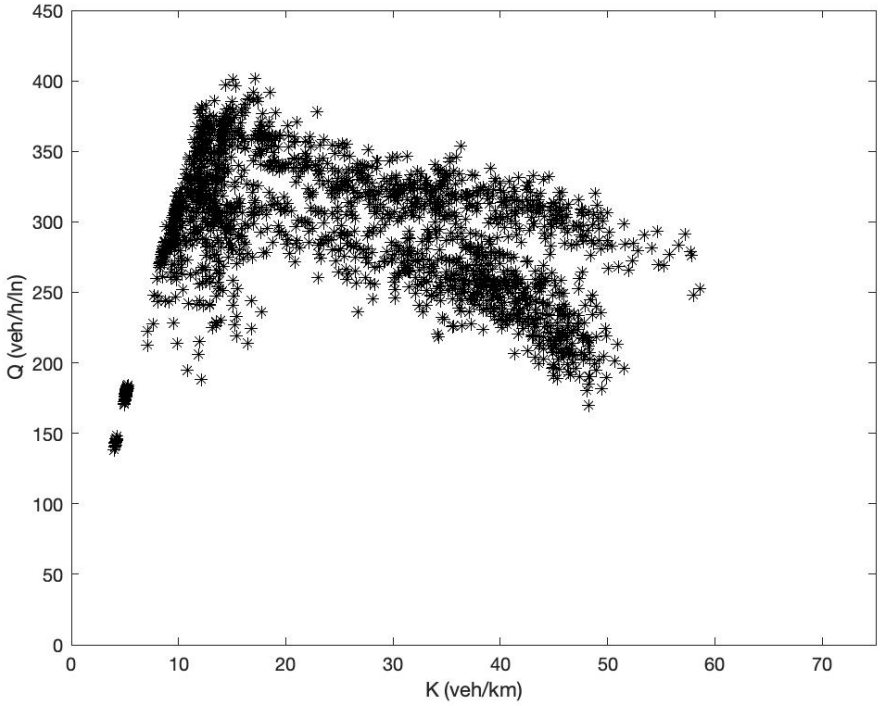

Figure A.5: MFD of the 40% automated vehicles penetration rate

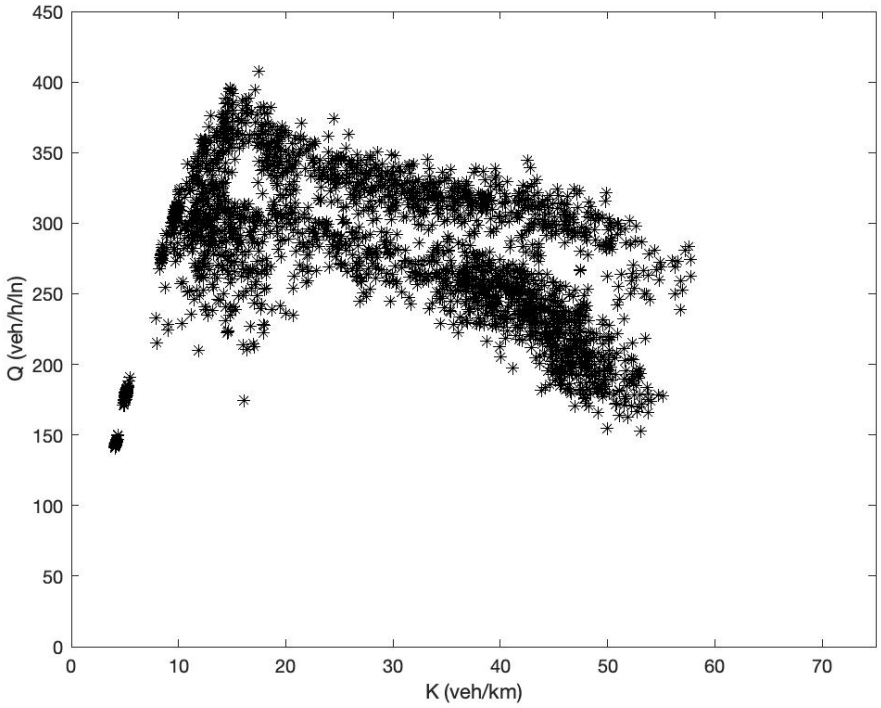

Figure A.6: MFD of the 50% automated vehicles penetration rate

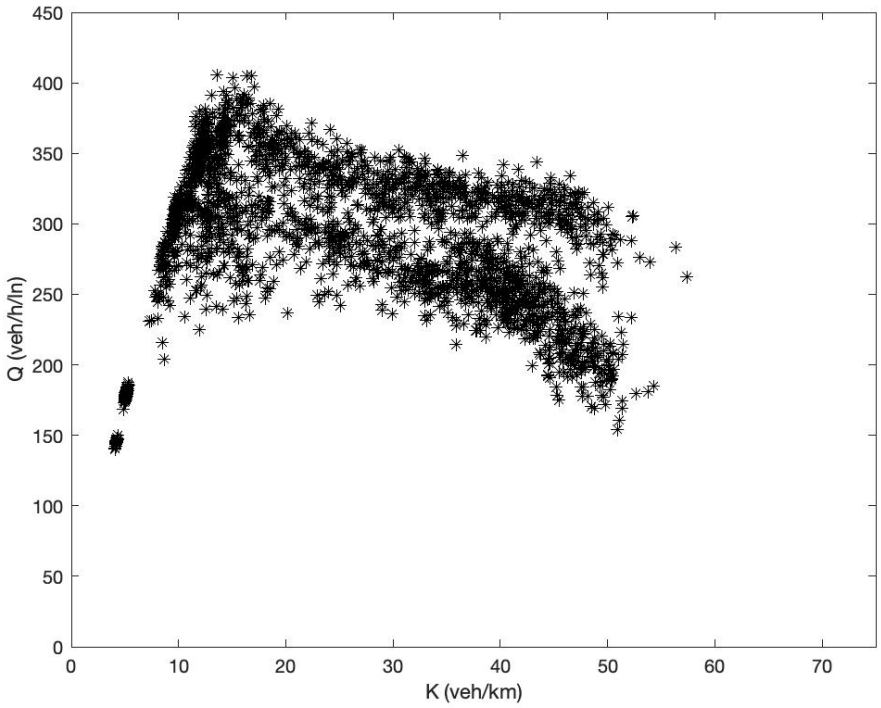

Figure A.7: MFD of the 60% automated vehicles penetration rate

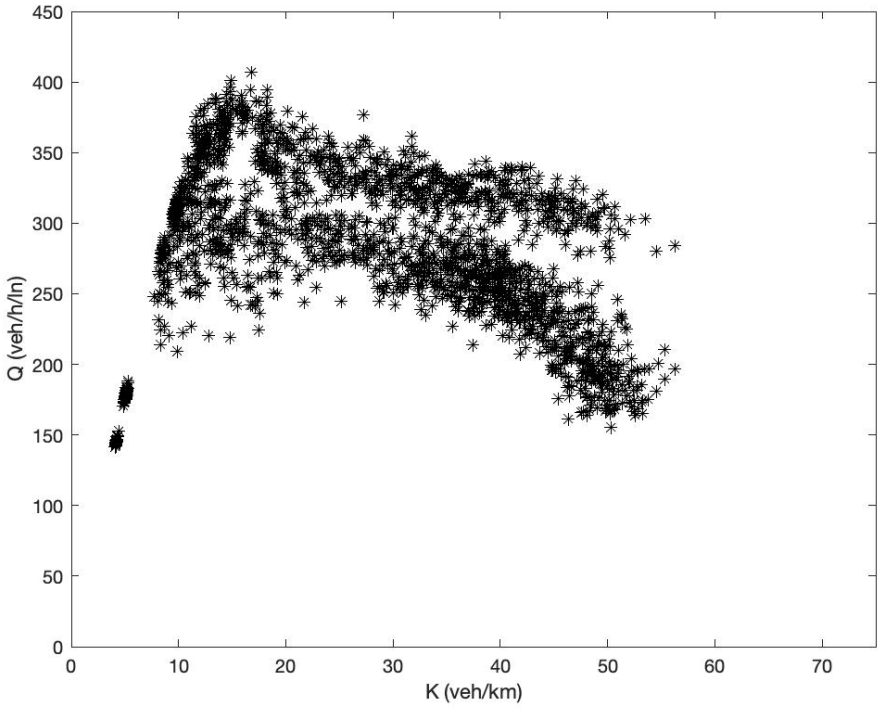

Figure A.8: MFD of the 70% automated vehicles penetration rate

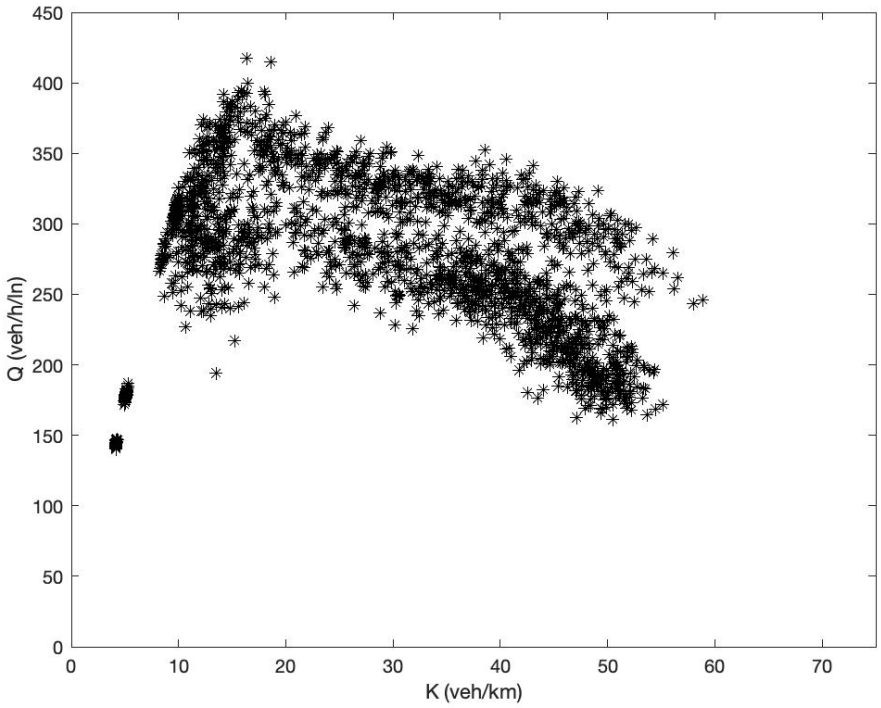

Figure A.9: MFD of the 80% automated vehicles penetration rate

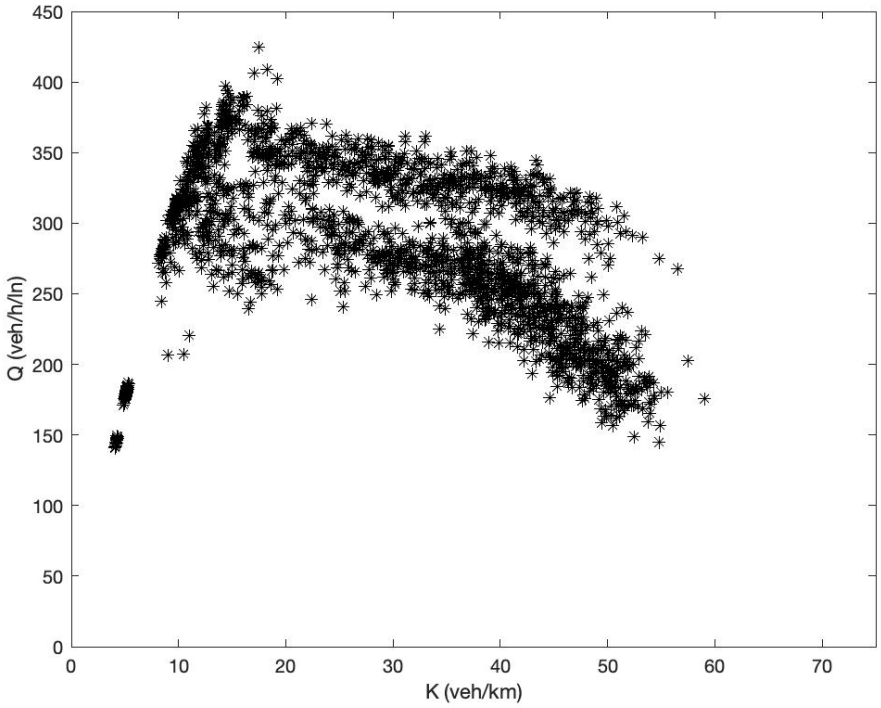

Figure A.10: MFD of the 90% automated vehicles penetration rate

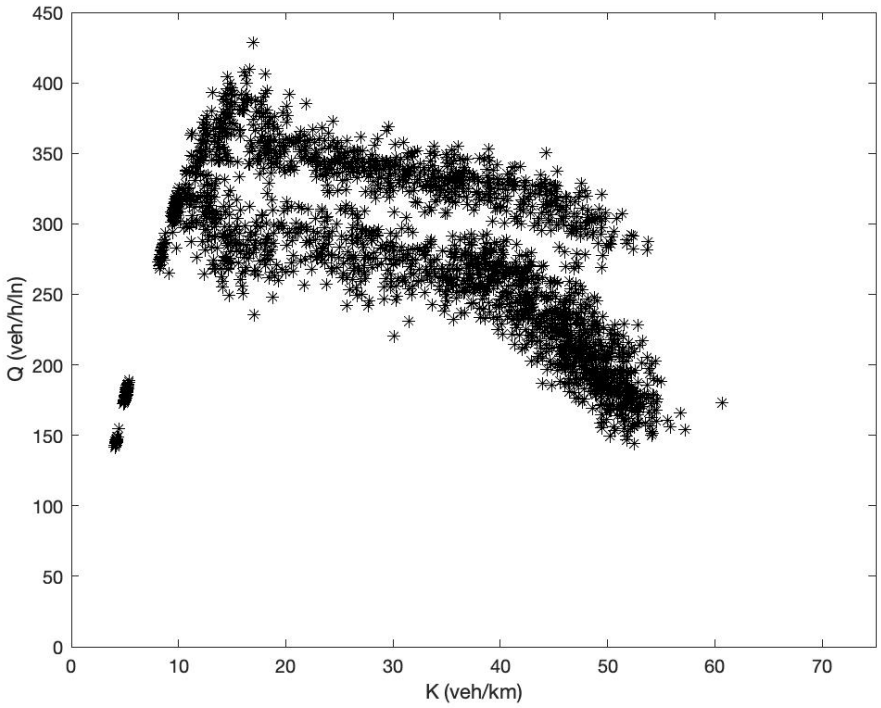

Figure A.11: MFD of the 100% automated vehicles penetration rate

Bibliography

[1] Pablo Alvarez Lopez, Michael Behrisch, Laura Bieker-Walz, Jakob Erdmann, Yun-Pang Flötteröd, Robert Hilbrich, Leonhard Lücken, Johannes Rummel, Peter Wagner, and Evamarie Wießner. "Microscopic Traffic Simulation using SUMO". In: *2019 IEEE Intelligent Transportation Systems Conference (ITSC)* (November 2018), pp. 2575–2582.

[2] Lukas Ambühl, Allister Loder, Michiel C.J. Bliemer, Monica Menendez, and Kay W. Axhausen. "A functional form with a physical meaning for the macroscopic fundamental diagram". In: *Transportation Research Part B: Methodological* 137 (July 2020), pp. 119–132. DOI: 10.1016/j.trb.2018.10.013.

[3] Eleonora Andreotti, Pinar Boyraz, and Selpi Selpi. "Simulation-based impact projection of autonomous vehicle deployment using real traffic flow". In: (2021).

[4] Various Authors. *Highway Capacity Manual*. Chapter 17. Washington, D.C.: Transportation Research Board, 2000. ISBN: 0-309-06681-6.

[5] SAE - Society of Automotive Engineers. "Taxonomy and definitions for terms related to driving automation systems for on-road motor vehicles". In: *SAE International* (September 2016).

[6] Mohamed Berrazouane, Kailin Tong, Selim Solmaz, Martijn Kiers, and Jacqueline Erhart. "Analysis and Initial Observations on Varying Penetration Rates of Automated Vehicles in Mixed Traffic Flow utilizing SUMO". In: *2019 IEEE International Conference on Connected Vehicles and Expo (ICCVE)* (Nov. 2019). DOI: 10.1109/ICCVE45908.2019.8965065.

[7] Christine Buisson and Cyril Ladier. "Exploring the impact of homogeneity of traffic measurements on the existence of macroscopic fundamental diagrams". In: *Transportation Research Record* 2124.1 (2009), pp. 127–136.

[8] D.L.R. German Aerospace Center. *SUMO Definition of vehicles, vehicle types, and routes*.

[9] Carlos F. Daganzo and Nikolas Geroliminis. "An analytical approximation for the macroscopic fundamental diagram of urban traffic". In: *Transportation Research Part B: Methodological* 42.9 (Nov. 2008), pp. 771–781. DOI: 10.1016/j.trb.2008.06.008.

[10] Richard Dowling, Alexander Skabardonis, and Vassili Alexiadis. *Traffic analysis toolbox, volume III: Guidelines for applying traffic microsimulation modeling software*. Tech. rep. United States. Federal Highway Administration. Office of Operations, 2004.

[11] Richard Dowling, Alexander Skabardonis, John Halkias, Gene McHale, and Grant Zammit. "Guidelines for calibration of microsimulation models: framework and applications". In: *Transportation Research Record* 1876.1 (2004), pp. 1–9.

[12] Jakob Erdmann. "SUMO's Lane-Changing model". In: *Lecture notes in control and information sciences, 13* (2015), pp. 105–123.

[13] Bernhard Friedrich. "The effect of autonomous vehicles on traffic". In: *Autonomous driving*. Springer, 2016, pp. 317–334. DOI: 10.1007/978-3-662-48847-8_16.

[14] Nikolas Geroliminis and Carlos F. Daganzo. "Existence of urban-scale macroscopic fundamental diagrams: Some experimental findings". In: *Transportation Research Part B: Methodological* 42.9 (Nov. 2008), pp. 759–770. DOI: 10.1016/j.trb.2008.02.002.

[15] Douglas Gettman and Larry Head. "Surrogate safety measures from traffic simulation models". In: *Transportation Research Record* 1840.1 (2003), pp. 104–115. DOI: 10.3141/1840-12.

[16] Bruce R Hellinga. "Requirements for the calibration of traffic simulation models". In: *Proceedings of the Canadian Society for Civil Engineering* 4 (1998), pp. 211–222.

[17] John Houston, Guido Zuidhof, Luca Bergamini, Yawei Ye, Long Chen, Ashesh Jain, Sammy Omari, Vladimir Iglovikov, and Peter Ondruska. "One thousand and one hours: Self-driving motion prediction dataset". In: *arXiv preprint* (2020).

[18] Yangbeibei Ji, Winnie Daamen, Serge Hoogendoorn, Sascha Hoogendoorn-Lanser, and Xiaoyu Qian. "Investigating the Shape of the Macroscopic Fundamental Diagram Using Simulation Data". In: *Transportation Research Record: Journal of the Transportation Research Board* 2161 (Dec. 2010), pp. 40–48. DOI: 10.3141/2161-05.

[19] Ozgenur Kavas-Torris, Nathan Lackey, and Levent Guvenc. "Simulating the Effect of Autonomous Vehicles on Roadway Mobility in a Microscopic Traffic Simulator". In: *International Journal of Automotive Technology* 22.3 (2021), pp. 713–733.

[20] Daniel Krajzewicz. "Traffic simulation with SUMO–simulation of urban mobility". In: *Fundamentals of traffic simulation*. Springer, 2010, pp. 269–293.

[21] Daniel Krajzewicz, Jakob Erdmann, Michael Behrisch, and Laura Bieker. "Recent development and applications of SUMO-Simulation of Urban MObility". In: *International journal on advances in systems and measurements* 5.3&4 (2012).

[22] Daniel Krajzewicz, Georg Hertkorn, Christian Rössel, and Peter Wagner. "SUMO (Simulation of Urban MObility)-an open-source traffic simulation". In: *Proceedings of the 4th middle East Symposium on Simulation and Modelling (MESM20002)*. 2002, pp. 183–187.

[23] Nathan Lackey. "Simulating autonomous vehicles in a microscopic traffic simulator to investigate the effects of autonomous vehicles on roadway mobility". PhD thesis. The Ohio State University, 2019, pp. 1–43.

[24] Suzanne E Lee, Erik CB Olsen, Walter W Wierwille, et al. *A comprehensive examination of naturalistic lane-changes*. Tech. rep. United States. National Highway Traffic Safety Administration, 2004.

[25] Qiong Lu, Tamás Tettamanti, Dániel Hörcher, and István Varga. "The impact of autonomous vehicles on urban traffic network capacity: an experimental analysis by microscopic traffic simulation". In: *Transportation Letters* 12.8 (Sept. 2019), pp. 540–549. DOI: 10.1080/19427867.2019.1662561.

[26] Qiong Lu, Tamás Tettamanti, and István Varga. "Impacts of autonomous vehicles on the urban fundamental diagram". In: (2018).

[27] Margarita Martìnez-Dìaz and Francesc Soriguera. "Autonomous vehicles: theoretical and practical challenges". In: *Transportation Research Procedia* (2018), pp. 275–282. DOI: 10.1016/j.trpro.2018.10.103.

[28] Michiel M Minderhoud and Piet HL Bovy. "Extended time-to-collision measures for road traffic safety assessment". In: *Accident Analysis & Prevention* 33.1 (2001), pp. 89–97. DOI: 10.1016/s0001-4575(00)00019-1.

[29] Evangelos Mintsis, Dimitris Koutras, Kallirroi Porfyri, Evangelos Mitsakis, Leonhard Lücken, Jakob Erdmann, Yun-Pang Flötteröd, Robert Alms, Michele Rondinone, Sven Maerivoet, Kristof Carlier, Xiaoyun Zhang, Robbin Blokpoel, Martijn Harmenzon, and Steven Boerma. "Modelling, simulation and assessment of vehicle automations and automated vehicles' driver behaviour in mixed traffic". In: *TransAID Deliverable 3.1* (Sept. 2019), pp. 1–71.

[30] Sara Moridpour, Majid Sarvi, and Geoff Rose. "Lane changing models: a critical review". In: *Transportation letters* 2.3 (July 2010), pp. 157–173. DOI: 10.3328/TL.2010.02.03.157-173.

[31] Ronald Nippold, Peter Wagner, Olaf Angelo Banse Bueno, and Christian Rakow. "Investigation of the effect of autonomous vehicles (AV) on the capacity of an urban transport network". In: (2021).

[32] Mario Olivari. *Teoria e tecnica del deflusso veicolare*. Ed. by ARACNE editrice. Chapter 1. Roma, 2011. ISBN: 9788854838680.

[33] Erik CB Olsen, Suzanne E Lee, Walter W Wierwille, and Michael J Goodman. "Analysis of distribution, frequency, and duration of naturalistic lane changes". In: *Proceedings of the Human Factors and Ergonomics Society Annual Meeting*. Vol. 46. 22. SAGE Publications Sage CA: Los Angeles, CA. 2002, pp. 1789–1793.

[34] Federico Orsini, Gregorio Gecchele, Massimiliano Gastaldi, and Riccardo Rossi. "Large-scale road safety evaluation using extreme value theory". In: *IET Intelligent Transport Systems* 14.9 (2020), pp. 1004–1012. DOI: 10.1049/iet-its.2019.0633.

[35] Byungkyu Park, Jongsun Won, and Michael A Perfater. *Microscopic simulation model calibration and validation handbook.* Tech. rep. Virginia Transportation Research Council, 2006.

[36] Perkins and J. Harris. "Traffic conflicts characteristics: Accident potential at intersections". In: *Highway Research Record* 225 (1967), pp. 35–43.

[37] *Report FHWA-03-050*. Tech. rep. FHWA, U.S. Department of Transportation, 2003.

[38] *Research on the impacts of connected and autonomous vehicles (CAVs) on traffic flow*. Tech. rep. Atkins Ltd, May 2016. URL: https://www.gov.uk/government/uploads/system/uploads/attachment_data/file/530091/impacts-of-connected-and-autonomous-vehicles-on-traffic-flow-summary-report.pdf.

[39] Andrew P Tarko. "A unifying view on traffic conflicts and their connection with crashes". In: *Accident Analysis & Prevention* 158 (2021), pp. 106–187. DOI: 10.1016/j.aap.2021.106187.

[40] Andrew P Tarko. "Surrogate measures of safety". In: *Safe mobility: challenges, methodology and solutions*. Vol. 11. Emerald Publishing Limited, 2018, pp. 383–405.

[41] Joseph Treiterer and Jeffrey Myers. "The hysteresis phenomenon in traffic flow". In: *Transportation and traffic theory* 6 (1974), pp. 13–38.

[42] François Vaudrin, Jakob Erdmann, and Laurence Capus. "Impact of autonomous vehicles in an urban environment controlled by static traffic lights system". In: *SUMO 2017–Towards Simulation for Autonomous Mobility* (2017), p. 81.

[43] Chang Wang, Qinyu Sun, Rui Fu, Zhen Li, and Qiong Zhang. "Lane change warning threshold based on driver perception characteristics". In: *Accident Analysis &amp Prevention* 117 (Aug. 2018), pp. 164–174. DOI: 10.1016/j.aap.2018.04.013.

[44] Yang Yang Wang, Guangda Chen, and Zhiguang Liu. "Modified car following and lane changing simulations model for autonomous vehicle on highway". In: (2018). DOI: 10.4271/2018-01-1647.

[45] Wikipedia. *Vahrenwald-List — Wikipedia, The Free Encyclopedia*. [Online; accessed on 21-January-2022]. 2022. URL: https://de.wikipedia.org/wiki/Vahrenwald-List.

[46] Minming Yang, Xuesong Wang, and Mohammed Quddus. "Examining lane change gap acceptance, duration and impact using naturalistic driving data". In: *Transportation Research Part C: Emerging Technologies* 104 (July 2019), pp. 317–331. DOI: 10.1016/j.trc.2019.05.024.

[47] Wei Zeng and Richard L Church. "Finding shortest paths on real road networks: the case for A". In: *International journal of geographical information science* 23.4 (2009), pp. 531–543. DOI: 10.1080/13658810801949850.

[48] Lele Zhang, Zhongqi Yuan, Li Yang, and Zhiyuan Liu. "Recent developments in traffic flow modeling using macroscopic fundamental diagram". In: *Transport Reviews* 40.4 (Mar. 2020), pp. 529–550. DOI: 10.1080/01441647.2020.1743918.